

UNCERTAINTY QUANTIFICATION IN STRUCTURAL SYSTEMS USING UNIVERSAL GREY THEORY

Thesis

Submitted in partial fulfilment of the requirements for the degree of

DOCTOR OF PHILOSOPHY

by

AKSHAY KUMAR



DEPARTMENT OF CIVIL ENGINEERING
NATIONAL INSTITUTE OF TECHNOLOGY KARNATAKA
SURATHKAL, MANGALORE – 575025

AUGUST, 2024



**UNCERTAINTY QUANTIFICATION IN
STRUCTURAL SYSTEMS USING UNIVERSAL
GREY THEORY**

A Thesis

Submitted in partial fulfilment of the requirements for the degree of

DOCTOR OF PHILOSOPHY

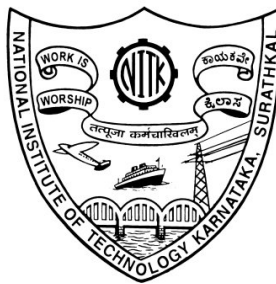
by

AKSHAY KUMAR

(197089CV002)

Under the guidance of

Dr. A S BALU



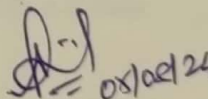
DEPARTMENT OF CIVIL ENGINEERING
NATIONAL INSTITUTE OF TECHNOLOGY KARNATAKA
SURATHKAL, MANGALORE – 575025

AUGUST, 2024



DECLARATION

I hereby *declare* that the Research Thesis entitled **UNCERTAINTY QUANTIFICATION IN STRUCTURAL SYSTEMS USING UNIVERSAL GREY THEORY** which is being submitted to the **National Institute of Technology Karnataka, Surathkal** in partial fulfilment of the requirements for the award of the Degree of **Doctor of Philosophy in Civil Engineering** is a *bonafide report of the research work carried out by me*. The material contained in this Research Thesis has not been submitted to any University or Institution for the award of any degree.

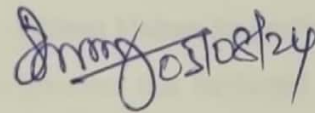

AKSHAY KUMAR
(197089CV002)
Research Scholar
Department of Civil Engineering

Place: Surathkal - 575025.

Date: 05/08/2024

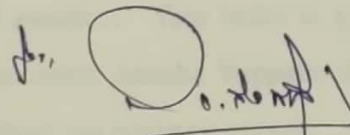
CERTIFICATE

This is to *certify* that the Research Thesis entitled **UNCERTAINTY QUANTIFICATION IN STRUCTURAL SYSTEMS USING UNIVERSAL GREY THEORY** submitted by **Akshay Kumar** (Register Number:197089CV002) as the record of the research work carried out by him, is *accepted as the Research Thesis submission* in partial fulfillment of the requirements for the award of degree of **Doctor of Philosophy**.



Research Supervisor

Dr. A S Balu



Chairman-DRPC

Chairman (DRPC)
Department of Civil Engineering
National Institute of Technology Karnataka
Surathkal, Mangalore - 575 025, Karnataka, INDIA

ACKNOWLEDGEMENT

I am immensely thankful to God for being my guiding strength, providing unwavering wisdom, and being the compass that led me through the completion of this research study.

First and foremost, I extend my heartfelt gratitude to my research supervisor, **Dr. A. S. Balu**, whose expertise, encouragement, and invaluable insights have steered me through every phase of this research journey. Your dedication and mentorship have been truly inspiring.

I am thankful to my RPAC members, **Dr. Vijaya Vengadesh Kumar** and **Dr. Murgan V.**, for their constructive feedback, scholarly guidance, and invaluable suggestions that significantly enriched this thesis.

I am also thankful to Chairman-DRPC **Prof. Subhash C Yaragal**, Head of the Civil Engineering Department and DRPC-Secretary **Dr. Mithun Mohan** for providing the necessary resources and a conducive academic environment that facilitated this research endeavor.

I want to express my heartfelt thanks to my fellow Ph.D. research scholars **Sushma M, Nagesh M, Sachin H, Utino W, Vinod S, Sreya M V, Arichandran, Amoke Shabari, and Afsal K P.** Your discussions and shared experiences brought depth and perspective to this study, and I truly appreciate it.

I owe an immeasurable debt of gratitude to my beloved parents, **Anant Mankal** and **Aruna Mankal**, and my in-laws, **K N Venkatesh** and **K V Jyothi** for their boundless love, unwavering encouragement, and sacrifices. Your belief in me has been my driving force. Special thanks to my dear sister, **Anusha Vuppala**, for her encouragement, support, and understanding throughout this academic pursuit.

Last but not least, I extend a special thanks to my loving wife, **Dr. Meghana K V.** Your understanding, encouragement, and unwavering support during the highs and lows of this academic pursuit have been my strength and motivation.

AKSHAY KUMAR



ABSTRACT

In recent times, there has been a growing demand for addressing uncertainties in engineering systems, both aleatory and epistemic nature. Aleatory uncertainties arise from the inherent randomness of physical systems, while epistemic uncertainties realize from limited knowledge. The present study exclusively focuses on the quantification of epistemic uncertainty within engineering systems. When the information about the system is grey (i.e., partially available as range or interval), methods such as combinatorial approach, interval methods (IM), and universal grey theory (UGT) are commonly employed to handle these uncertainties. However, as the dimension of the uncertain system increases, challenges emerge. Combinatorial optimization, although effective, becomes computationally expensive for large systems, and interval analysis tends to overestimate due to violations of physical laws and dependency issues. To mitigate these challenges, the UGT offers a promising solution by obeying distributive laws which addresses the dependency problems and enhances the computational efficiency.

However, the traditional UGT encounters limitations in some situations where one or both bounds are negative, with the upper bound having a smaller absolute value. (i.e., $|\bar{x}| \leq |\underline{x}|$). This study proposes a necessary modification in the arithmetic operations within the UGT framework to overcome the above limitation.

In addition, another key consideration for efficient analysis of systems with epistemic uncertainty is the computational cost. The analysis of large systems is computationally expensive while using finite element methods. However, metamodeling techniques such as Response Surface Method (RSM) and Kriging techniques can be adopted to mimic the original models. However, these techniques can also become too expensive as system dimensions increase. A High Dimensional Model Representation (HDMR) is an RSM which stands out as a computationally efficient technique while dealing with large systems.

To address the quantification of epistemic uncertainty in large-dimensional systems, this study further proposed the HDMR-UGT based formulation. The UGT handles the ambiguity more efficiently by addressing the dependency issues. Moreover,

in order to avoid the model errors being carried over into the uncertainty quantification, HDMR in conjunction with UGT has been developed in this study. The method integrates finite element modeling, utilizes the HDMR metamodel technique to develop response surfaces, and employs UGT for explicit uncertainty analysis to predict response bounds.

The proposed methodology is evaluated through numerical examples, demonstrating its accuracy and computational efficiency in exclusively quantifying epistemic uncertainty. Comparative assessments with conventional techniques further validate the effectiveness of the HDMR-UGT based formulation in terms of reducing computational efforts while maintaining high accuracy in engineering system analysis subjected to epistemic uncertainty.

Keywords: Aleatory, Epistemic, Interval method, Universal grey theory, Finite element analysis, High dimensional model representation.

TABLE OF CONTENTS

Title	Page No.
ABSTRACT	i
LIST OF TABLES	v
LIST OF FIGURES	vi
SYMBOLS AND ABBREVIATION	viii
CHAPTER 1 INTRODUCTION	1
1.1 UNCERTAINTY	1
1.2 METHODS TO QUANTIFY UNCERTAINTY	3
1.3 METAMODEL	5
1.4 NEED FOR THE PRESENT WORK	7
1.5 THESIS ORGANISATION	8
CHAPTER 2 LITERATURE REVIEW	9
2.1 INTERVAL METHODS	9
2.2 GREY THEORY	12
2.3 HIGH DIMENSIONAL MODEL REPRESENTATION	14
2.4 COMBINATORIAL OPTIMIZATION	16
2.5 SUMMARY OF LITERATURE REVIEW	18
2.6 OBJECTIVES OF RESEARCH WORK	18
2.7 SCOPE OF PRESENT RESEARCH	19
CHAPTER 3 INTERVAL APPROACH	21
3.1 BACKGROUND	21
3.2 DEPENDENCY PROBLEM	22
3.3 NUMERICAL EXAMPLES	25
3.3.1 Lamina Stiffness Element	25
3.3.2 Axially Loaded Stepped Bar	25

3.4	COMBINATORIAL METHOD	27
CHAPTER 4 GREY THEORY		29
4.1	BACKGROUND	29
4.2	GREY NUMBER	30
4.3	UNIVERSAL GREY NUMBER THEORY	30
4.3.1	Example : Lamina Stiffness Element	32
4.3.2	Example : Three Bar System	33
4.3.3	Example : Nonlinear Explicit Function	36
4.3.4	Example : Vibration Analysis of Spring Mass Damper System	38
4.4	IMPROVED UNIVERSAL GREY NUMBER	42
4.4.1	Example : Non-linear Explicit Function (Revisited)	45
4.4.2	Example : Three Bar Stepped System	47
4.4.3	Example : Planar Truss System	50
4.4.4	Example : Buckling analysis for the column structure	54
4.5	METAMODEL	56
4.6	FIRST ORDER HDMR APPROXIMATION	57
4.7	NUMERICAL EXAMPLES	62
4.7.1	A Truncated Conical Structure	62
4.7.2	Static Analysis of Fixed Beam	64
4.7.3	Shear Wall Frame Subjected to Lateral Load	66
4.7.4	Multi-Storied Frame Structure	70
CHAPTER 5 SUMMARY AND CONCLUSION		73
5.1	SUMMARY AND RESEARCH FINDINGS	73
5.2	FUTURE SCOPE	75
APPENDIX A		77
REFERENCES		85
PUBLICATIONS		94

LIST OF TABLES

Table No.	Title	Page No.
3.1	Material properties of graphite and epoxy	25
4.1	Stresses in different element	36
4.2	Response of explicit nonlinear function	37
4.3	Variation of displacement transmissibility (Deterministic analysis) . . .	40
4.4	Variation of displacement transmissibility (Interval method)	42
4.5	Variation of displacement transmissibility (UGT)	42
4.6	Ranges of stresses	46
4.7	Stress in element 1	49
4.8	Response of stress in element 2	49
4.9	Response of stress in element 3	50
4.10	Stresses in truss members obtained by interval method	51
4.11	Stresses in truss members obtained by by UGT	52
4.12	Stresses in truss members obtained by combinatorial approach	53
4.13	Material and geometric properties of column member	54
4.14	Critical buckling load	56
4.15	Material and geometrical properties of fixed beam	65
4.16	Material and geometric properties of the single-storey building	68
4.17	Input data for the frame structure	72

LIST OF FIGURES

Figure No.	Title	Page No.
1.1	Comparison of certainty and uncertainty	2
1.2	Illustration of surrogate-modelling	6
3.1	Two bar stepped system	26
4.1	Universal Grey number based Gaussian elimination Procedure	32
4.2	Three bar system	33
4.3	Response of explicit function	38
4.4	A spring mass damper system	39
4.5	Variation of displacement transmissibility for $\zeta = 0.1$	40
4.6	Variation of transmissibility for $\zeta = 0.3$	41
4.7	Variation of transmissibility for $\zeta = 0.5$	41
4.8	Response function, $f(x)$	46
4.9	Three bar stepped system	47
4.10	Variation of stress in element 1	48
4.11	Variation of stress in element 2	48
4.12	Variation of stress 3	49
4.13	Planar truss system	50
4.14	Variation of Stress in member 2	51
4.15	Variation of Stress in member 4	52
4.16	Variation of Stress in member 11	53
4.17	Axially loaded column	54
4.18	Sampling points along each variable axis in first-order HDMR	59
4.19	UGT–HDMR based uncertainty analysis	61
4.20	Performance function, G	64
4.21	Maximum deflection at mid span	66
4.22	Floor plan of the building	67
4.23	Rigid floor plan with degree of freedom	67

4.24 Displacement, U_1	69
4.25 Displacement, U_2	69
4.26 Five story three bay portal frame	71
4.27 Displacement, U_x	72

SYMBOLS AND ABBREVIATION

A	Cross sectional area
C	Damping constant
E	Young's modulus
E_e	Young's modulus of epoxy matrix
E_{g11}	Young's modulus of graphite fiber in longitudinal direction
E_{g22}	Young's modulus of graphite fiber in transverse direction
K	Stiffness matrix
L	Length
M	Bending Moment
P	Load
T_d	Transmissibility ratio
U	Displacement matrix
$U_g^{(0)}$	Universal zero unit
$U_g^{(0)}$	Universal grey number unit element
U_g	Universal grey number
V_e	Volume fraction of epoxy matrix
V_g	Volume fraction of graphite fiber
$[Aug]$	Augmented matrix
μ	Poisson's ratio
μ_e	Poisson's ratio of epoxy matrix
μ_g	Poisson's ratio of graphite fiber
ω	Base excitation frequency
ω_n	Natural frequency
σ	Stress
θ	Slope angle
ζ	Damping ratio

c	Reference point
m	Mass
r_1	internal radius
r_1	Thickness
r_m	Mean frequency ratio
w	Load per meter run

ABBREVIATIONS

FEA	F inite E lement A nalysis
HDMR	H igh D imensional M odel R epresentation
IA	I nterval A nalysis
UGN	U niversal G rey N umber
UGT	U niversal G rey T heory

CHAPTER 1

INTRODUCTION

1.1 UNCERTAINTY

There has been growing interest in the modeling and analysis of structural systems with input uncertainties, as these input variables play a crucial role in determining the performance and behavior of the structures. The source of uncertainty can be due to model imperfection, system inaccuracies, statistical error, material uncertainty, load uncertainty, and many more (Ranganathan, 1999). The complexity of most structural systems necessitates accounting for uncertainties to avoid uncertainty in the output response. In structural mechanics, uncertainties are inevitable and can arise from various sources, including geometry, material properties, load parameters, model formulation, and analysis procedures. For example, in civil engineering, live loads imposed on structures introduce uncertainty due to variations in magnitude and distribution. These uncertainties result in responses of structural systems such as displacement, stress, and vibration frequencies by exhibiting inherent uncertainty. Incorporating these uncertainties into modeling and analysis requires careful effort but provides valuable information for decision-making. By accounting for uncertainties, engineers can enhance the accuracy of predictions and assessments, leading to more informed and reliable decisions in civil engineering applications.

Uncertainties are generally classified as either aleatory or epistemic, based on their source and nature (Li et al. 2016; Der Kiureghian and Ditlevsen 2009). Aleatory uncertainties arise due to the intrinsic random nature of the physical system. Aleatory (random) is also known as objective or stochastic uncertainty or irreducible uncertainty. Ideally, there would be accessible objective information on both the range and the possibility of the quantity within the range (i.e., distribution). Epistemic uncertainty realize on account of insufficient knowledge about the physical system, usually expressed as ranges (interval numbers), vague statements (fuzzy numbers), etc. It is also known as subjective uncertainty or reducible uncertainty. Unlike aleatory uncertainty, which is inherent and irreducible, epistemic uncertainty has the potential to be reduced through the acquisition of additional data, improved modeling, or more accurate parameter estimation. Incomplete information or knowledge about the system

is the root cause of epistemic uncertainty. In engineering practice, it is essential to distinguish between aleatory and epistemic uncertainty because they require different approaches for quantification. The comparison of certainty and uncertainty (Hang Hou et al., 2019) is shown in Figure 1.1 is Both types of uncertainty play significant roles in risk assessment, decision-making, uncertainty analysis, and modeling complex systems. Some examples of epistemic uncertainty are as follows:

- i. **Statistical uncertainty as a result of inadequate data:** When the sufficient information is unavailable to make precise statistical predictions.
- ii. **Expert opinion range of possible values:** Sometimes, experts provide a range of values for a physical quantity based on their judgment and expertise rather than precise measurements.
- iii. **Model uncertainty as a result of limited understanding of complex system:** In structural mechanics, model uncertainty occurs due to simplified assumptions about materials and forces, because of limited understanding about the complex structural system.

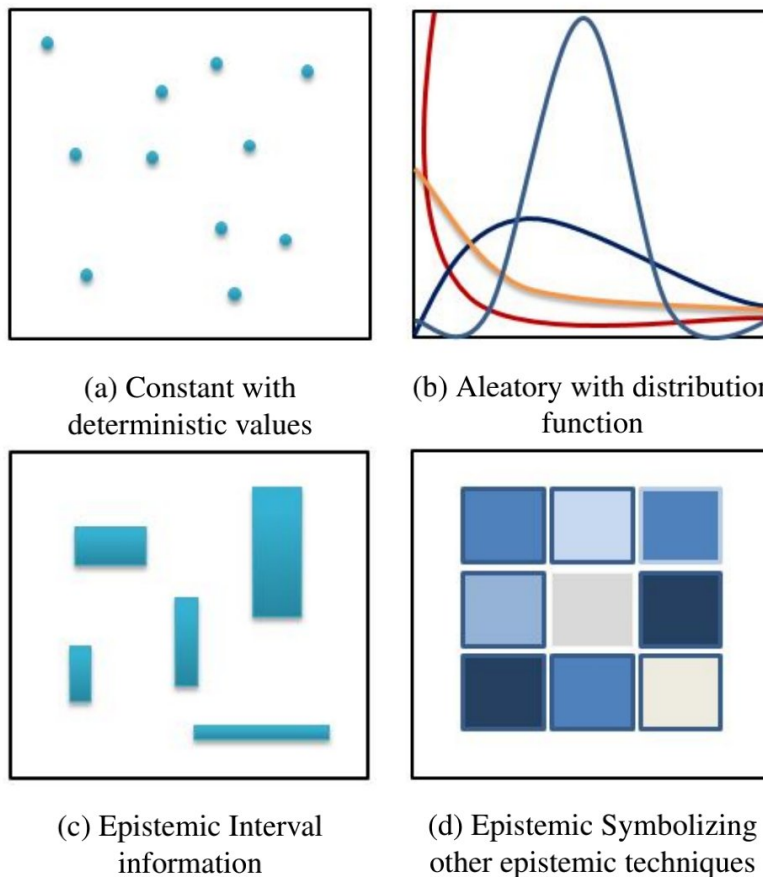


Figure 1.1 Comparison of certainty and uncertainty

1.2 METHODS TO QUANTIFY UNCERTAINTY

In most cases, statistical or probabilistic approaches are used to quantify stochastic or aleatory uncertainty. In the probabilistic method, uncertainty levels are quantified as random variables, time-dependent characteristics are characterized by stochastic processes and spatial attributes are represented by random fields. The basic goal of probabilistic analysis is to determine the reliability of a system. Methods such as the response surface method, the Monte Carlo and Latin Hypercube sampling methods, the first-order and second-order reliability methods (FORM and SORM, respectively), and other techniques are frequently used to propagate uncertainty. Many of the researchers have concluded that probabilistic and stochastic approaches are best suited methods for the quantification of aleatory uncertainty (Der Kiureghian and Ditlevsen, 2009).

It is often difficult to obtain sufficient information about the system parameters. In such cases, few researchers have carried out the analysis using a probabilistic approach by assuming uncertainty parameters as random variables with known uniform distribution functions. However, which is not the case in the practical system. A slight error in the probabilistic data/model results in a huge difference in the system output (Du et al., 2006). Stochastic methods are effective in modeling and propagating uncertainty; however, their applicability is constrained in cases where parameter distributions are unavailable.

Non-probabilistic approaches have emerged and developed as a result of the shortcomings of stochastic methods. These include fuzzy set theory (Zadeh, 1965), possibility theory (Dubois and Prade, 2015), probability bounds approach (Berleant et al., 2005), convex models (Ben-Haim 1994; Ben-Haim and Elishakoff 2013), evidence theory (Wang et al., 2022a), interval methods (Moore et al. 2009; Jansson 1991; Impollonia and Muscolino 2011), imprecise probability theory (Walley, 1991), and many more. Based on the nature of uncertainty in the structural system, the non-probabilistic approaches listed above can be used. Among these, the interval method is widely accepted when information is available in ranges or bounds due to its practicality and efficiency.

Moore et al. (2009) pioneered the interval method, where the basic interval arithmetic operations and solutions to the set of linear and non-linear interval equations are explained. Although the basic fundamental relationships of interval arithmetic and their solutions were presented in the early 90's, the use of interval concepts in engineering and structural analysis is more recent. However, the interval method face a dependency problem (Jansson, 1991), when the same interval variable is encountered multiple times within a system. As a result, the estimates predicted by the

interval arithmetic are usually wider than the actual ranges. To mitigate this problem, researchers have proposed approaches such as the interval truncation method (Rao and Berke 1997; Rao and Alazwari 2020), interval perturbation method (Qiu and Elishakoff 1998; Chen and Yang 2000), interval and subinterval methods (Zhou et al. 2006; Wang et al. 2023), interval-based control methods (Wang et al. 2022b; Wang et al. 2023) and interval parameterization (Elishakoff and Thakkar, 2014), element-by-element technique (Muhanna and Mullen, 2001), interval finite element technique (Fedele et al. 2015; Muhanna and Mullen 1999; Muhanna et al. 2005; Muhanna et al. 2007) and many more. Interval finite element technique has been proven to be particularly effective in recent decades for structural uncertainty analysis. Nevertheless, interval approaches cannot be immediately applied to every situation; the physical nature of the problem must first be understood to adjust the interval calculations as necessary by the presented methods to reduce response quantity widths.

In the real world system, when the information about the system parameter is completely known then the system is called white. When the information about the system parameter is completely unknown it is treated as black. Only partial information about the system is known then it is termed as grey. The grey system technique may be utilized to manage an uncertain system with only partial knowledge. Grey system theory was proposed by Julong et al. (1989) to deal with systems having parameters whose values are partially known. In this theory, grey numbers are used to capture the information and implement a grey arithmetic operation to predict the response bounds of the system. Initially the Grey theory was used in the field of meteorological disaster risk assessment, flood disaster risk analysis, construction risk assessment and system security.

Although generic grey numbers are expressed similar to the interval numbers and their arithmetic operations performed are similar to interval arithmetic. A universal grey number theory (UGT), which falls under a specific class of grey number theory, satisfies the physical laws (distributive law) that arise out of defining the grey arithmetic relations and contributes the theory free from dependency problem. For the first time, Rao and Liu (2017) adopted UGT for the analysis of structural system subjected to interval uncertainty. Small sample sizes and limited knowledge regarding uncertain systems are typical in the natural world. In recent times the application of UGT in engineering mechanics has gained much attention over the interval method because the results obtained from interval analysis were found to be overestimated due to violations of the physical law and the dependency problem in its arithmetic process. Whereas, satisfaction of the physical law (distributive law) that arises out of defining the arithmetic relations, contributes to the UGT free from dependency problem, and

makes the approach more efficient. The present study mainly focus on the analysis of structural system subjected to epistemic uncertainty. In this study, the UGT, interval arithmetic method and combinatorial optimization techniques are adopted to study the behavior of the structural system subjected to epistemic uncertainty (partially available as range or interval).

1.3 METAMODEL

In the real-world engineering system, the computational time required for the analysis of complex structures in the computer is quite expensive in terms of cost and time. Hence, metamodel (surrogate) techniques have evolved to solve the mitigation of complex computer analysis. The primary purpose of surrogate modeling is to create a simplified and computationally efficient model (the surrogate or meta-model) that approximates the behavior of a complex and computationally expensive simulation or process. The actual behavior of the complex system is achieved by developing the relationship between input variables and output response. The surrogate model can then be used for various applications, such as optimization, sensitivity analysis, or uncertainty quantification while reducing the computational cost significantly. However, by selecting a better model, the accuracy of the metamodel can be improved to more accurately reflect the real system and imitate the performance of a system that has the ideal design configurations and set of design parameters.

The metamodel development approach typically consists of a three-step process: In the first step, the focus is on choosing a set of typical and representative sample points within the design space. The selection process aims to gather comprehensive data that covers the entire design space. The specific choice of sample points depends on the type of metamodel being developed. Secondly, the outputs corresponding to each of the selected sample points are carefully evaluated. This assessment helps in determining a set of design points and their corresponding responses. These design points represent critical aspects of the system or model under consideration. The final step involves the development of a mathematical model. Surrogate models are constructed from a given set of n observations $Z_n = (z_1, \dots, z_n)$, where each $Z_j = (x_j, y_j)$ for $1 \leq j \leq n$ and $y_j = f(x_j)$, also known as design points. The primary goal of surrogate modeling is to approximate the costly function f with a simpler response surface \hat{f}_{z_n} , thus accelerating the estimation of a characteristic of f using \hat{f}_{z_n} . The precision of the surrogate model depends significantly on the quality of the training set. Naturally, there is a balance to be struck between the accuracy of feature estimation and the number of evaluations of f . As a result, the design of experiments (DOE), which involves selecting the sampling

points $(x_j)_{1 \leq j \leq n}$, is a vital and actively studied area. The illustration for surrogate modelling (Forrester et al., 2008) is shown in Figure 1.2.

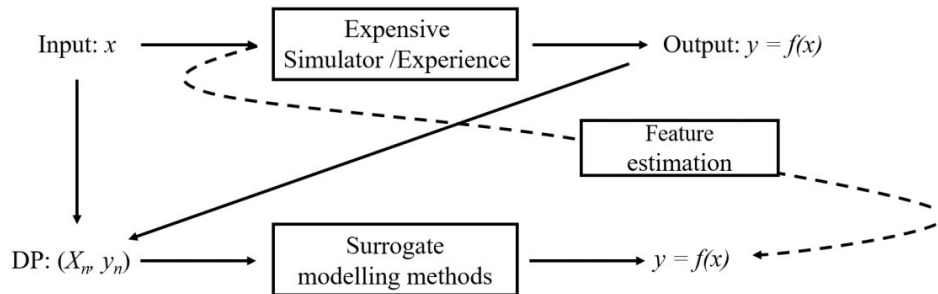


Figure 1.2 Illustration of surrogate-modelling

This model serves as a mapping tool that defines the relationship between inputs (design points) and outputs. Essentially, it provides a mathematical representation of how changes in the input variables affect the output variables (Dey et al., 2017). Various types of surrogate models are commonly used, such as polynomial regression (Zhou et al., 2005), Gaussian processes (Wan et al., 2014), neural networks (Alam et al., 2004), and support vector machines (Pan and Dias, 2017), Kriging meta-models (Sudret (2012); Zhang et al. (2015); Zhao et al. (2015)).

The theories mentioned above are only suitable for basic models and not for complex, high-dimensional structural models due to their high computational demands. However, Li et al. (2001a) has proposed an alternative approach called high-dimensional model representation (HDMR) to overcome this challenge. It was first introduced in the field of the chemistry and later was widely used in the structural reliability areas because of its simplicity and adoptability. It approximates complex mathematical or computer models by representing them as explicit functions, composed of component functions ordered by their contribution to variance. HDMR is particularly useful for systems with numerous input variables, where lower order terms adequately capture the system's behavior, while higher order terms have minimal impact.

In most of the practical cases, higher order terms of the inputs usually have a negligible impact on the output response of the system. HDMR technique usually used to formulate the mathematical model from the experimental available data, Finite element modeling (Balu and Rao, 2012a) and so on. Hence there is a considerable interest in quantifying interval uncertainties in assessing the behavior of structural systems. Response surface methods facilitate metamodels to reduce the effort involved in analysing multidimensional systems. Therefore in the present work,

HDMR technique is utilised for response surface generation and HDMR-UGT based uncertainty analysis is developed for studying the behavior of complex system in the presence of epistemic uncertainties.

1.4 NEED FOR THE PRESENT WORK

In recent times, there has been a notable interest directed toward the modeling and analysis of structural systems with uncertainties. Since input variables significantly play an important role in the performance of the structure. Also, there is a demand for computationally efficient approximation techniques in terms of cost and effort for the analysis of uncertain systems. Especially quantifying the epistemic uncertainty in the structural system is the main concern in this present study. In recent times the application of UGT in engineering mechanics has gained much attention over the interval method because the results obtained from interval analysis were found to be overestimated due to violations of the physical law (distributive law) and the dependency problem in its arithmetic process. Whereas, satisfaction of the physical law (distributive law) that arises out of defining the arithmetic relations, contributes to the UGT free from dependency problem, and makes the approach more efficient. Therefore, in this study UGT is adopted to deal with epistemic uncertainty.

The traditional UGT is ineffective in certain conditions like case 1: if the uncertain quantity ($x \in [\underline{x}, \bar{x}]$) has negative values in its upper and lower bounds (i.e., $|\bar{x}| \leq |\underline{x}|$) and case 2: if the uncertainty quantity has a negative value in its lower and positive value in its upper bound (if the magnitude of the lower bound is greater than upper bound i.e., $|\bar{x}| \leq |\underline{x}|$). Ineffectiveness of traditional UGT in certain cases is due to not satisfying the basic definition of UGN (i.e., $|\underline{x}| \leq |\bar{x}|, |\underline{y}| \leq |\bar{y}|$). Therefore, the present study proposes a necessary modification in arithmetic operations to overcome the incapability of traditional UGT. The efficiency of the proposed UGT is then demonstrated through various numerical examples.

The study further proposes HDMR based UGT formulation to develop the computationally efficient technique in terms of accuracy and effort for the analysis of large dimensional systems subjected to epistemic uncertainty, which involves an integrated FE modeling, development of response surface using HDMR, the establishment of objective function, and explicit uncertainty analysis using UGT for predicting the bounds of the response. The efficiency of the proposed HDMR based UGT is then demonstrated through various numerical examples. This approach is particularly useful for research applications where accurate results are essential, but computational resources are limited.

1.5 THESIS ORGANISATION

In this present study, a computationally efficient UGT technique is developed for the analysis of structural systems subjected to epistemic uncertainty. Also HDMR-UGT based formulation is proposed to develop the computationally efficient technique in terms of accuracy and effort for the analysis of large dimensional systems subjected to epistemic uncertainty. The thesis is organised as follows.

- i. The first chapter introduces the concept of uncertainty, types of uncertainty, metamodel techniques, need for the present work
- ii. The second chapter presents a detailed review of relevant literature on interval methods, universal grey theory, and high dimensional model representation, followed by a summary of the literature and objectives of the proposed research work.
- iii. The third chapter demonstrates the concept of interval analysis, dependency problem and numerical examples solved using interval method.
- iv. The fourth chapter provides a brief introduction to Grey theory, Universal grey number theory, and the contradiction stated in traditional UGT. Numerical examples are solved using traditional and proposed UGT. Finally quantification of the uncertainties of structural systems using HDMR based UGT is performed.
- v. The last chapter presents the conclusions based on the key findings from the present work, and the scope for future work.

CHAPTER 2

LITERATURE REVIEW

2.1 INTERVAL METHODS

In engineering design and analysis, uncertainties play a crucial role, and addressing uncertainties is essential. In situations where comprehensive information regarding the probability distribution of input parameters is lacking, and only a range of values is accessible, the utilization of a non-probabilistic approach emerges as a particularly advantageous technique for analyzing such systems. Various researchers have concluded that the most suitable way to represent uncertainty is by using the information available to us, which is the interval itself (Ferson and Ginzburg 1996; Joslyn 2004; Oberkampf and Helton 2004; Sentz and Ferson 2002). Few mathematical modeling approaches, such as probabilistic, fuzzy, or interval methods, can efficiently account for these uncertainties. The interval method is widely accepted when information is available in ranges or bounds due to the simplicity in its computation. Interval arithmetic was introduced by Moore (1966), the importance of interval arithmetic were emphasized and presented the operational laws of interval arithmetic, including the property of sub-distributive. However, distributive law does not always hold in interval arithmetic because of the dependency issue in interval arithmetic. Rohn (1989) proposed the theory and methods for computing the exact bounds of a linear system of equations whose coefficients and right-hand sides vary in intervals. Finite and iterative methods were proposed based on results from linear complementarity theory. Similar work was carried out by Jansson (1991) by addressing the challenges of handling dependencies in interval linear systems with symmetric and skew-symmetric matrices, providing algorithms and methods for computing sharp bounds for the solution sets. The concept of interval algebra is discussed in several books, including Alefeld and Herzberger (2012), Hansen and Walster (1992), Neumaier (1990).

Köylüoğlu et al. (1995) employed interval algebra to address structural and loading uncertainties, achieving computational ease and simplicity in linear static analysis by discretizing material uncertainty and determining conservative bounds for response quantities. Similarly, Rao and Berke (1997) demonstrated various solution methods for linear interval equations which encompasses direct and Gaussian

elimination-based methods, combinatorial approach, and inequality-based method. It is observed that range of response parameters expands with problem size. To manage this expansion an interval truncation approach was proposed to limit the growth of intervals of response parameters, ensuring realistic and accurate solutions in the presence of uncertainty. Qiu et al. (1996) utilized the perturbation method as a straightforward analytical tool to determine static responses, specifically interval displacements in finite element equilibrium equations with interval parameters. The numerical findings demonstrates the exceptional effectiveness of the proposed method. In the later work, Qiu and Elishakoff (1998) discussed the efficacy of the subinterval perturbation method in presenting the range of static displacements of structures with large uncertain but non-random parameters. Concluded that the subinterval perturbation method yields tighter bounds compared to the interval perturbation method. For large dimensional problem Makino and Berz (1999) demonstrated the Taylor model for effective handling of functional dependencies. It was found that reduced overestimation with increased interval precision and manageable computational complexity for higher-dimensional systems, making it a promising approach for complex dependencies.

Chen and Yang (2000) proposed a method of matrix perturbation to solve uncertainty problems of the beam structures using the interval finite element method. The proposed method is validated through numerical examples, demonstrating its effectiveness in capturing the uncertainties and providing reliable results. Similar work were carried out for the other mechanics problems using first order matrix perturbation technique. The computational accuracy is limited if the number and width of the interval parameters are too large (Chen et al., 2002). Uncertainty analysis in solid mechanics was studied by Muhanna and Mullen (2001) by formulating an element-by-element technique and the Lagrange multiplier method eliminates most sources of overestimation and obtains a very sharp solution. Shary (2001) developed a numerical technique that extends the interval Gauss-Seidel method to enclose generalized AE-solution sets in interval linear systems, with a theoretical study proving optimality for interval matrix systems.

Dessombz et al. (2001) introduced iterative algorithm for addressing mechanical systems with bounded parameters in finite element problems. By employing interval calculations, guarantees accurate transfer function envelopes and convergence for linear mechanical problems were found. Polyak and Nazin (2004) proposed an overbounding technique for large-scale problems, enhancing interval solution approximations. Their work extends robust linear algebra to linear interval systems and explores the polytope nature of solution sets for modeling uncertainty. Nedialkov et al. (2004) analyzed optimal approximations for interval computations, including linear and polynomial

methods like affine arithmetic and Taylor series, introducing the Hermite-Obreschkoff method to reduce excess width and explore alternative approaches for efficient approximations.

Wu and Rao (2004) presented an interval analysis approach for precise modeling of assembly tolerances and clearances, outperforming probabilistic methods. It guarantees 100 % confidence intervals, bounding errors, while contrasting with the fuzzy analysis method that offers diverse response information based on preference and confidence levels. A penalty-based solution for interval finite-element methods, ensuring reliable mechanical system approximations by treating parameter uncertainty as intervals (Muhanna et al., 2005). The approach maintains computational efficiency, guarantees results, and extends its applicability to various uncertainty theories reliant on interval arithmetic.

Zhou et al. (2006) studied interval and subinterval analysis methods, using Taylor expansion and error estimations, to calculate structural displacement response bounds with uncertain parameters, enhancing design reliability in engineering applications. Jiang et al. (2007) proposed method by merging nonlinear interval number programming and interval analysis with a genetic algorithm for Pareto optimum solutions, suitable for low-uncertainty linear elastic structural problems, and adaptable for nonlinear structures using numerical differentiation.

Degrauwe et al. (2010) recommend interval-based uncertainty models in structural safety engineering, introducing affine arithmetic to mitigate dependency issues, providing precise bounds and sensitivity information. Khodaparast et al. (2011) proposed interval model updating solutions using parameter vertex solutions and a Kriging predictor metamodel. Numerical validation demonstrates accurate parameter identification with limited data, benefiting frame structure updates. Xiao et al. (2015) used INTLAB to develop an efficient interval finite element approach, addressing parameter dependence and effectively handling material and load uncertainties with element-by-element (EBE) techniques and the penalty method. The method predicts sharp sharp response enclosures. Modified Interval Perturbation Finite Element Method for precise static response interval determination in structures with interval parameters, addressing higher accuracy (Xia and Yu, 2013) . However, computational challenges arise with numerous interval parameters, where fast algorithms like local and global searches can be beneficial in structural analysis.

Sofi and Romeo (2016) developed Interval Finite Element Method utilizing the Extra Unitary Interval (EUI) approach, for static analysis of linear-elastic structures with interval parameters and improved accuracy were observed. Rao and Alazwari (2020) introduced interval-based failure analysis for composite materials, utilizing

truncation-based interval analysis and universal grey system theory, relying on lower and upper bounds of uncertain parameters for realistic and meaningful failure assessments.

Santoro et al. (2020) proposed a approach for computing response bounds in beams under static loads with multiple cracks and uncertain parameters. It employs a monotonicity test and sensitivity-based or global optimization methods, offering accurate bounds for various response functions, while reducing computational efforts compared to other techniques. Ge et al. (2021) developed a method using interval theory to calculate dam failure-induced loss of life, accounting for influencing factors. Validation against real-world data showed close estimates and addressed uncertainty intervals for potential loss of life.

2.2 GREY THEORY

In real-world structural systems, information is frequently characterized by partial knowledge and partial uncertainty, leading to imprecise data. Grey system theory, developed by Julong et al. (1989), deals with uncertain parameters in control problem systems, categorizing data as known (white), unknown (black), or partially known (grey). The central objective was to transform and analyze imprecise information, making it a valuable tool in fields like forecasting, decision-making, and control, where conventional approaches struggle with uncertainties and limited data. Over the years, grey system theory has evolved and expanded, finding applications in various domains, including economics, engineering, and environmental science.

Grey Linear Programming method was developed for managing municipal solid waste under uncertainty, utilizing a model with grey numbers to handle uncertain decisions (Huang et al., 1992). Lin et al. (2004) gave a comprehensive overview of grey systems theory, covering its foundation in the 1980s, fundamental concepts, and practical applications, emphasizing its relevance and efficacy across various domains. LiuSF et al. (2010) discussed in detail, the theory and practical application of grey information in various domains. Later the advancement in grey system research was discussed by Liu and Forrest (2010). The importance of grey system theory in numerous industries by defining grey number inverse operations, introducing an optimized operator to correct errors, and demonstrating its efficiency in computing operations with interval grey numbers (Wei et al., 2009).

Grey system theory has been used to a variety of practical challenges, including information system security (Shi and Deng, 2012), meteorological disaster risk analysis

and assessment (Gong and Forrest, 2014), grey data analysis: methods, model and applications (Liu et al., 2017), and risk assessment of construction projects (Zavadskas et al., 2010). The utilization of grey system theory has predominantly been observed in non-engineering sectors.

The general grey numbers share similarities with interval numbers in terms of definition and mathematical operations, a certain class of grey number called UGN, satisfies the physical laws (distributive law) that arises out of defining the grey arithmetic relations and contributes the theory free from dependency problem. Rao and Jin (2014) analysed the beams subjected coupled bending-torsional vibrations under uncertainties, employing various approaches. The universal grey system approach was used for coefficient derivation, while natural frequencies were determined using an interval analysis-based technique. The results were compared with the Monte Carlo simulations. Rao and Liu (2017) proposed UGT technique for the analysis of structural systems subjected to interval uncertainty and demonstrates computational feasibility through numerical examples when compared with the other interval techniques. The universal grey system approach is a viable methodology for the accurate analysis of structural and other engineering problems involving uncertain parameters that are described in terms of ranges or intervals. Rao and Wang (2019) performed uncertainty modeling in vibrating systems using approaches like interval and UGT. For response quantities predicted by UGT is better than the interval approach, which suffers by the dependency problem. Hybrid structural reliability analysis under multisource uncertainties based on UGT was studied (Yang et al., 2018). Where interval and fuzzy parameters are incorporated, and an effective solution to structural reliability analysis with random-interval-fuzzy hybrid parameters was developed. The proposed strategy yielded more conservative hybrid structural reliability results.

Alazwari and Rao (2019) used interval analysis and the universal grey theory to model the uncertainty in the macro mechanics of composite laminates by describing the primitive parameters as intervals. In addition, for comparison, a probabilistic strategy with plus/minus three standard deviations from the response mean is shown. UGT performed better in predicting the response. Rao and Wang (2019) performed interval parameter-based optimum design of structural components using graphical optimization and genetic algorithm. UGT is used for the analysis of optimization problem in order to avoid dependency problem of the interval method.

Nejadpak and Rao (2020) introduced universal grey number-based fuzzy analysis for heat transfer problems, demonstrating its superior efficiency and accuracy compared to interval-based fuzzy analysis, effectively reducing response parameter widths at each α - cut value of the fuzzy analysis. The influence of various error

intervals on the performance of the wiper structural system using the universal grey system Liang et al. (2021). UGT is a viable methodology for the accurate analysis of the uncertain structural system. The result obtained from the grey number theory will shrink too much, which is too conservative for engineering analyses. Further, Liu et al. (2021) in their study proposed an improved interval truncation method and improved grey number theory for safety analysis of aircraft landing gear. Alazwari and Rao (2022) presented the Universal Grey Number-Based Gaussian Elimination method for solving linear interval algebraic equations in large structures. The proposed method found to be computational efficient.

2.3 HIGH DIMENSIONAL MODEL REPRESENTATION

In structural analysis, the behavior of complex systems, such as mechanical system, structures, or bridges, is examined. These systems can be computationally demanding and time-consuming to simulate accurately, especially when numerous design factors, load situations, and uncertainties are taken into account. Metamodel or surrogate model is the simplified mathematical or computer model that approximates the behavior of such a complex system (Baran et al. (2017); Kleijnen (1987)). While performing the structural simulations or analyses, these surrogate models are employed to reduce the computational burden. Various types of surrogate models are commonly used, such as polynomial regression (Zhou et al., 2005), Gaussian processes (Wan et al., 2014), neural networks (Alam et al., 2004), and support vector machines (Pan and Dias, 2017), Kriging meta-models (Sudret 2012; Zhang et al. 2015; Zhao et al. 2015). The theories mentioned above are only suitable for basic models and not for complex, high-dimensional structural models due to their high computational demands. An alternative approach called high-dimensional model representation (HDMR) is a powerful method for approximating the complex model (Rabitz and Aliş, 1999). It was first introduced in the field of chemistry and later was widely used in structural reliability areas because of its simplicity and adaptability.

The HDMR is a tool for approximating the input and output relationships of complicated and computationally demanding models to build a function with hierarchical correlation expansions. To understand the hierarchy of correlations among the input variables, a set of non-parametric multivariate approximation functions was developed (Rabitz and Aliş, 1999). The inputs and outputs were ordered into a mapping strategy. Aliş and Rabitz (2001) presented the formulation of HDMR assuming that the data is randomly scattered throughout the domain of the output. The number of samples

necessary for representation to a particular tolerance under these conditions and the HDMR assumptions is independent of the dimensionality of the function, providing a feasible technique for high dimensional interpolation.

The HDMR is capable of developing a mathematical model by ordered mapping between inputs and outputs for a variety of well-defined physical systems. The HDMR approximation techniques are extremely helpful in many fields if they can accurately reflect the output at sufficiently low orders. ANOVA-HDMR and cut-HDMR are two specific HDMR expansions used to determine the component functions. ANOVA-HDMR evaluates component function contributions to output variance, whereas Cut-HDMR captures output in a variable space hyperplane via a reference point. Higher-order terms of cut-HDMR expansions are written as lower-order terms with monomial multipliers in a preconditioned HDMR approach based on monomials (Li et al., 2001b). In this case, extra input-output samples are needed since the first and second-order cut-HDMR correlation functions approximation, which avoid using higher-order terms, are insufficient.

HDMR can be applied for various purposes, including global uncertainty assessments, construction of computational models, identification of key variables, and quantitative risk assessments (Li et al., 2002). Sobol' (2003) introduced HDMR for approximating multivariable mathematical models and outlines criteria for evaluating the influence of input variables. Also introduced the cut-HDMR for model representation and emphasizes the importance of selecting quasi-random trial points and computing crude estimates to improve approximations.

Kaya et al. (2004) introduced a symbolic algebra-based computer program for calculating individual components of HDMR resolution and global sensitivity indices in multivariate functions. The program employs recursive procedures and efficiently stores intermediate calculations, although some areas, such as the transformation from sets to integers, may benefit from further enhancements, making it a valuable tool for HDMR research. Tunga and Demiralp (2006) addressed multivariate interpolation challenges using HDMR and introduced a Hybrid HDMR method, combining conventional HDMR and Factorized HDMR for improved handling of hybrid multivariate data.

The application of the HDMR approach to uncertainty analysis has increased recently due to its adaptability in capturing the relationship between inputs and outputs. A HDMR-based Response Surface Model is used to analyze the response of the structures when the uncertainties are expressed in terms of fuzzy membership functions Balu and Rao (2012a). Suggested methodology involves integrated finite element modeling with HDMR, using both implicit and explicit fuzzy analysis. The use of HDMR to approximate the fuzzy FE response quantity is proven to be computationally

less expensive. Balu and Rao (2012b) proposed efficient method for inverse reliability analysis using HDMR for limit state function approximation, reliability index update, and most probable point (MPP) estimation. Proposed approach is demonstrated through numerical examples and a parametric study, emphasizing accuracy and efficiency.

Balu and Rao (2014) proposed an efficient method for estimating structural reliability under mixed uncertain variables using HDMR, transformations, and fast Fourier transform. Accurate and computationally efficient failure probability estimates for problems with various distributions and numerous fuzzy and random variables were obtained. The stochastic natural frequency of angle ply composite plates is investigated using a random sampling-HDMR technique (Dey et al., 2015). Uncertainty in input variables (modulus of elasticity, orientation angle of fiber, density of material) is accounted for while performing global sensitivity analysis. Naveen and Balu (2019) developed a practical model updating method based on high-dimensional model representation (HDMR), demonstrating its effectiveness in improving accuracy while reducing computational effort in examples involving a simply supported beam and an existing bridge, thereby facilitating structural damage identification.

Kesava Rao and Balu (2019) proposed a computationally efficient HDMR-based method for cohesive parameter determination in mixed mode cohesive zone models (CZM) for bonded joints, accurately predicting failure mechanisms across different modes and applicable to various adhesive joints. Ji et al. (2022) proposed the Iterative Interval Analysis Method based on Kriging-HDMR. This method combines Kriging-HDMR for response meta-modeling with the Genetic Algorithm and Sequential Quadratic Programming for optimization, resulting in improved accuracy and efficiency in numerical cases while emphasizing lower sample requirements.

2.4 COMBINATORIAL OPTIMIZATION

Finding the best configuration / value among several options is the focus of optimization problems. Due to their practical importance, combinatorial optimization problems with uncertain input data have gained much attention. Typically, uncertainty is handled in two main ways: through the stochastic approach or worst-case analysis. The stochastic approach deals with uncertainty by using probability distribution techniques to model it. In the worst-case approach, scenarios are described deterministically, encompassing all potential situations. The goal is to find a solution that performs well across all scenarios, aiming for the best performance even in the most challenging scenario, hence the term worst-case performance. The minmax version of the worst-case approach aims to minimize and maximize the objective function value for a solution.

Averbakh (2001) work focuses on the complexity of a class of combinatorial optimization problems with uncertainty in weights. And proposed a polynomial algorithm for the minmax-regret version of the problem with interval representation of uncertainty. Mazyavkina et al. (2021) discussed exploration of Reinforcement Learning (RL) techniques to handle combinatorial optimization problems. In terms of these specific problems: Traditional Heuristics and their Limitations Traditional Heuristics. Akpan et al. (2001) studied Practical fuzzy finite element analysis of structures. Following an approximation of the response surface, combinatorial optimization is employed to identify binary combinations of fuzzy variables leading to extreme responses at a specified α -level. These extreme responses' actual values at the α -level are acquired by implementing the identified binary combinations of fuzzy variables within the finite element model.

Balu and Rao (2012a) adopted Combinatorial optimization in their study to identify the key binary combinations of fuzzy variables causing extreme responses, aiding the understanding of structural behavior under uncertainties. It efficiently determines critical scenarios impacting the structure, utilized for formulating closed-form expressions and deriving response bounds at specific confidence levels through HDMR. Rao and Berke (1997) adopted combinatorial approach to explore exhaustive combinations of extreme values within interval numbers, aiding in the solution of uncertain structural systems represented by interval equations, thereby addressing the inherent uncertainty in the analysis.

Muhanna et al. (2005) proposed the Penalty-Based Solution for the Interval, where the accuracy of the proposed method is evaluated with the results of the combinatorial optimization. Rao and Liu (2017) proposed a more accurate approach called a universal grey number theory for handling uncertain parameters in engineering problems. Finite-Element method is adopted to analyse the uncertainty of the system. The results of the proposed method as compared with combinatorial approach results treating it as exact. Alazwari and Rao (2022) utilized combinatorial method to solve systems of linear interval equations in uncertain structural and engineering systems, demanding substantial computational resources due to its requirement of 2^n analyses, where ' n ' represents the number of uncertain input quantities.

2.5 SUMMARY OF LITERATURE REVIEW

Performances of structures mainly depend upon the input variables, whose information is never certain, precise, and complete. If a range of information is only available, then interval analysis is best suited for the analysis. However, the accuracy of the results given by the interval analysis suffers dependency problem. Although several approaches, such as numerical truncation, parameterization of interval, use of subintervals within an interval and many more techniques have been suggested to limit the growth of the intervals of the results predicted. The computational efficiency becomes an issue in choosing the appropriate technique.

One such approach called UGT is computationally efficient (compared to the interval analysis) for the analysis of systems whose parameters are described as intervals. Hence, in the present study the UGT approach is adopted for the analysis of structural system subjected to interval uncertainty. Physical experiments and simulations performed during engineering design are the time consuming tasks, in addition with increase in design cost. High dimensional or large number of input variables makes the design problem complex. Hence, a metamodel techniques are generally adopted such as Response Surface Method, HDMR and so on. However, these techniques can also become too expensive as system dimensions increase. One such approach called HDMR is a powerful method in approximating high dimensional and expensive problems. Hence, HDMR model is preferred over other meta-models in the present study. There is the need for the account for epistemic uncertainty in the large dimensional system.

2.6 OBJECTIVES OF RESEARCH WORK

The main objectives of the proposed research work are as follows:

- i. To study the universal grey theory (UGT) for estimating the responses of structural systems and suggest any required modifications to UGT.
- ii. To develop a computationally efficient UGT in conjunction with the high dimensional model representation (HDMR).
- iii. To quantify the uncertainties of structural systems using HDMR based UGT.

2.7 SCOPE OF PRESENT RESEARCH

The scope of present work is as follows:

- i. To study the response of the structural elements subjected to interval uncertainty with traditional UGT and comparisons have been made with the conventional techniques such as the Interval method and the Combinatorial Method.
- ii. Necessary modifications are made in the traditional UGT arithmetic to develop a computationally efficient technique.
- iii. Explicit formulation of structural system response using HDMR approximation technique.
- iv. The obtained explicit response function is subjected to epistemic uncertainty and evaluating the response bounds using the UGT approach.
- v. To compare the results obtained from the proposed HDMR-UGT based uncertainty analysis with conventional methods like the interval method and combinatorial method.



CHAPTER 3

INTERVAL APPROACH

3.1 BACKGROUND

In many cases, there exists only a range of possible values for an uncertain quantity, with no available information about the likelihood of specific values within that range. Ferson and Ginzburg (1996) provided evidence that the probabilistic approach may not always yield accurate results in this specific situation. In such case the most suitable way to perform the uncertain analysis is by using the information available to us, which is the interval itself. The interval approach is one such approach which is widely accepted when dealing with the uncertain interval variable.

The interval approach makes the assumption that an uncertain variable is unknown but bounded and has lower and upper bounds (endpoints) in the absence of a given probability structure. Consequently, the interval representation of a variable x is given by

$$\mathbf{x} = [\underline{x}, \bar{x}] = \{x \in \mathbb{R} | \underline{x} \leq x \leq \bar{x}\} \quad (3.1)$$

where \underline{x} and \bar{x} represents lower and upper bound of the interval quantity x respectively. x is an arbitrary (generic) element in the interval \mathbf{x} . \mathbb{R} represents the collection of all real numbers. Moore (1966) introduced the interval approach to handle rounding and truncation errors in finite precision arithmetic. For instance, in a computer with five significant digits, the number $\sqrt{3}$ can be represented as an interval, such as $\sqrt{3} \in [1.7320, 1.7321]$, effectively capturing the rounding error. Interval arithmetic not only contains rounding errors but also enables efficient and reliable exploration of function behaviors across entire sets of arguments. Its inherent characteristics provide rigorous bounds for operation and function ranges, yielding results in intervals that must encompass the exact outcomes. Interval arithmetic is helpful in scientific computing because of its characteristics, which includes: Confining the impacts of rounding and truncation errors (Moore 1966), Restraining function ranges (Moore (1966); Zuhe et al. (1990)), Limiting error terms in Taylor's theorem (Neumaier (1990)), Facilitating global optimization (Hansen and Walster (2003)), Solving nonlinear systems.

In the mid-nineties, the interval approach emerged as a method for characterizing engineering system parameters. This approach is a straightforward and computationally efficient means of representing uncertainties exclusively through range information. For example, the manufacturing tolerance affects the thickness of a metal plate, which is specified as $t \pm \delta$ or in an interval form $[t - \delta; t + \delta] = [\underline{t}, \bar{t}]$. The distributed live load can be represented as an interval $[1.5, 2.0]$ kN/m² if it is known to range between 1.5 kN/m² and 2.0 kN/m². Information for defining bounds on possible ranges of these quantities can be found in experimental data, measurements, statistical analysis, and expert knowledge (Ferson and Hajagos, 2004). Intervals can be extended to the four basic operations of real arithmetic, namely addition (+), subtraction (-), multiplication (\times), and division (\div). The general rule governs operations $\circ \in \{+, -, \times, \div\}$ over intervals.

$$\mathbf{x} \circ \mathbf{y} = \{x \circ y | x \in \mathbf{x}, y \in \mathbf{y}\} \quad (3.2)$$

The set of all feasible solutions for $x \in \mathbf{x}$ and $y \in \mathbf{y}$ easily forms a closed interval (for 0 not in a denominator interval), and the bounds can be computed by

$$\mathbf{x} \circ \mathbf{y} = [\min(x \circ y), \max(x \circ y)] \text{ for } \circ \in \{+, -, \times, \div\} \quad (3.3)$$

The arithmetic operations of the interval approach are shown in the appendix A. An interval function refers to a function that produces interval values based on one or more interval arguments, effectively mapping the values of these interval arguments onto an interval range. For a real-valued function $f(x_1, \dots, x_n)$ an interval-valued function $\mathbf{f}(x_1, \dots, x_n)$ exhibits this property if: $\mathbf{f}(x_1, \dots, x_n) = f(x_1, \dots, x_n)$ for real arguments. In particular, each real variable x_i is replaced with an interval variable x_i , and each real operation is replaced with its equivalent interval arithmetic operation to obtain the natural interval extension of f .

3.2 DEPENDENCY PROBLEM

Interval evaluation of $\mathbf{f}(\mathbf{x})$ typically yields an enclosure or outer bound for the range of f , rather than the exact range. Achieving a sharp enclosure is desirable, but in some instances, interval arithmetic tends to be overly conservative, resulting in significantly wider bounds than the actual range, making it ineffectiveness. When evaluating the natural interval extension function for the arithmetic expression $f(x) = x^2 - x$, with \mathbf{x}

in the interval $[1, 3]$, the obtained result is:

$$\begin{aligned} f(x) &= x^2 - x = [1, 3]^2 - [1, 3]. \\ &= [1, 9] - [1, 3] = [-2, 8]. \end{aligned} \quad (3.4)$$

However, the exact bounds are $[0, 6]$. The computed interval function f contains the exact range. However, it overestimates the lower and upper bound. In interval computations, each interval variable is regarded as a different and independent variable. Following the computation of the sub-expression x^2 , interval arithmetic does not recognize the strong correlation between the values of x and x^2 . It implicitly assumes that all intervals are independent, treating $x^2 - x$ as if it is evaluating $x_1^2 - x_2$. This causes the overestimation in the results computed using interval arithmetic, as a result it is difficult to achieve the sharp enclosure for the complicated problems. The additional growth of interval width is known as the overestimation due to the dependence problem (Moore (1966); Hansen and Walster (2003)). To eliminate a dependency problem, it is sometimes possible to minimize the number of occurrences of each variable in the interval expression. In the above example, the dependency can be avoided by re-writing the interval functional expression as $g(x) = (x - 0.5)^2 - 0.25$, which when evaluated with interval arithmetic is equivalent to $f(x)$ evaluated in real arithmetic. Since the occurrence of interval variable is only once in $g(x)$, hence predicts the exact range for the expression.

$$\begin{aligned} g &= (x - 0.5)^2 - 0.25 \\ &= [1, 3]^2 - 0.25 = [1, 9] - 0.25 = [0, 6] \end{aligned} \quad (3.5)$$

The dependency problem in interval arithmetic results in the strict validity of only certain algebraic laws that apply to real numbers, while others maintain their validity in a more limited manner. There are two main laws governing the algebraic characteristics of interval operations (Zuhe et al., 1990).

- i) In interval arithmetic, two arithmetic expressions that are equivalent in real arithmetic remain equivalent when each variable appears only once on each side. For instance, the following laws hold good for the interval variable $x, y, z \in \mathbb{IR}$:

$$\begin{aligned} x + y &= y + x \\ xy &= yx \end{aligned} \quad (3.6)$$

- ii) If f and g are equivalent arithmetic expressions in real arithmetic, then in interval arithmetic, the relationship $f \subseteq g$ holds true when each variable appears more than once in f . For instance, the following laws holds good for the interval variable

$x, y, z \in \mathbb{IR}$:

$$\begin{aligned} x(y \pm z) &\subseteq xy \pm xz, \\ (x \pm y) &\subseteq xz \pm yz \text{ (subdistributivity)} \end{aligned} \quad (3.7)$$

$$\begin{aligned} x - y &\subseteq (x + z) - (y + z), \\ x/y &\subseteq (xz)/(yz) \text{ (subcancellation)} \end{aligned} \quad (3.8)$$

$$\begin{aligned} 0 &\in x - x, \\ 1 &\in x/x \text{ (subcancellation)} \end{aligned} \quad (3.9)$$

The dependency problem in interval analysis disrupts basic algebraic laws like distributivity and cancellation, making it difficult to calculate accurate results for complex interval computations. Effective interval analysis is based on eliminating this dependence because occurrence of an interval variable several times in a computation results in a much wider computed range than the actual one.

The satisfaction of the distributive property by interval method is shown with the numerical example. Let a , b and c be the interval variable, whose values are defined as: $a = [3, 4]$, $b = [-1, 2]$ and $c = [2, 3]$

$$\begin{aligned} P &= a(b + c) & Q &= ab + ac \\ &= [3, 4] \times ([-1, 2] + [2, 3]) & &= ([3, 4] \times [-1, 2]) + ([3, 4] \times [2, 3]) \\ &= [3, 20] & &= [2, 20] \end{aligned}$$

$$P \subseteq Q \text{ (subdistributivity)}$$

$$\begin{aligned} R &= a(b - c) & S &= ab - ac \\ &= [3, 4] \times ([-1, 2] - [2, 3]) & &= ([3, 4] \times [-1, 2]) - ([3, 4] \times [2, 3]) \\ &= [-16, 0] & &= [-16, 2] \end{aligned}$$

$$R \subseteq S \text{ (subdistributivity)}$$

$$\begin{aligned} J &= a - b & K &= (a + c) - (b + c) \\ &= [3, 4] - [-1, 2] & &= ([3, 4] + [2, 3]) - ([-1, 2] + [2, 3]) \\ &= [1, 5] & &= [0, 6] \end{aligned}$$

$$J \subseteq K \text{ (subcancellation)}$$

3.3 NUMERICAL EXAMPLES

3.3.1 Lamina Stiffness Element

A graphite-epoxy matrix lamina system is considered for the uncertainty analysis. Uncertainty in the material constituent is considered, the lamina stiffness K_{22} is calculated using following formula:

$$K_{22} = \frac{E_e (V_g E_{g11} + V_e E_e)}{(V_g E_{g11} + V_e E_e) \left(1 - \sqrt{V_g} \left(1 - \frac{E_e}{E_{g22}}\right)\right) - E_e (V_g \mu_{g12} + V_e \mu_e)^2} \quad (3.10)$$

where E , V , μ represents modulus of elasticity, volume fraction and poison's ratio. By considering $\pm 1\%$ variation in the material parameters whose mean values are given in Table 3.1. The bounds of stiffness of lamina system are calculated using interval method arithmetic operation. The bounds of stiffness element K_{22} using interval arithmetic is [4.97, 5.65] Gpa, which are wider than the results predicted by a deterministic analysis where stiffness is computed based on mean parameter values, the stiffness value found to be 5.30 GPa.

Table 3.1 Material properties of graphite and epoxy

Material	Properties
Graphite fiber	$V_g = 0.5$, $E_{g11} = 250$ GPa, $E_{g22} = 6.78$ GPa, $\mu_{g12} = 0.2$.
Epoxy matrix	$V_e = 0.5$, $E_e = 3.45$ GPa, $\mu_e = 0.35$

3.3.2 Axially Loaded Stepped Bar

The displacement analysis of two bar stepped system shown in Figure 3.1 subjected to axial load at node 2 and 3 is performed. Where E_i , A_i and L_i ($i = 1$ to 2) represents the young's modulus, cross-sectional area and length of the bar element respectively. K_1 and K_2 are the element stiffness of the bar element and is represented by

$$\begin{bmatrix} \frac{A_1 E_1}{L_1} + \frac{A_2 E_2}{L_2} & -\frac{A_2 E_2}{L_2} \\ -\frac{A_2 E_2}{L_2} & \frac{A_2 E_2}{L_2} \end{bmatrix} \begin{bmatrix} u_1 \\ u_2 \end{bmatrix} = \begin{bmatrix} P_1 \\ P_2 \end{bmatrix} \quad (3.11)$$

The displacement of node 2 and 3 is represented by u_1 and u_2 . Considering the uncertainty in stiffness element and are represented by $k_1 = [0.85, 1.01]$ and $k_2 = [1.85, 2.05]$. The axial load is applied at the node 2 and 3 are 0.5 and 1. Substituting the element stiffness and load value in Eq.(3.11) and is given by

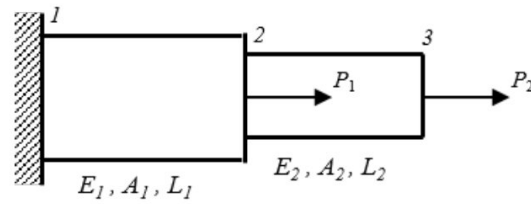


Figure 3.1 Two bar stepped system

$$\begin{bmatrix} [2.69, 3.06] & [-2.05, -1.85] \\ [-2.05, -1.85] & [1.85, 2.05] \end{bmatrix} \begin{bmatrix} u_1 \\ u_2 \end{bmatrix} = \begin{bmatrix} 0.5 \\ 1 \end{bmatrix} \quad (3.12)$$

the solution for the linear interval equation is found by using the *verifylss* function (Intlab) and the nodal displacement are obtained as

$$u_1 = [-0.60, 3.84]$$

$$u_2 = [-0.53, 4.79]$$

On the other hand, the exact nodal displacement bounds can be obtained by solving analytically. The inverse of the stiffness matrix is given by

$$K^{-1} = \begin{bmatrix} \frac{1}{k_1} & \frac{1}{k_1} \\ \frac{1}{k_1} & \frac{k_1+k_2}{k_1k_2} \end{bmatrix}$$

The displacements are therefore obtained as:

$$\begin{aligned} u_1 &= \frac{p_1}{k_1} + \frac{p_2}{k_1} = \frac{p_1 + p_2}{k_1} \\ &= \frac{1.5}{[0.85, 1.01]} = [1.485, 1.764] \\ u_2 &= \frac{p_1}{k_1} + \frac{(k_1 + k_2)p_2}{k_1k_2} = \frac{p_1 + p_2}{k_1} + \frac{p_2}{k_2} \\ &= \frac{1.5}{[0.85, 1.01]} + \frac{1}{[1.85, 2.05]} = [1.973, 2.305] \end{aligned}$$

To obtain the exact solution for the interval expression. In the above interval expression, the each interval variable is made to appear only once to avoid the dependency issue which usually occurs during the interval analysis. It is observed that the bounds predicted by the interval method are wider than the exact bonds.

3.4 COMBINATORIAL METHOD

The combinatorial technique is utilized in to determine the exact range for an arbitrary function denoted by f in Eq.(3.13), the parameters of which are represented by the ranges. The technique takes into account every possible combination of upper and lower limits of parameters and then determines the values for each possible combination of parameters based on those limits.

$$f = (\chi_1, \chi_2, \dots, \chi_n) \quad (3.13)$$

The variable χ_i denotes the interval parameter. By considering the minimum and maximum value of interval parameter χ_i

$$\chi_i = [\underset{-i}{\chi}, \bar{\chi}_i] = [\chi_i^{(1)}, \chi_i^{(2)}] \quad (3.14)$$

For all n parameters, different combinations of the extreme left and extreme right of the interval parameter are used to determine f , which is represented by

$$f = f(\chi_1^{(i)}, \chi_2^{(j)}, \dots, \chi_n^{(k)}); i = 1, 2; j = 1, 2; \dots, k = 1, 2 \quad (3.15)$$

Where f represents the value of $\chi_1, \chi_2, \chi_3, \dots, \chi_n$. This method is straightforward method to apply for the interval finite element method. However, as the number of interval parameters increases, the method becomes more time-consuming and computationally expensive (increases exponentially). Generally, 2^n analyses are required for the combinatorial method, where n is the number of uncertain quantities in the analysis. Usually, n is very large, in most practical systems.



CHAPTER 4

GREY THEORY

4.1 BACKGROUND

Generally the available system information tends to contain various kinds of uncertainty and noise. Along with the development of science and technology and the progress of mankind, our understanding of uncertainties of systems has been gradually deepened and the research of uncertain systems has reached a new height. Over the time various theories and methodologies of unascertained systems have been developed. For instance, Zadeh (1965) established fuzzy mathematics, and Polyak and Nazin (2004) advanced rough set theory.

Grey system theory is a mathematical framework designed to tackle systems characterized by uncertain parameters. In the natural world, uncertain systems with small samples and poor information exist commonly. This theory classifies data into three distinct categories: known (white), unknown (black), and partially known (grey). The central objective is to transform and analyze imprecise information, making it a valuable tool in fields like forecasting, decision-making, and control, where conventional approaches struggle with uncertainties and limited data. Over the years, grey system theory has evolved and expanded, finding applications in various domains, including economics, engineering, and environmental science. Its adaptability and ability to extract insights from ambiguous data make it a robust analytical tool in the uncertain world.

There are four possible cases that can arise in situations involving incomplete system information:

- i. The available information about the parameter (element) is incomplete;
- ii. The available information about the system is incomplete;
- iii. The information about the boundary of the system is incomplete; and
- iv. The data about the behavior of system is incomplete.

Being *grey* simply means having *incomplete information*.

4.2 GREY NUMBER

A grey number is a term used to describe a number when its exact value is unknown, and it is represented as a single value rather than a range. The grey number is the fundamental unit of the grey systems. In practical scenarios, a grey number refers to an uncertain number that takes values within an interval or a general set of numbers. The symbol \otimes is generally used to represent the grey number. Grey numbers can be only with the lower bound i.e., $\otimes \in [\underline{x}, \infty)$ or $\otimes(\underline{x})$ Grey numbers with only upper bound i.e., $\otimes \in (-\infty, \bar{x}]$ or $\otimes(\bar{x})$. In interval grey numbers that have clearly defined upper and lower bounds i.e., $\otimes \in [\underline{x}, \bar{x}]$. In this present study, we only deal with the interval grey numbers. Which is expressed as

$$\otimes \in [\underline{x}, \bar{x}] = \{t \mid \underline{x} \leq t \leq \bar{x}\} \quad (4.1)$$

4.3 UNIVERSAL GREY NUMBER THEORY

In the region $U \in \mathbb{R}$, where \mathbb{R} is the set of real number. The representation of universal grey number set for \mathbb{R} is $U_g(\mathbb{R})$, and the element of $U_g(\mathbb{R})$ is termed as universal grey number (UGN) is defined as

$$U_g = (x_0, [x_1, x_2]) \text{ where } x_0, x_1, x_2 \in \mathbb{R} \quad (4.2)$$

where x_0 is the observation value, $[x_1, x_2]$ is the grey information part of x_0 . The zero element and unit element of $U_g(\mathbb{R})$ are $U_g^{(0)} = (0, [0, 0])$ and $U_g^{(1)} = (1, [1, 1])$ respectively. The UGN whose observation part is zero but whose information part is not zero, it is referred as $U_{g'}$ and given the term subzero unit. The zero unit and subzero unit are referred to collectively as the universal zero unit, denoted as $g'(0)$. The UGN is a certain class of grey numbers that satisfies the physical laws (distributive law) that arise out of defining the grey arithmetic relations and contributes the theory free from dependency problem. According to the basic concept of UGN, the lowest and highest trust levels can be represented by x_1 and x_2 of $(x_0, [x_1, x_2])$. Thus, an interval number can be used to define a UGN when and is represented as

$$(x_0, [x_1, x_2]) = [x_0x_1, x_0x_2] \quad (4.3)$$

Normalization of the upper bound is done while performing the basic arithmetic operation to avoid the dependency problem. Hence, the UGN is further defined as

$$\left(x_0x_2, \left[\frac{x_0x_1}{x_0x_2}, 1 \right] \right) = \left(\bar{x}, \left[\frac{x}{\bar{x}}, 1 \right] \right) \quad (4.4)$$

where \underline{x} and \bar{x} represents lower bound and upper bound. Basic arithmetic relation operation for the UGN's are defined in Appendix A. The computational effort required in the combinatorial optimization is 2^n times the deterministic analyses (where n is the number of interval variables), while in the UGT, it is a single analysis.

Advantage of UGT

- i. Simple approach to carry-out the computation.
- ii. Results predicted are nearer to the exact range irrespective of multiple occurrence of same interval quantity.
- iii. Does not violate distributive laws.
- iv. Computational effort is less when compared with the combinatorial optimization.

Considering same example as in the earlier case of interval approach for the functional evaluation $f(x) = x^2 - x$ using UGT. The interval variable $x = [\underline{x}, \bar{x}] = [1, 3]$ is re-written in the form of UGN as $x = (\bar{x}, [\frac{x}{\bar{x}}, 1]) = x = (3, [\frac{1}{3}, 1])$.

$$\begin{aligned} f(x) = x^2 - x &= \left(3, \left[\frac{1}{3}, 1 \right] \right) \times \left(3, \left[\frac{1}{3}, 1 \right] \right) - \left(3, \left[\frac{1}{3}, 1 \right] \right) \\ &= \left(6, \left[\frac{0}{6}, 1 \right] \right) = [0, 6] \end{aligned} \quad (4.5)$$

which is the exact solution as represented in section 3.2. Therefore universal grey system provides better results when compared to the interval analysis.

Universal Grey Number based Gaussian elimination method

This flowchart emphasizes the unique considerations required when working with UGNs, such as handling uncertainties and maintaining consistency with grey number arithmetic during Gaussian elimination.

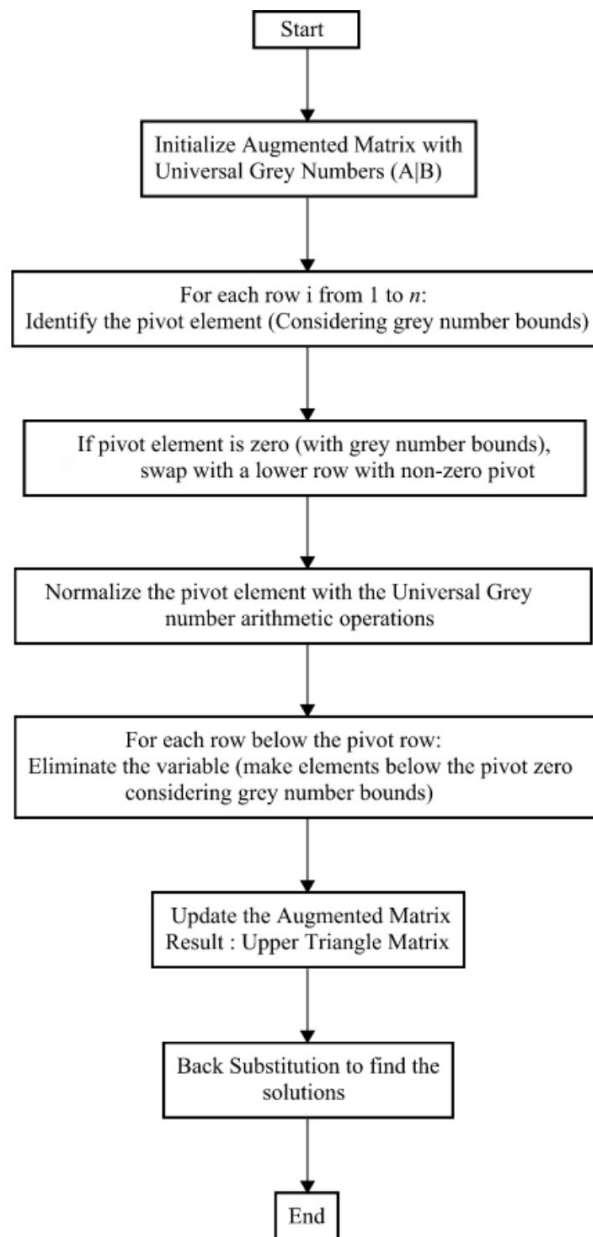


Figure 4.1 Universal Grey number based Gaussian elimination Procedure

4.3.1 Example : Lamina Stiffness Element

A graphite-epoxy matrix lamina system whose stiffness is considered for the uncertainty analysis. Uncertainty in the material constituent is considered, the lamina stiffness K_{22} is calculated using following formula:

$$K_{22} = \frac{E_e (V_g E_{g_{11}} + V_e E_e)}{(V_g E_{g_{11}} + V_e E_e) \left(1 - \sqrt{V_g} \left(1 - \frac{E_e}{E_{g_{22}}}\right)\right) - E_e (V_g \mu_{g_{12}} + V_e \mu_e)^2} \quad (4.6)$$

where E , V , μ represents modulus of elasticity, volume fraction and poisson's ratio. By considering $\pm 1\%$ variation in the material parameters whose mean values are given in Table 3.1. The bound of stiffness of lamina system is calculated using UGT and interval analysis using their respective arithmetic operation. The Eq. (4.6) is re-written in the form of UGN and is expressed as

$$K_{22} = [a, (b, 1)] \quad (4.7)$$

$$\text{where } a = \frac{(\overline{V_g \times E_{g11}} + \overline{V_e \times E_e}) \times \overline{E_e}}{(\overline{V_g \times E_{g11}} + \overline{V_e \times E_e}) \left(\frac{E_{g22} - (E_{g22} - E_e) \sqrt{V_g}}{E_{g22}} \right) - (\overline{V_g \times \mu_{g12}} + \overline{V_e \times \mu_e})^2 \times \overline{E_e}}$$

$$b = \frac{\left[(\overline{V_g \times E_{g11}} + \overline{V_e \times E_e}) \times \left(\frac{E_{g22} - (E_{g22} - E_e) \sqrt{V_g}}{E_{g22}} \right) - (\overline{V_g \times \mu_{g12}} + \overline{V_e \times \mu_e})^2 \times \overline{E_e} \right] (\overline{V_g \times E_{g11}} + \overline{V_e \times E_e}) \times \overline{E_e}}{\left[(\overline{V_g \times E_{g11}} + \overline{V_e \times E_e}) \left(\frac{E_{g22} - (E_{g22} - E_e) \sqrt{V_g}}{E_{g22}} \right) - (\overline{V_g \times \mu_{g12}} + \overline{V_e \times \mu_e})^2 \times \overline{E_e} \right] (\overline{V_g \times E_{g11}} + \overline{V_e \times E_e}) \times \overline{E_e}}$$

The bounds of stiffness element K_{22} using UGT was found to be [5.03, 5.58] Gpa, however, the bounds predicted by interval arithmetic was [4.97, 5.65] Gpa, which are wider than the results predicted by UGT. Conversely, in a deterministic analysis where stiffness is computed based on mean parameter values, the stiffness value found to be 5.30 GPa.

4.3.2 Example : Three Bar System

The three bar stress system made up with steel, aluminium and copper is subjected to axial load as shown in Figure 4.2. A static analysis is performed considering the uncertainty in its material, geometry and load parameters. It is assumed that the fundamental input parameters, such as the elastic moduli, the cross-sectional areas, and the applied load, will lie within certain intervals or ranges (written in the form of UGN).

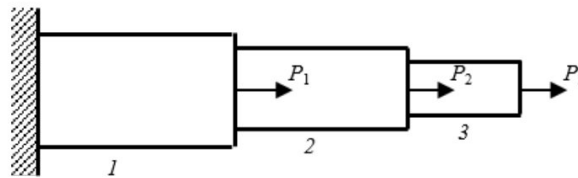


Figure 4.2 Three bar system

Modulus of elasticity: $E_{ugn(i)} \in \left(\overline{E_i}, \left[\frac{E_i}{\overline{E_i}}, 1 \right] \right)$, $i = 1, 2, 3$.

Cross-sectional areas: $A_{ugn(i)} \in \left(\overline{A_i}, \left[\frac{A_i}{\overline{A_i}}, 1 \right] \right)$, $i = 1, 2, 3$.

Length : $L_{ugn(i)} \in \left(\bar{L}_i, \left[\frac{L_i}{\bar{L}_i}, 1 \right] \right)$, $i = 1, 2, 3$.

Applied load : $P_{ugn(i)} \in \left(\bar{P}_i, \left[\frac{P_i}{\bar{P}_i}, 1 \right] \right)$, $i = 1, 2, 3$.

The numerical computations are made considering variation in input parameters as follows $\pm 1\%$ in L_1, L_2, L_3 , $\pm 2\%$ in A_1, A_2, A_3 , $\pm 2\%$ in P_1 and P_3 , $\pm 3\%$ in E_1, E_2, E_3 . Where, $L_1 = 700$ mm, $L_2 = 900$ mm, and $L_3 = 500$ mm, $A_1 = 1600$ mm², $A_2 = 1100$ mm², $A_3 = 600$ mm², $P_1 = 1200$ kN, $P_2 = 0$ kN, $P_3 = 1600$ kN. The element stiffness matrix is represented as

$$[k_i] = \begin{bmatrix} \frac{A_{ugn(i)}E_{ugn(i)}}{L_{ugn(i)}} & -\frac{A_{ugn(i)}E_{ugn(i)}}{L_{ugn(i)}} \\ -\frac{A_{ugn(i)}E_{ugn(i)}}{L_{ugn(i)}} & \frac{A_{ugn(i)}E_{ugn(i)}}{L_{ugn(i)}} \end{bmatrix}_{i=1,2,3} \quad (4.8)$$

The global stiffness matrix is developed, and upon applying boundary conditions the matrix is reduced to

$$[K] = \begin{bmatrix} \frac{A_{ugn(1)}E_{ugn(1)}}{L_{ugn(1)}} + \frac{A_{ugn(2)}E_{ugn(2)}}{L_{ugn(2)}} & -\frac{A_{ugn(2)}E_{ugn(2)}}{L_{ugn(2)}} & 0 \\ -\frac{A_{ugn(2)}E_{ugn(2)}}{L_{ugn(2)}} & \frac{A_{ugn(2)}E_{ugn(2)}}{L_{ugn(2)}} + \frac{A_{ugn(3)}E_{ugn(3)}}{L_{ugn(3)}} & -\frac{A_{ugn(3)}E_{ugn(3)}}{L_{ugn(3)}} \\ 0 & -\frac{A_{ugn(3)}E_{ugn(3)}}{L_{ugn(3)}} & \frac{A_{ugn(3)}E_{ugn(3)}}{L_{ugn(3)}} \end{bmatrix} \quad (4.9)$$

$$[K] = \begin{bmatrix} [541874, 587018] & [-87723, -80977] & [0, 0] \\ [-87723, -80977] & [230768, 249994] & [-162270, -149791] \\ [0, 0] & [-162270, -149791] & [149791, 162270] \end{bmatrix} \quad (4.10)$$

The above matrix is re-written in the form of the augmented matrix, which is represented as

$$[Aug] = \begin{bmatrix} [541874, 587018] & [-87723, -80977] & [0, 0] & : [1176, 1224] \\ [-87723, -80977] & [230768, 249994] & [-162270, -149791] & : [0, 0] \\ [0, 0] & [-162270, -149791] & [149791, 162270] & : [1568, 1632] \end{bmatrix} \quad (4.11)$$

The universal grey number-based Gaussian elimination method is developed to reduce augmented matrix to upper triangular matrix. The MATLAB code for universal grey number-based Gauss elimination is represented in Appendix A.

$$[Aug] = \begin{bmatrix} [541874, 587018] & [-87723, -80977] & [0, 0] & : [1176, 1224] \\ [0, 0] & [218667, 236884] & [-162270, -149791] & : [175.74, 182.91] \\ [0, 0] & [0, 0] & [47181, 51112] & : [1688.39, 1757.30] \end{bmatrix} \quad (4.12)$$

By using the reduced augmented matrix the nodal displacements for the three bar system is obtained by the back substitution technique.

$$u_3 \in \left(\frac{\overline{Aug}_{34}^{(2)}, \left[\frac{Aug_{34}^{(2)}}{\overline{Aug}_{34}^{(2)}}, 1 \right]}{\overline{Aug}_{33}^{(2)}, \left[\frac{Aug_{33}^{(2)}}{\overline{Aug}_{33}^{(2)}}, 1 \right]} \right) \in \left(\frac{Aug_{34}^{(2)}, \left[\overline{Aug}_{34}^{(2)} \times Aug_{33}^{(2)}, 1 \right]}{Aug_{33}^{(2)}, \left[\overline{Aug}_{34}^{(2)} \times Aug_{33}^{(2)}, 1 \right]} \right), \quad (4.13)$$

$$u_2 = \left(\frac{\overline{Aug}_{24}^{(2)} + \left(\overline{u_3} \left| \overline{Aug}_{24}^{(2)} \right| \right)}{Aug_{22}^{(2)}}, \left[\frac{\left[Aug_{24}^{(2)} + \left(\overline{u_3} \left| \overline{Aug}_{23}^{(2)} \right| \right) \right] \overline{Aug}_{22}^{(2)}}{\left[\overline{Aug}_{24}^{(2)} + \left(\overline{u_3} \left| \overline{Aug}_{23}^{(2)} \right| \right) \right] \overline{Aug}_{22}^{(2)}}, 1 \right] \right)$$

$u_3 \in 0.0357 \times [0.96078, 1] \in [0.0343, 0.0357]$ mm and $u_2 \in 0.02528 \times [0.9632, 1]$. The bounds of the u_1 are similarly determined and found as $u_1 \in 0.00586 \times [0.98976, 1] = [0.00580, 0.00586]$. By utilizing the above displacements the stresses in the bar are determined as follows:

$$\sigma_1 = \left(\frac{u_1 E_{ugn(1)}}{L_{ugn(1)}} \right) \in [1.7077, 1.7939] \quad (4.14)$$

$$\sigma_2 = \left(\frac{(u_2 - u_1) \times E_{ugn(2)}}{L_{ugn(2)}} \right) \in [1.3931, 1.5184] \quad (4.15)$$

$$\sigma_3 = \left(\frac{(u_3 - u_2) \times E_{ugn(3)}}{L_{ugn(3)}} \right) \in [2.5540, 2.7839] \quad (4.16)$$

Deterministic analysis of the 3 bar system is carried out considering the crisp value of the above input variables. The element stiffness matrix is represented as

$$[k_i] = \begin{pmatrix} \frac{A_i E_i}{L_i} & -\frac{A_i E_i}{L_i} \\ -\frac{A_i E_i}{L_i} & \frac{A_i E_i}{L_i} \end{pmatrix}_{i=1,2,3} \quad (4.17)$$

The global stiffness matrix is developed, and upon applying boundary conditions the matrix is reduced to

$$[K] = \begin{bmatrix} \frac{A_1 E_1}{L_1} + \frac{A_2 E_2}{L_2} & -\frac{A_2 E_2}{L_2} & 0 \\ -\frac{A_2 E_2}{L_2} & \frac{A_2 E_2}{L_2} + \frac{A_3 E_3}{L_3} & -\frac{A_3 E_3}{L_3} \\ 0 & -\frac{A_3 E_3}{L_3} & \frac{A_3 E_3}{L_3} \end{bmatrix} \quad (4.18)$$

$$[K] = \begin{bmatrix} 564333 & -84333 & 0 \\ -84333 & 240333 & -156000 \\ 0 & -156000 & 156000 \end{bmatrix} \quad (4.19)$$

The above matrix is re-written in the form of the augmented matrix, which is represented as

$$[Aug] = \begin{bmatrix} 564333.333 & -84333.333 & 0 & : & 1200 \\ -84333.333 & 240333.333 & -156000 & : & 0 \\ 0 & -156000 & 156000 & : & 1600 \end{bmatrix} \quad (4.20)$$

The Gaussian elimination method is used to reduce augmented matrix to upper triangular matrix and is represented as

$$[Aug] = \begin{bmatrix} 564333.333 & -84333.333 & 0 & : & 1200 \\ 0 & 227730.655 & -156000 & : & 179.326 \\ 0 & 0 & 49136.916 & : & 1722.842 \end{bmatrix} \quad (4.21)$$

By using the reduced augmented matrix the nodal displacements for the three bar system is obtained by the back substitution technique. Calculating u_3 the nodal displacements using the back substitution technique.

$$u_3 \in \frac{1722.842}{49136.916} \in 0.03506 \quad (4.22)$$

$$u_2 \in \frac{179.326 - (u_3 \times -156000)}{227730.655} \in 0.02480 \quad (4.23)$$

$$u_1 \in \frac{1200 - (u_2 \times -84333.333)}{564333.333} \in 0.00583 \quad (4.24)$$

$$\sigma_1 = \left(\frac{u_1 E_1}{L_1} \right) \in 1.7499 \quad (4.25)$$

$$\sigma_2 = \left(\frac{(u_2 - u_1) \times E_2}{L_2} \right) \in 1.4545 \quad (4.26)$$

$$\sigma_3 = \left(\frac{(u_3 - u_2) \times E_3}{L_3} \right) \in 2.6666 \quad (4.27)$$

Similarly, Interval analysis is carried out for the above 3 bar system using interval arithmetic operation. The stresses in the bar calculated by different methods are presented in Table 4.1.

Table 4.1 Stresses in different element

Methods	σ_1 N/mm ²	σ_2 N/mm ²	σ_3 N/mm ²
Interval method	[1.2134, 3.1413]	[0.4376, 3.5099]	[-6.4316, 12.7462]
Deterministic method	1.7499	1.4545	2.6666
Universal grey theory	[1.7077, 1.7939]	[1.3931, 1.5184]	[2.5540, 2.7839]

4.3.3 Example : Nonlinear Explicit Function

An explicit nonlinear response function (Balu and Rao, 2012a) is represented as

$$f(x) = 16x_1^4 - 96x_1^3 + 216x_1^2 - 216x_1 - 64x_2^3 + 240x_2^2 - 300x_2 + 36x_3^2 - 84x_3 - 8x_4 + 264 \quad (4.28)$$

Numerical computation are made using the percentage variation from 1% to 10 % about the mean data ($x_1^0 = 2$, $x_2^0 = 5$, $x_3^0 = 3$, and $x_4^0 = 15$). The variation in the input paramaters are introduced through δ , which allows the assumed range of unknown parameters to be determined. The interval parameters are written in the form of UGN as shown in Eq. (4.29). The interval and universal grey number arithmetic operations are used to evaluate the explicit nonlinear response function. The values of evaluated response function for percentage variation in the input parameters are represented in Table 4.2. The graphical variation of response function for the input percentage variation is shown in Figure 4.3.

$$x_i = \left(x_i^0 (1 + \delta), \left[\frac{x_i^0 (1 - \delta)}{x_i^0 (1 + \delta)}, 1 \right] \right)_{i=1 \text{ to } 4} \quad (4.29)$$

Table 4.2 Response of explicit nonlinear function

δ	Combinatorial optimization	Universal grey theory	Interval analysis
0	-2980.000	-2980.000	-2980.000
2	[-3297.696, -2674.832]	[-3230.016, -2742.511]	[-3835.776, -2136.752]
4	[-3628.352, -2381.757]	[-3492.992, -2517.117]	[-4704.513, -1305.598]
6	[-3972.402, -2100.343]	[-3769.361, -2303.383]	[-5586.642, -486.103]
8	[-4330.273, -1830.153]	[-4059.553, -2100.873]	[-6482.594, 322.167]
10	[-4702.398, -1570.750]	[-4363.998, -1909.150]	[-7392.798, 1119.650]

For the maximum percentage variation in the input variable, the response predicted by the UGT differ by 7.19 % and 21.54 % in its lower and upper bound when compared with the combinatorial optimization, whereas the interval method results differ by 57.21 % and 171.28 %. As the percentage of variation in input parameter increases, the deviation in results are observed by both the methods. However, deviation observed are less in UGT than interval method. At lower δ value, the UGT results converges with the combinatorial optimization.

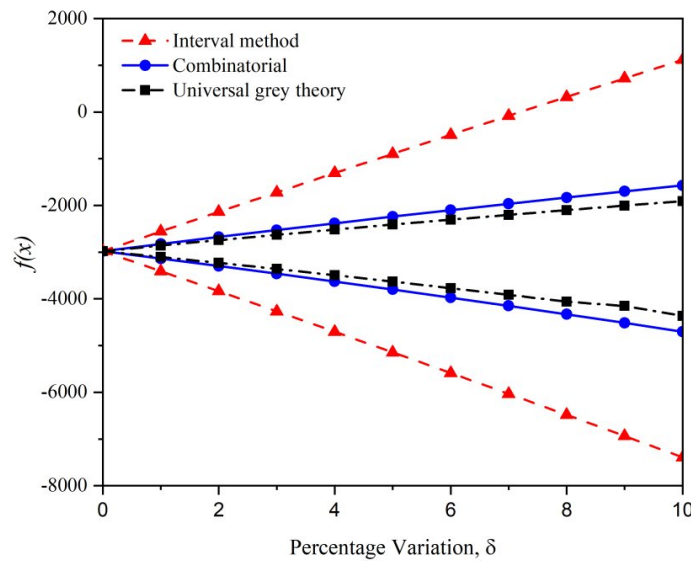


Figure 4.3 Response of explicit function

4.3.4 Example : Vibration Analysis of Spring Mass Damper System

Response of spring mass damper system subjected harmonic excitation is shown in Figure 4.4. Uncertainty analysis of the system is performed considering the uncertainty in the system parameters. The numerical computations are made considering variation in input mean parameters as follows $\pm 1\%$ in k^0 (stiffness, 12000 k/m), $\pm 4\%$ in m^0 (mass, 45kg). The damping ratio (ζ), whose mean value is assumed to vary between 0 and 0.5, is used to define the range of c ($c = 146.96$ N-s/m for $\zeta = 0.1$). ω is the base excitation frequency varies as interval with $\underline{\omega}$ being the lower bound and $\bar{\omega}$ be the upper bound. The natural frequency of the vibrating system for the considered mean value is given by $\omega_n = \sqrt{\frac{k}{m}} = 16.329$ rad/s. The ratio of average excitation frequency and natural frequency is defined by $r_m = \left(\frac{\omega + \bar{\omega}}{\omega_n + \bar{\omega}_n}\right)$ as mean frequency ratio. The equation of motion of the spring mass damper system is represented as

$$m\ddot{x} + c(\dot{x} - \dot{y}) + k(x - y) = 0 \quad (4.30)$$

where $y(t) = y \sin(\omega t)$ denotes the base harmonic motion at frequency ω . Upon simplification the Eq. (4.30) can be written as

$$m\ddot{x} + c\dot{x} + kx = ky + c\dot{y} = kY \sin \omega t + c\omega Y \cos \omega t = A \sin(\omega t - \alpha) \quad (4.31)$$

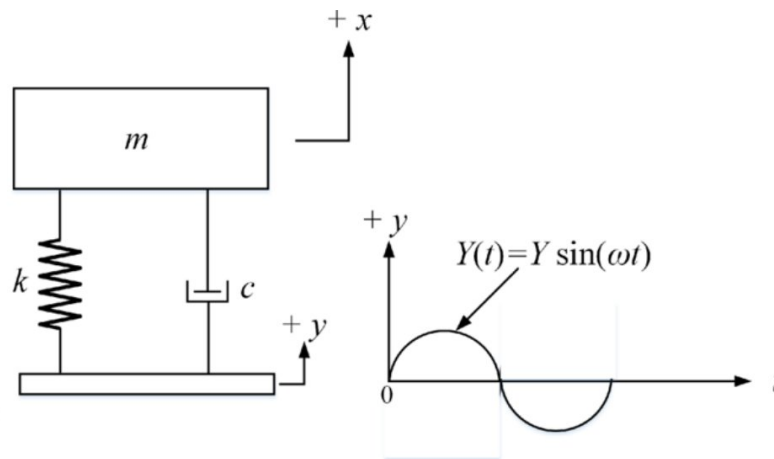


Figure 4.4 A spring mass damper system

The steady state solution for Eq. (4.31) is expressed in terms of amplitude mass motion and phase angle and is given by

$$x_p(x) = X \sin(\omega t - \phi) \quad (4.32)$$

The amplitude of mass motion is of importance in this system. The displacement transmissibility of the vibrating system is determined as

$$T_d = \frac{X}{Y} = \left[\frac{k^2 + (c\omega)^2}{(k - m\omega^2)^2 + (c\omega)^2} \right]^{\frac{1}{2}} \quad (4.33)$$

The variation in the displacement transmissibility ratio with the mean frequency ratio is studied using interval method and UGT analysis. Considering uncertainty in the parameters, each uncertain parameters are written in the interval and UGN form during interval and UGT analysis for the. Deterministic analysis is also performed to compare the results of above two approach considering the mean value of the uncertain parameters. The variation in bounds of displacement transmissibility with the mean frequency ratio r_m ranging from 0 to 3 is plotted in Figures 4.5, 4.6 and 4.7 for the mean value of $\zeta = 0.1, 0.3$ and 0.5 . And their values are depicted in Tables 4.3, 4.4 and 4.5 respectively.

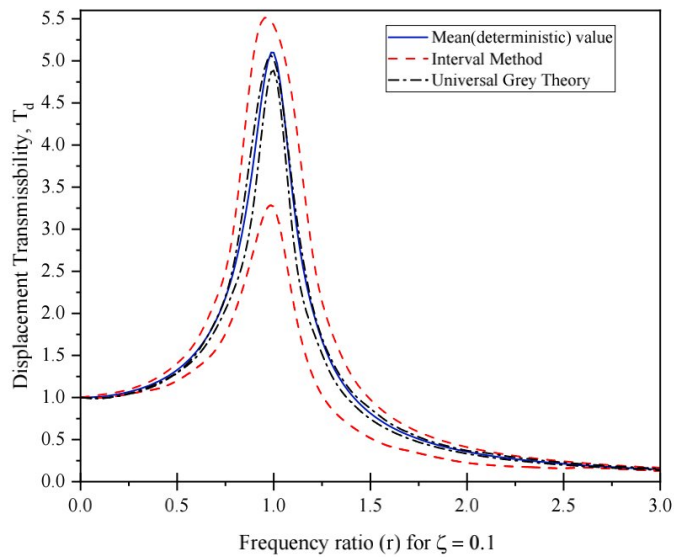


Figure 4.5 Variation of displacement transmissibility for $\zeta = 0.1$

Table 4.3 Variation of displacement transmissibility (Deterministic analysis)

mean ratio	$\zeta = 0$	$\zeta = 0.1$	$\zeta = 0.3$	$\zeta = 0.5$
0	1	1	1	1
0.5	1.333	1.328	1.294	1.240
1	-	5.099	1.943	1.414
1.5	0.799	0.812	0.873	0.923
2	0.333	0.355	0.483	0.620
2.5	0.190	0.212	0.330	0.463
3	0.125	0.145	0.251	0.370

It is observed that for the value of r ranging from 0.5 to 3, the displacement transmissibility T_d bounds predicted by the interval method is wider than that of UGT. The upper bounds obtained from the UGT for non-zero r values are generally anticipated to be higher than the values calculated using deterministic analysis for any set of r and ζ combination. The results when compared with the deterministic analysis, the maximum percentage variation in the output response predicted by the interval method is 14.52% and 17.27 % for $\zeta = 0.3$; and 13.26% and 15.45 % for $\zeta = 0.5$ in its lower and upper bounds. On the other hand, the variation in the displacement transmissibility predicted by UGT is 3.19% and 8.25 % for $\zeta = 0.3$; and 4.68 % and 4.85 % for $\zeta = 0.5$. It is evident that the anticipated variation in the displacement

transmissibility are excessively significant, leading to the conclusion that the results obtained from interval analysis do not seem to align with accuracy when compared to those derived from the universal grey system theory.

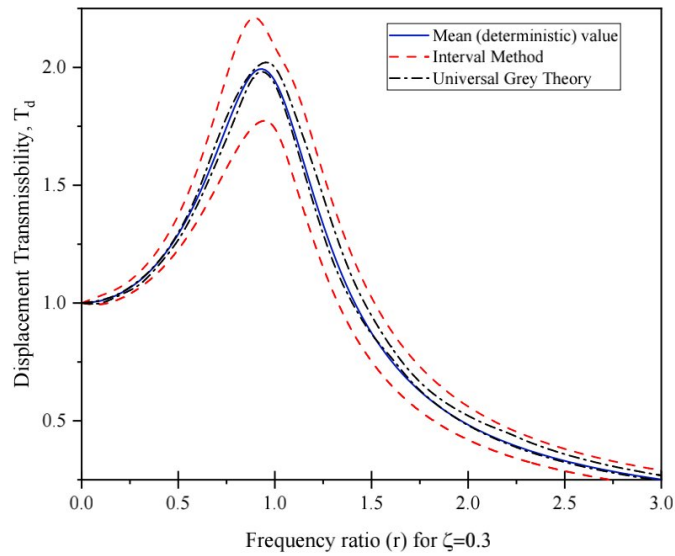


Figure 4.6 Variation of transmissibility for $\zeta = 0.3$

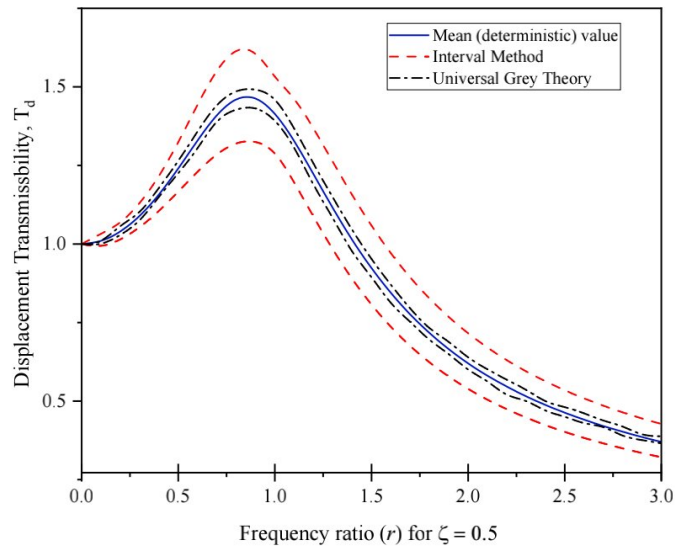


Figure 4.7 Variation of transmissibility for $\zeta = 0.5$

Table 4.4 Variation of displacement transmissibility (Interval method)

r	$\zeta = 0$	$\zeta = 0.1$	$\zeta = 0.3$	$\zeta = 0.5$
0	1	1	1	1
0.5	[1.2667, 1.4098]	[1.1890, 1.4050]	[1.2225, 1.3720]	[1.1661, 1.3240]
1	–	[3.6890, 5.4231]	[1.7874, 2.0865]	[1.2996, 1.5326]
1.5	[0.6726, 0.9655]	[0.5089, 0.9757]	[0.7479, 1.0237]	[0.8050, 1.0584]
2	[0.2923, 0.3818]	[0.2210, 0.4093]	[0.4180, 0.5608]	[0.5379, 0.7158]
2.5	[0.1692, 0.2149]	[0.2866, 0.3811]	[1.2667, 1.4098]	[0.4017, 0.5343]
3	[0.1117, 0.1400]	[0.1286, 0.1645]	[0.2183, 0.2892]	[0.3212, 0.4268]

Table 4.5 Variation of displacement transmissibility (UGT)

r	$\zeta = 0$	$\zeta = 0.1$	$\zeta = 0.3$	$\zeta = 0.5$
0	1	1	1	1
0.5	[1.3343, 1.3345]	[1.2934, 1.2979]	[1.2250, 1.2645]	[1.1661, 1.3240]
1	[16.159, 17.16]	[4.8840, 5.0268]	[1.9280, 2.0003]	[1.3918, 1.4589]
1.5	[0.7198, 0.8938]	[0.7452, 0.8678]	[0.8943, 0.9523]	[0.8050, 1.0584]
2	[0.3079, 0.3615]	[0.3323, 0.3694]	[0.4810, 0.52149]	[0.6002, 0.6391]
2.5	[0.1774, 0.2074]	[0.1994, 0.2273]	[0.3246, 0.3589]	[0.4500, 0.4805]
3	[0.1168, 0.1338]	[0.1373, 0.1547]	[0.2456, 0.26843]	[0.36598, 0.3881]

In the above sections details explanation of traditional UGT is carried out. A few numerical examples are solved. In the next section the major contribution of present work is explained, where the ineffectiveness of traditional UGT in certain cases are explained and necessary modifications are suggested.

4.4 IMPROVED UNIVERSAL GREY NUMBER

The definition of UGN and basic arithmetic relation associated with it satisfies the distributive property. However, the traditional UGT is ineffective in certain conditions like case (i): if the uncertain quantity ($x \in [\underline{x}, \bar{x}]$) having negative values in its upper and lower bounds (i.e., $|\bar{x}| \leq |\underline{x}|$, \underline{x} and $\bar{x} < 0$). Case (ii): uncertain quantity having negative value in its lower and positive value in its upper bound (if the magnitude of the lower bound is greater than upper bound i.e., $|\bar{x}| \leq |\underline{x}|$, $\underline{x} < 0$ and $\bar{x} > 0$). It does not satisfy the basic definition of UGN (i.e., $|\underline{x}| \leq |\bar{x}|$, $|\underline{y}| \leq |\bar{y}|$). Hence, for the case (i): The definition of UNG needs to be modified to reflect the inequality, in order to be fulfilled, the UGN representation needs to be written in the form of

$$x \in \left(|-x|, \left[\frac{|\bar{x}|}{|x|}, 1 \right] \right) \text{ and } y \in \left(|-y|, \left[\frac{|\bar{y}|}{|y|}, 1 \right] \right) \quad (4.34)$$

For the case (ii): The definition of UNG is modified to reflect the inequality, in order to be fulfilled (i.e., $|\bar{x}| \leq |x|, |\bar{y}| \leq |y|$), the UGN representation needs to be written in the form of

$$x \in \left(|-x|, \left[\frac{-\bar{x}}{|-x|}, 1 \right] \right) \text{ and } y \in \left(|y|, \left[\frac{-\bar{y}}{|y|}, 1 \right] \right) \quad (4.35)$$

where the arithmetic relations are developed to account for the negative sign and basic four arithmetic (+, -, ×, ÷) relations of UGN are defined using Intlab (a MATLAB toolbox for interval arithmetic (Rump, 1999), to perform rigorous error analysis of numerical computations implemented in MATLAB (The Mathworks, 2021). To check the fulfilment of the distributive property, two examples are solved using proposed universal grey arithmetic and general interval arithmetic. Example 1: Considering a uncertainty quantity with a negative value in its lower and upper bounds. Example 2: Considering a uncertainty quantity with negative in its lower bound and positive in its upper bound, magnitude of lower bound is greater than upper bound $|\bar{x}| \leq |x|$).

Example. 1

Let $x = [2, 4]$, $y = [-3, -1]$ and $z = [3, 8]$. x , y and z are re-written in the form of proposed UGN representation, i.e.,

$$x \in \left(4, \left[\frac{2}{4}, 1 \right] \right), y \in \left(|-3|, \left[\frac{|-1|}{|-3|}, 1 \right] \right) \text{ and } z \in \left(8, \left[\frac{3}{8}, 1 \right] \right)$$

negative sign is taken care during the arithmetic operations

Case (i)

$$\begin{aligned} A_I &= x \times (y + z) = [2, 4] \times ([-3, -1] + [3, 8]) = [0, 28] \\ B_I &= xy + xz = ([2, 4] \times [-3, -1]) + ([2, 4] \times [3, 8]) = [-6, 30] \\ A_U &= x \times (y + z) = \left(4, \left[\frac{2}{4}, 1 \right] \right) \times \left\{ - \left(|-3|, \left[\frac{|-1|}{|-3|}, 1 \right] \right) + \left(8, \left[\frac{3}{8}, 1 \right] \right) \right\} \\ &= \left(20, \left[\frac{4}{20}, 1 \right] \right) = [4, 20] \\ B_U &= xy + xz = \left(4, \left[\frac{2}{4}, 1 \right] \right) \times \left\{ - \left(|-3|, \left[\frac{|-1|}{|-3|}, 1 \right] \right) \right\} + \left(4, \left[\frac{2}{4}, 1 \right] \right) \times \\ &\quad \left(8, \left[\frac{3}{8}, 1 \right] \right) \\ &= \left(20, \left[\frac{4}{20}, 1 \right] \right) = [4, 20] \end{aligned}$$

Case (ii)

$$\begin{aligned} C_I &= (x + y) \times z = ([2, 4] + [-3, -1]) \times [3, 8] = [-8, 24] \\ D_I &= xz + yz = ([2, 4] \times [3, 8]) + ([-3, -1] \times [3, 8]) = [-18, 29] \\ C_U &= (x + y) \times z = \left(4, \left[\frac{2}{4}, 1 \right] \right) + \left\{ - \left(|-3|, \left[\frac{|-1|}{|-3|}, 1 \right] \right) \right\} \times \left(8, \left[\frac{3}{8}, 1 \right] \right) \\ &= \left(8, \left[\frac{3}{8}, 1 \right] \right) = [3, 8] \\ D_U &= xz + yz = \left(4, \left[\frac{2}{4}, 1 \right] \right) \times \left(8, \left[\frac{3}{8}, 1 \right] \right) + \left\{ - \left(|-3|, \left[\frac{|-1|}{|-3|}, 1 \right] \right) \right\} \times \\ &\quad \left(8, \left[\frac{3}{8}, 1 \right] \right) \\ &= \left(8, \left[\frac{3}{8}, 1 \right] \right) = [3, 8] \end{aligned}$$

Example. 2

Let $x = [-2, 1]$, $y = [3, 8]$ and $z = [-3, 2]$

x , y and z are re-written in the form of proposed UGN representation, i.e.,

$$x \in \left(|-2|, \left[\frac{-1}{|-2|}, 1 \right] \right), y \in \left(8, \left[\frac{3}{8}, 1 \right] \right) \text{ and } z \in \left(|-3|, \left[\frac{-2}{|-3|}, 1 \right] \right)$$

Case (i)

$$A_I = x \times (y + z) = [-2, 1] \times ([3, 8] + [-3, 2]) = [-20, 10]$$

$$B_I = xy + xz = ([-2, 1] \times [3, 8]) + ([-2, 1] \times [-3, 2]) = [-20, 14]$$

$$A_U = x \times (y + z) = - \left(|-2|, \left[\frac{-1}{|-2|}, 1 \right] \right) \times \left\{ \left(8, \left[\frac{3}{8}, 1 \right] \right) + \left\{ - \left(|-3|, \left[\frac{-2}{|-3|}, 1 \right] \right) \right\} \right\}$$

$$= \left(5, \left[\frac{-10}{5}, 1 \right] \right) = [-10, 5]$$

$$B_U = xy + xz = - \left(|-2|, \left[\frac{-1}{|-2|}, 1 \right] \right) \times \left(8, \left[\frac{3}{8}, 1 \right] \right) + \left\{ - \left(|-2|, \left[\frac{-1}{|-2|}, 1 \right] \right) \times \left\{ - \left(|-3|, \left[\frac{-2}{|-3|}, 1 \right] \right) \right\} \right\}$$

$$= \left(5, \left[\frac{-10}{5}, 1 \right] \right) = [-10, 5]$$

Case (ii)

$$C_I = (x + y) \times z = ([-2, 1] + [3, 8]) \times [-3, 2] = [-27, 18]$$

$$D_I = xz + yz = ([2, 4] \times [3, 8]) + ([-3, -1] \times [3, 8]) = [-18, 29]$$

$$C_U = (x + y) \times z = \left\{ - \left(|-2|, \left[\frac{-1}{|-2|}, 1 \right] \right) + \left(8, \left[\frac{3}{8}, 1 \right] \right) \right\} \times \left\{ - \left(|-3|, \left[\frac{-2}{|-3|}, 1 \right] \right) \right\}$$

$$= \left(8, \left[\frac{-18}{8}, 1 \right] \right) = [-18, 8]$$

$$D_U = xz + yz = - \left(|-2|, \left[\frac{-1}{|-2|}, 1 \right] \right) \times \left\{ - \left(|-3|, \left[\frac{-2}{|-3|}, 1 \right] \right) \right\} + \left(8, \left[\frac{3}{8}, 1 \right] \right) \times \left\{ - \left(|-3|, \left[\frac{-2}{|-3|}, 1 \right] \right) \right\}$$

$$= \left(8, \left[\frac{-18}{8}, 1 \right] \right) = [-18, 8]$$

A_I , B_I , C_I and D_I represents the arithmetic operation performed using interval arithmetic and A_U , B_U , C_U and D_U represents the arithmetic operation performed using universal grey number arithmetic. For the first example, one of the uncertainty quantity with negative in its lower and upper bound is considered, in this case it can be seen that sub-distributive property is satisfied in the case of interval arithmetic i.e., ($A_I \subset B_I$ and $C_I \subset D_I$), which is considered to be the main reason for the dependency problem and further leading to overestimation in the results. In the case of proposed UGT arithmetic, there is the satisfaction of the distributive property i.e., ($A_U = B_U$ and $C_U = D_U$) and hence it is free from the dependency problem. Mathematically is represented by ($A_I \supset A_U = B_U \subset B_I$) and ($C_I \supset C_U = D_U \subset D_I$).

For the second example, a uncertainty quantity considered is negative in its lower bound and positive in its upper bound (magnitude of lower bound is greater than upper bound), similar to the first example there is satisfaction of sub-distributive property i.e. ($A_I \subset B_I$ and $C_I \subset D_I$) by interval method and distributive property

i.e. $(A_U = B_U \text{ and } C_U = D_U)$ by UGT. Mathematically it can be represented by $(A_I \supset A_U \text{ and } B_U \subset B_I)$ and $(C_I \supset C_U \text{ and } D_U \subset D_I)$. Hence, from the proposed arithmetic relation it can be seen that there is the satisfaction of distributive property and the arithmetic relations are developed to account for the negative sign and basic four arithmetic $(+, -, \times, \div)$ relations of UGN are defined using MATLAB. In the following section, the proposed method is utilized to solve three numerical examples involving input uncertainty.

4.4.1 Example : Non-linear Explicit Function (Revisited)

An explicit nonlinear response function is considered and solved using universal grey theory, interval and combinatorial optimization.

$$f(x) = 16x_1^4 - 96x_1^3 + 216x_1^2 - 216x_1 - 64x_2^3 + 240x_2^2 - 300x_2 + 36x_3^2 - 84x_3 - 8x_4 + 264 \quad (4.28)$$

The notation δ is used to introduce variation, which allows the assumed ranges of the unknown parameters to be determined. Following parameters are written in the form of UNG.

$$x_1 = \left(x_1^0 (1 + \delta_1), \left[\frac{x_1^0 (1 - \delta_1)}{x_1^0 (1 + \delta_1)}, 1 \right] \right), x_2 = \left(x_2^0 (1 + \delta_2), \left[\frac{x_2^0 (1 - \delta_2)}{x_2^0 (1 + \delta_2)}, 1 \right] \right)$$

$$x_3 = \left(x_3^0 (1 + \delta_3), \left[\frac{x_3^0 (1 - \delta_3)}{x_3^0 (1 + \delta_3)}, 1 \right] \right) \text{ and } x_4 = \left(x_4^0 (1 + \delta_4), \left[\frac{x_4^0 (1 - \delta_4)}{x_4^0 (1 + \delta_4)}, 1 \right] \right)$$

where x_1^0, x_2^0, x_3^0 and x_4^0 base value of x_1, x_2, x_3 and x_4 . ($x_1^0 = 1.95, x_2^0 = -0.5, x_3^0 = -4.5$ and $x_4^0 = 15$). The fractional maximum variation in the parameters ± 0.01 in $x_1, \pm 0.001$ in $x_2, \pm 0.15$ in x_3 and ± 0.5 in x_4 are considered. The variation in the parameters is studied by considering a uniform steps size i.e., $\alpha \delta_i$, ($i = 1$ to 4) with α ranging in steps as $0.0, 0.2, 0.4, 0.6, 0.8, 1.0$. Thus, the maximum variability on a single side of every parameter (when $\alpha = 1$) is considered and solution for the response function is found using proposed UGT. The following results are compared with those obtained using interval method and combinatorial optimization. As the variation are introduced through the step size, in certain step size the variation in the bounds tends to have the negative in its lower bound and positive in its upper bounds with magnitude less than the lower bound. In both the situation the response variation predicted by UGT found to be comparable with the combinatorial optimization. The graphical representation of response of explicit equation obtained by three methods considering variation in the input parameters is shown in Figure 4.8 and corresponding values are depicted in Table. 4.6. As expected, wider bounds are obtained while using direct interval method which is due to the dependency problem. The proposed UGT handles the uncertain quantity having negative in its bound and

also the response variation predicted are comparable with the combinatorial approach.

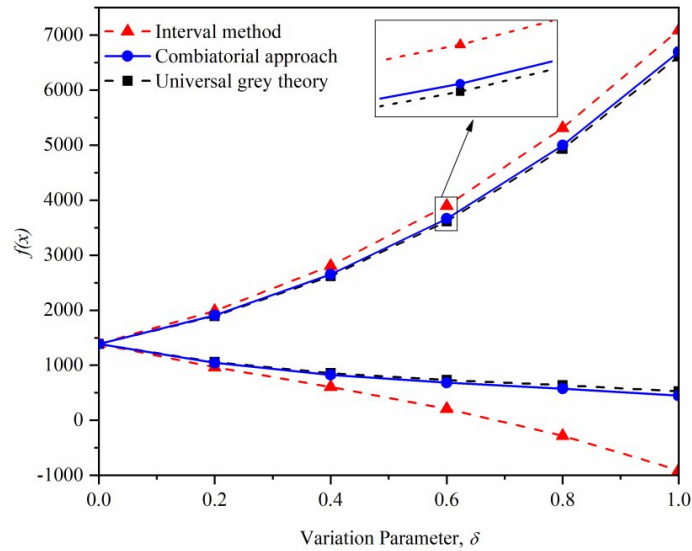


Figure 4.8 Response function, $f(x)$

Table 4.6 Ranges of stresses

α	Interval method	Combinatorial optimization	Universal Grey theory
0	1388.65	1388.65	1388.65
0.2	[964.60, 1987.20]	[1043.33, 1908.48]	[1059.3, 1892.5]
0.4	[607.1, 2808.3]	[824.53, 2650.84]	[856.5, 2618.9]
0.6	[208, 3899.9]	[684.22, 3663.72]	[732.2, 3615.8]
0.8	[-280.6, 5310.2]	[574.42, 4995.12]	[638.4, 4931.2]
10	[-906.9, 7087.1]	[447.12, 6693.07]	[527.1, 6613.1]

For the maximum variation in the input parameters, lower bounds predicted by two approaches (UGT and Combinatorial) differ by 11.83 % and upper bounds differ by 1.30 %. Whereas, in interval method bounds shows much more variation in its response bounds. When there is an increase in the width of the interval parameter values, the predicted outcomes of both the UGT and interval methods tend to deviate from the combinatorial results. However, the deviation is more pronounced and outward in the case of the interval method, whereas the deviation in the UGT method is comparatively smaller and inward. This shrinkage in the results may be attributed to the normalization of the upper bound after each arithmetic operation.

4.4.2 Example : Three Bar Stepped System

The static analysis for the three bar stepped system shown in Figure 4.9 is performed considering the uncertainty in its material, geometry and load parameters. The uncertainty in the input parameters are defined as intervals. It is assumed that the fundamental input parameters, such as the elastic moduli, the cross-sectional areas, and the applied load, will lie within certain intervals or ranges (In the universal grey number notation). The numerical computations are made considering variation in input parameters as follows $\pm 2\%$ in A_1, A_2, A_3 , $\pm 3\%$ in E (same for all the bars) and $\pm 4\%$ in P_3 , where $A_1 = 1000 \text{ mm}^2$, $A_2 = 800 \text{ mm}^2$, $A_3 = 600 \text{ mm}^2$, $P_1 = 0 \text{ kN}$, $P_2 = 0 \text{ kN}$, $P_3 = 1050 \text{ kN}$, $L_1 = 700 \text{ mm}$, $L_2 = 650 \text{ mm}$ and $L_3 = 500 \text{ mm}$. Each uncertain parameter defined in the ranges or interval are re-written in the form of UGN during the UGT analysis. Similar to the previous problem, the variation in the parameters is studied by considering a uniform steps size i.e., with α ranging in steps as 0.0, 0.2, 0.4, 0.6, 0.8, and 1.0. When $\alpha = 1$ shows the maximum variation in each parameter considered, and the stress analysis of three bar stepped system is studied using proposed universal grey arithmetic and the following stress results are evaluated against those obtained using interval method and combinatorial optimization as shown in Table 4.7-4.9. The variation of stresses in bar are obtained, by considering the percentage variation in input parameter and are shown in Figures 4.10, Figure 4.11 and Figure 4.12 respectively.

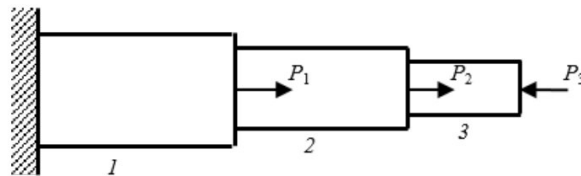


Figure 4.9 Three bar stepped system

It can be seen that the values obtained using proposed universal grey arithmetic shows converging with the combinatorial optimization values, whereas interval method showed diverging pattern. For the large uncertainty in the input parameters, the UGT predicts slight shrink in the results than the combinatorial optimization. The maximum percentage variation in the lower bound found to be 1.98% and 8.33% in the upper bound. As the α value increases, the predicted outcomes of both the UGT and interval methods tend to deviate from the combinatorial results. However, at lower values, the proposed method demonstrates a tendency to converge with the actual result. The deviations are observed more at higher values of α . The cause of deviation is due to percentage increase in the input uncertainty and normalization of the upper bound after each arithmetic operation.

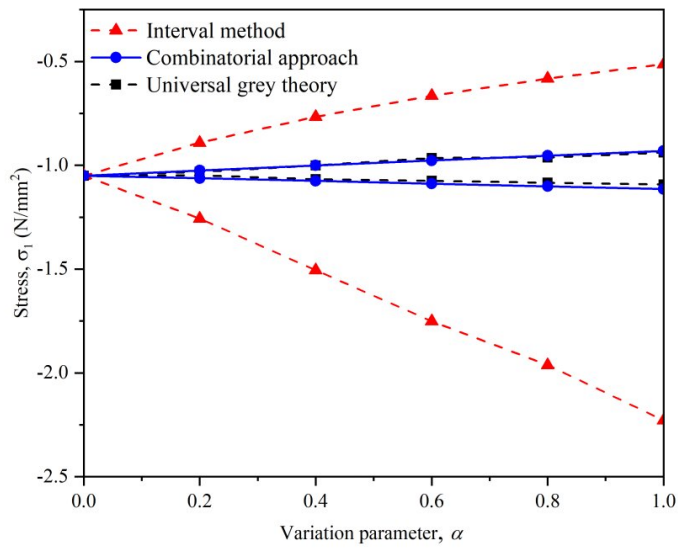


Figure 4.10 Variation of stress in element 1

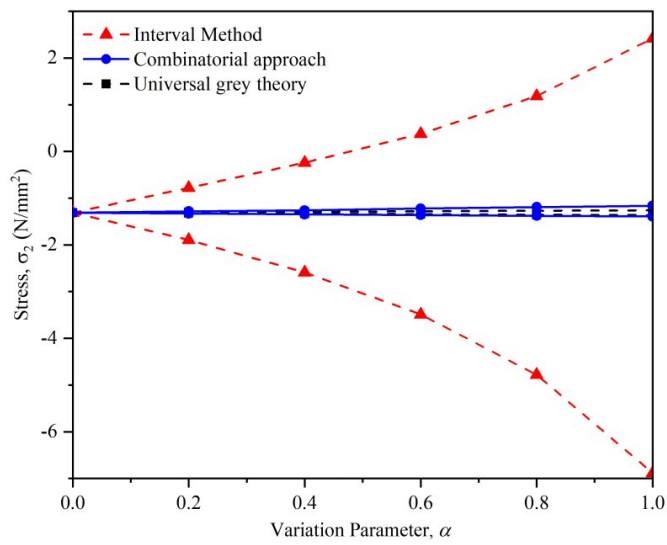


Figure 4.11 Variation of stress in element 2

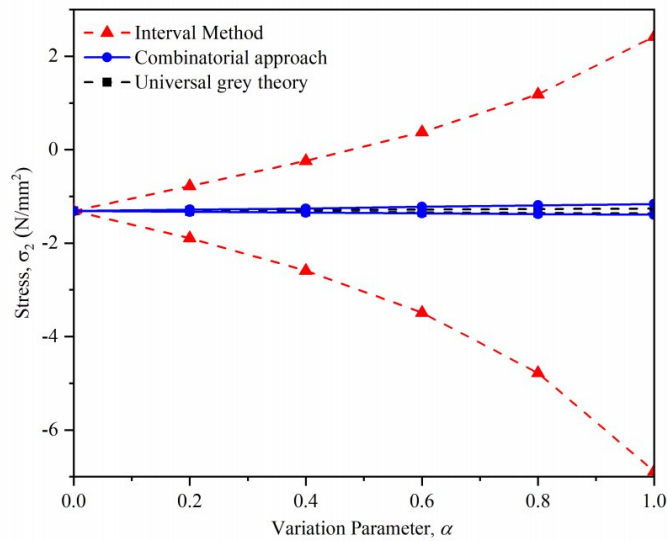


Figure 4.12 Variation of stress 3

Table 4.7 Stress in element 1

α	Interval method	Combinatorial optimization	Universal Grey theory
0	-1.05	-1.05	-1.05
0.2	[-1.256, -0.8913]	[-1.0626, -1.0250]	[-1.0484, -1.0316]
0.4	[-1.5056, -0.7661]	[-1.0754, -1.0006]	[-1.0668, -1.0003]
0.6	[-1.7510, -0.6650]	[-1.0882, -0.9768]	[-1.0752, -0.9648]
0.8	[-1.9619, -0.5821]	[-1.1012, -0.9535]	[-1.0837, -0.9625]
10	[-2.2287, -0.5129]	[-1.1142, -0.9306]	[-1.0921, -0.9387]

Table 4.8 Response of stress in element 2

α	Interval method	Combinatorial optimization	Universal Grey theory
0	-1.3125	-1.3125	-1.3125
0.2	[-1.8947, -0.7788]	[-1.3283, -1.2813]	[-1.3230, -1.3020]
0.4	[-2.5880, -0.2408]	[-1.3456, -1.3125]	[-1.3335, -1.2915]
0.6	[-3.4891, 0.3760]	[-1.3603, -1.2210]	[-1.3440, -1.2811]
0.8	[-4.7808, 1.1871]	[-1.3765, -1.1918]	[-1.3546, -1.2706]
10	[-6.8850, 2.4208]	[-1.3928, -1.1633]	[-1.3652, -1.2602]

Table 4.9 Response of stress in element 3

α	Interval method	Combinatorial optimization	Universal Grey theory
0	-1.75	-1.75	-1.75
0.2	[-2.8098, -0.7231]	[-1.7710, -1.7084]	[-1.7640, -1.7360]
0.4	[-4.0104, 0.3809]	[-1.7851, -1.6744]	[-1.7780, -1.7220]
0.6	[-5.5070, 1.7278]	[-1.8137, -1.6280]	[-1.7921, -1.7081]
0.8	[-7.5833, 3.5553]	[-1.8353, -1.5891]	[-1.8062, -1.6942]
10	[-10.8858, 6.4183]	[-1.8571, -1.5511]	[-1.8203, -1.6803]

4.4.3 Example : Planar Truss System

The 11 bar planar truss system shown in Figure 4.13 is studied to determine its stress behaviour. To demonstrate the effectiveness of the three approaches, namely the interval method, combinatorial approach and the proposed universal grey theory considering the input parameters uncertainty. Material uncertainty and load uncertainty is considered with variation from $\pm 0\%$ to $\pm 2\%$ from the base value $P_4^0 = 10\text{ kN}$, $P_6^0 = 20\text{ kN}$, $P_9^0 = 15\text{ kN}$, $P_{10}^0 = -20\text{ kN}$, $E_0^0 = 212\text{ kN/mm}^2$. The stress analysis is performed using FEA.

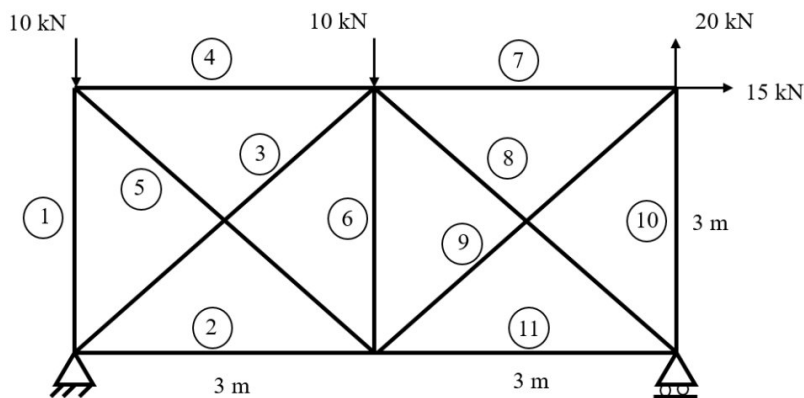


Figure 4.13 Planar truss system

The uncertainty in the input parameters (Young's modulus and applied load) are assumed to vary in specified interval for the analysis of truss system. Using uncertainty-based approaches, the above equilibrium equation is solved for the truss analysis by applying both the interval and universal grey theory computations. The interval simultaneous equations have been solved using a modified version of the general Gauss elimination method that can handle interval-bound values by considering interval arithmetic. Similarly universal grey arithmetic operations are used in order to solve the interval simultaneous equations.

The results of both the methods are compared with the combinatorial

optimization, in which a solution for the deterministic finite element approach is obtained for all the possible combinations in order to determine the exact bounds. For the given uncertainty the variation of stress in the member 2, 4 and 11 is plotted as shown in Figures 4.14, 4.15 and 4.16. The remaining member stresses are shown in Table 4.10- 4.12 for the interval method, Universal grey approach and combinatorial optimization respectively. The results from the proposed UGT are comparable to those from the combinatorial optimization shows that among the truss members with the high stresses, the stress error ranged from 0.153% to 3.49%, whereas the deviations are larger for the stresses which has smaller magnitude of stresses.

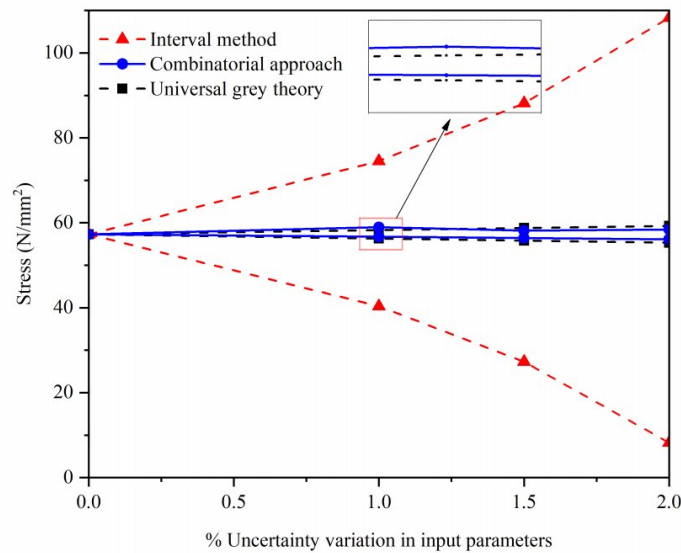


Figure 4.14 Variation of Stress in member 2

Table 4.10 Stresses in truss members obtained by interval method

Member	0%	1%	1.5%	2%
3	-13.817	[-55.335, 27.424]	[-88.437, 60.387]	[-137.533, 109.345]
5	10.93	[-16.792, 38.872]	[-38.938, 61.127]	[-71.813, 94.112]
7	41.766	[13.236, 70.864]	[-8.756, 93.541]	[-41.488, 126.691]
10	28.821	[-15.195, 73.415]	[-50.524, 109.032]	[-103.142, 161.939]

Table 4.11 Stresses in truss members obtained by by UGT

Member	0%	1%	1.5%	2%
3	-13.817	[-14.618, -13.025]	[-15.021, -12.632]	[-15.426, -12.24]
5	10.93	[10.276, 11.587]	[9.95, 11.917]	[9.624, 12.247]
7	41.766	[41.190, 42.349]	[40.905, 42.644]	[40.621, 42.94]
10	28.821	[27.227, 30.444]	[26.441, 31.267]	[25.661, 32.097]

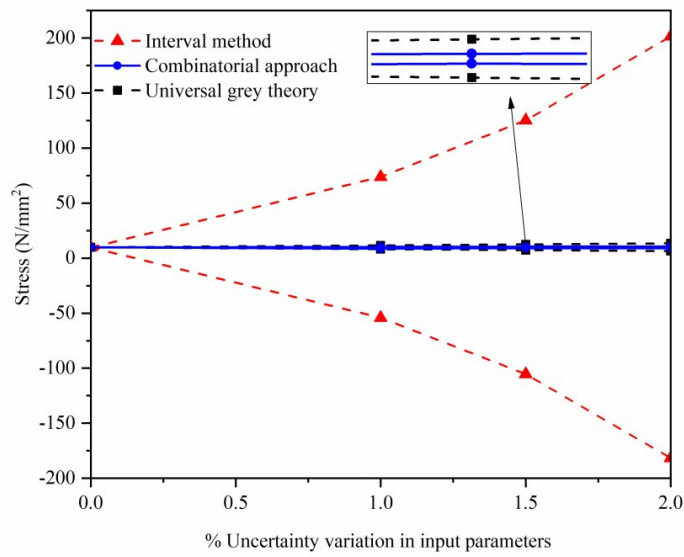


Figure 4.15 Variation of Stress in member 4

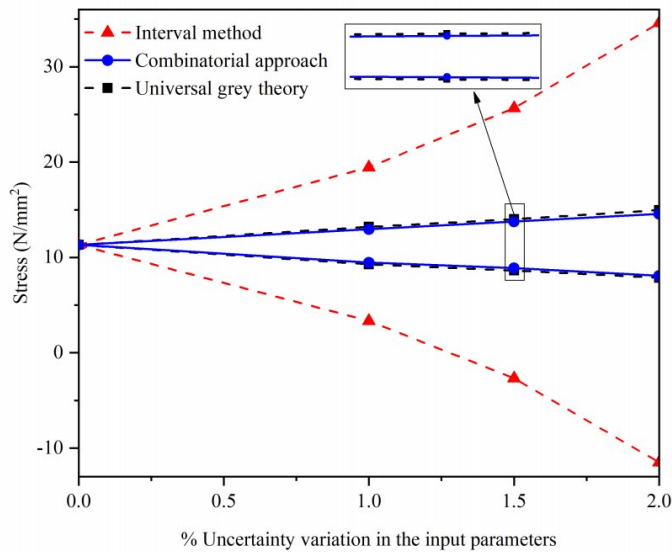


Figure 4.16 Variation of Stress in member 11

Table 4.12 Stresses in truss members obtained by combinatorial approach

Member	0%	1%	1.5%	2%
3	-13.817	[-14.450, -12.260]	[-14.770, -12.870]	[-15.090, -12.550]
5	10.93	[8.181, 12.100]	[9.179, 12.680]	[8.595, 13.270]
7	41.766	[41.350, 42.700]	[41.140, 42.390]	[40.930, 42.600]
10	28.821	[28.280, 30.910]	[28.010, 29.630]	[27.740, 29.900]

The results predicted by the interval method are wider than the actual bounds, the overestimation in the results is due to the multiple use of interval stiffness matrix and load matrix during solving of linear interval simultaneous equation using modified Gauss elimination method. Due to its sub-distributive property and dependency problem leads to overestimation in the predicted bounds. It is evident that the proposed UGT method dealing with the interval parameter with negative in its upper and lower bounds predicts better results for the small variation in the input parameters.

The deviations tend to be more significant for stresses characterized by smaller magnitudes, whereas for stresses with larger magnitudes, the deviations are comparatively smaller. However, the results remain satisfactory, given the longer computational time required for the combinatorial optimization, and they are notably superior in terms of accuracy when compared to the interval method.

4.4.4 Example : Buckling analysis for the column structure

A column structure whose one end is fixed and other end is free, and subjected to axial load P at free end and elastic hinge is considered at node 2 as shown in Figure 4.17. The base (nominal) values of elastic and geometric parameters are given in Table. 4.13. The elastic modulus of the structural member is considered as unknown but bounded by upper and lower limit values which could be expressed in universal grey number form as

$$[E] = \left(E^0 (1 + \alpha), \left[\frac{(1 - \alpha)}{(1 + \alpha)}, 1 \right] \right) \quad \alpha = 0.02 \text{ to } 0.1 \quad (4.36)$$

$$[I] = \left(I^0 (1 + \alpha), \left[\frac{(1 - \alpha)}{(1 + \alpha)}, 1 \right] \right), \quad \alpha = 0.02 \text{ to } 0.1 \quad (4.37)$$

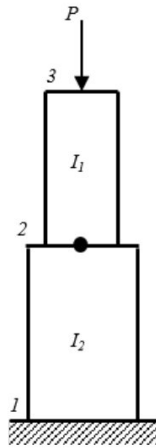


Figure 4.17 Axially loaded column

Table 4.13 Material and geometric properties of column member

variables	Values
E^0	$200 \times 10^6 \text{ kN/m}^2$
I_1^0	$1 \times 10^{-6} \text{ m}^4$
I_2^0	$2 \times 10^{-6} \text{ m}^4$
L	4 m

where and are the base (deterministic) value of E^0 and I_1^0 and is the parametric variation from 2 to 10% from the base value with step size of 2%. In general, the stability analysis of frame structure is performed considering the structural member are axially rigid. i.e., axial deformation is neglected in the stability analysis of frame structure. The elastic stiffness matrix of the member is expressed as:

$$[k_{e_i}] = \begin{bmatrix} \frac{12[E][I_1]}{L^3} & \frac{6[E][I_1]}{L^2} & \frac{-12[E][I_1]}{L^3} & \frac{6[E][I_1]}{L^2} \\ \frac{6[E][I_1]}{L^2} & \frac{4[E][I_1]}{L} & \frac{-6[E][I_1]}{L^2} & \frac{2[E][I_1]}{L} \\ \frac{-12[E][I_1]}{L^3} & \frac{-6[E][I_1]}{L^2} & \frac{12[E][I_1]}{L^3} & \frac{-6[E][I_1]}{L^2} \\ \frac{6[E][I_1]}{L^2} & \frac{2[E][I_1]}{L} & \frac{-6[E][I_1]}{L^2} & \frac{4[E][I_1]}{L} \end{bmatrix}_{i=1 \text{ to } 2} \quad (4.38)$$

$$k_{g_{i=1 \text{ to } 2}} = \frac{P}{30L} \begin{pmatrix} 36 & 3L & -36 & 3L \\ 3L & 4L^2 & -3L & -L^2 \\ -36 & -3L & 36 & -3L \\ 3L & -L^2 & -3L & 4L^2 \end{pmatrix} \quad (4.39)$$

By and combining and applying boundary conditions, the resultant global elastic and global geometric stiffness matrix is reduced to

$$[K_e] = \begin{bmatrix} \frac{12[E][I_1]}{L^3} & \frac{6[E][I_1]}{L^2} & \frac{-12[E][I_1]}{L^3} & \frac{6[E][I_1]}{L^2} \\ \frac{6[E][I_1]}{L^2} & \frac{4[E][I_1]}{L} & \frac{-6[E][I_1]}{L^2} & \frac{2[E][I_1]}{L} \\ \frac{-12[E][I_1]}{L^3} & \frac{-6[E][I_1]}{L^2} & \frac{12[E][I_1]}{L^3} + \frac{12[E][I_2]}{L^3} & \frac{-6[E][I_1]}{L^2} + \frac{-6[E][I_2]}{L^2} \\ \frac{6[E][I_1]}{L^2} & \frac{2[E][I_1]}{L} & \frac{-6[E][I_1]}{L^2} + \frac{-6[E][I_2]}{L^2} & \frac{4[E][I_1]}{L} + \frac{4[E][I_2]}{L} \end{bmatrix} \quad (4.40)$$

$$k_g = \frac{P}{30L} \begin{bmatrix} 36 & 3L & -36 & 3L \\ 3L & 4L^2 & -3L & -L^2 \\ -36 & -3L & 72 & 0 \\ 3L & -L^2 & 0 & 8L^2 \end{bmatrix} \quad (4.41)$$

Considering hinge at node 2, applying hinge condition, the elastic and geometric stiffness are reduced to

$$[K_e] = \begin{bmatrix} \frac{12[E][I_1]}{L^3} & \frac{6[E][I_1]}{L^2} & \frac{6[E][I_1]}{L^2} \\ \frac{6[E][I_1]}{L^2} & \frac{4[E][I_1]}{L} & \frac{2[E][I_1]}{L} \\ \frac{6[E][I_1]}{L^2} & \frac{2[E][I_1]}{L} & \frac{4[E][I_1]}{L} + \frac{4[E][I_2]}{L} \end{bmatrix} \quad (4.42)$$

$$k_g = \frac{P}{30L} \begin{bmatrix} 36 & 3L & 3L \\ 3L & 4L^2 & -L^2 \\ 3L & -L^2 & 8L^2 \end{bmatrix} \quad (4.43)$$

$$\det \{ [K_e]_{ugs} - \lambda_i K_g \} = 0 \quad (4.44)$$

The eigenvalue problem is solved using Rayleigh coefficient method and the critical buckling load for the stepped column bar element is found. Initial Eigenvector is assumed and iteration procedure was carried out to get the critical buckling load for the column structure.

$$\lambda^1_I = \min_{x \in R^n} \left(\frac{x^T [K_e]_{I \text{ or } ugn} x}{x^T [K_g]_{I \text{ or } ugn} x} \right) = \min_{x \in R^n} \left(\frac{x^T \left(\sum_{i=1}^n [K_{e_i}]_{I \text{ or } ugn} \right) x}{x^T \left(\sum_{i=1}^n ([fmin_i, fmax_i]) [K_{g_i}]_{I \text{ or } ugn} \right) x} \right) \quad (4.45)$$

By solving Eq. (4.45), we get the upper and lower bounds of buckling eigenvalue for the considered structural stepped column bar element with variation of uncertain parameter α . Considering the variation of $\pm 10\%$ (α) the upper and lower bounds of buckling eigenvalue is calculated by proposed method and combinatorial optimization are given in Table 4.14

Table 4.14 Critical buckling load

α	Combinatorial approach	Universal grey theory
2	[23.368, 25.067]	[27.613, 29.913]
4	[22.424, 26.317]	[26.500, 26.317]
6	[21.499, 24.244]	[25.405, 32.008]
8	[20.594, 28.381]	[24.336, 33.468]
10	[19.709, 29.441]	[23.289, 34.790]

4.5 METAMODEL

Metamodel techniques have evolved to solve the mitigation of complex computer analysis. The primary purpose of surrogate modeling is to create a simplified and computationally efficient model (the surrogate or meta-model) that approximates the behavior of a complex and computationally expensive simulation or process. The actual behavior of the complex system is achieved by developing the relationship between input variables and output response. The surrogate model can then be used for various applications, such as optimization, sensitivity analysis, or uncertainty quantification while reducing the computational cost significantly. This model serves as a mapping tool that defines the relationship between inputs (design points) and outputs. Essentially, it provides a mathematical representation of how changes in the input variables affect the output variables (Dey et al., 2017). Various types of surrogate models are commonly

used, such as polynomial regression (Zhou et al., 2005), Gaussian processes (Wan et al., 2014), neural networks (Alam et al., 2004), and support vector machines (Pan and Dias, 2017), Kriging meta-models (Sudret (2012); Zhang et al. (2015); Zhao et al. (2015)). The theories mentioned above are only suitable for basic models and not for complex, high-dimensional structural models due to their high computational demands. However, Li et al. (2001a) has proposed an alternative approach called high-dimensional model representation (HDMR) to overcome this challenge. It approximates complex mathematical or computer models by representing them as explicit functions, composed of component functions ordered by their contribution to variance. In most of the practical cases, higher order terms of the inputs usually have a negligible impact on the output response of the system.

4.6 FIRST ORDER HDMR APPROXIMATION

High dimensional model representation approximates complex mathematical or computer models by representing them as explicit functions composed of component functions ordered by their contribution to variance. HDMR is particularly useful for systems with numerous input variables, where lower-order terms adequately capture the system's behavior. In most practical cases, higher-order terms of the inputs typically have a negligible impact on the output response of the system.

In a large-dimensional system, the output $f(x)$ typically depends on numerous input variables $x = \{x_1, x_2, \dots, x_N\}$ with $N \geq 10^2$ or more. The HDMR represents the output as a hierarchical correlated function expansion based on the input variables as:

$$z(x) = z_0 + \sum_{i=1}^N z_i(x_i) + \sum_{1 \leq i_1 < i_2 \leq N} z_{i_1 i_2}(x_{i_1}, x_{i_2}) + \sum_{1 \leq i_1 < \dots < i_m \leq N} z_{i_1 i_2 \dots i_m}(x_{i_1}, x_{i_2}, \dots, x_{i_m}) + z_{12 \dots N}(x_1, x_2, \dots, x_N) \quad (4.46)$$

where the mean response z_0 represents the constant component, $z_i(x_i)$ represents the individual nonlinear effects of each variable x_i , and $z_{ij}(x_i, x_j)$ refer to the collective effects of variables x_i and x_j on the output. Higher-order terms account for the collective influence of multiple input variables while the last term, $z_{12 \dots N}(x_1, x_2, \dots, x_N)$ captures any residual dependence among all variables.

There are two specific HDMR expansions based on the approach used to determine the component functions in Eq. (4.46) (1): ANOVA-HDMR and cut-HDMR. ANOVA-HDMR assesses the contribution of every single component function to the total output variance. Cut-HDMR perfectly captures the output in the variable space hyperplane passing through a reference point. The cut-HDMR technique has

been adopted in this present study. The cut-HDMR method involves selecting a reference point C in the variable space. Regardless of the specific choice of c , the cut-HDMR method remains invariant in the convergence limit. By analyzing the system's input–output responses in relation to the reference point c along divisions in the input variable space referred as "cuts," the expansion functions are established. This process establishes relationships for the component functions represented as.

$$z_0 = z(c) \quad (4.47)$$

$$z_i(x_i) = z(x_i, c^i) - z_0 \quad (4.48)$$

where $z(x_i, c^i) = z(c_1, c_2, \dots, c_{i-1}, x_i, c_{i+1}, \dots, c_N)$ represents the value of component function at the reference point for all input variables except x_i . In order to obtain the value z_0 , all input variables are evaluated at the reference point c . In order to obtain the final output response $z(x)$, the following procedures are performed.

Step 1: Select the component function of first-order

$z(x_i, c^i) = z(c_1, c_2, \dots, c_{i-1}, x_i, c_{i+1}, \dots, c_N)$. For $x_i = x_i^j, n$, function values

$$z(x_i^j, c^i) = z(c_1, c_2, \dots, c_{i-1}, x_i^j, c_{i+1}, \dots, c_N), \quad j = 1, 2, \dots, n \quad (4.49)$$

The function value is determined by evaluating it at n sample points along the variable axis x_i

$$z(x_i^j, c^i) = \sum_{j=1}^n \phi_j(x_i) z(c_1, c_2, \dots, c_{i-1}, x_i^j, c_{i+1}, \dots, c_N) \quad (4.50)$$

When n function values are available, the generation of $z(x_i)$ can be achieved by utilizing Eq. (4.48). The procedure should then be repeated for the remaining component functions.

Step 2: By incorporating the aforementioned functions, we obtain the first-order expansion of $z(x)$ as follows.

$$\tilde{z}(x) = \sum_{i=1}^N \sum_{j=1}^n \phi_j(x_i) z(c_1, c_2, \dots, c_{i-1}, x_i^j, c_{i+1}, \dots, c_N) - (N-1)z_0 \quad (4.51)$$

The Lagrange interpolation function ($\phi_j(x_i)$) is defined as

$$\phi_j(x_i) = \frac{(x_i - x_i^1) \dots (x_i - x_i^{j-1}) (x_i - x_i^{j+1}) \dots (x_i - x_i^n)}{(x_i^j - x_i^1) \dots (x_i^j - x_i^{j-1}) (x_i^j - x_i^{j+1}) \dots (x_i^j - x_i^n)} \quad (4.52)$$

The total number of function evaluations required for interpolation purposes can be determined based on two parameters: the order of the component function taken into consideration (s) and the number of sample points obtained along each variable axis (n). The sampling scheme depicted in Figure 4.18 (a), (b) showcases the approach used for approximating a single and double variable. The computation for the total number of function evaluations, from the zeroth order up to the m^{th} order, is as follows:

$$\sum_{s=0}^m \frac{N!}{s!(N-1)!} (n-1)^s \quad (4.53)$$

The HDMR sampling technique holds significance in comparison to other sampling technique due to its ability to achieve more accurate results with a minimum number of component functions. Therefore, in uncertainty analysis utilizing HDMR, It is crucial to produce an precise reduced model utilizing a limited number of full model runs.

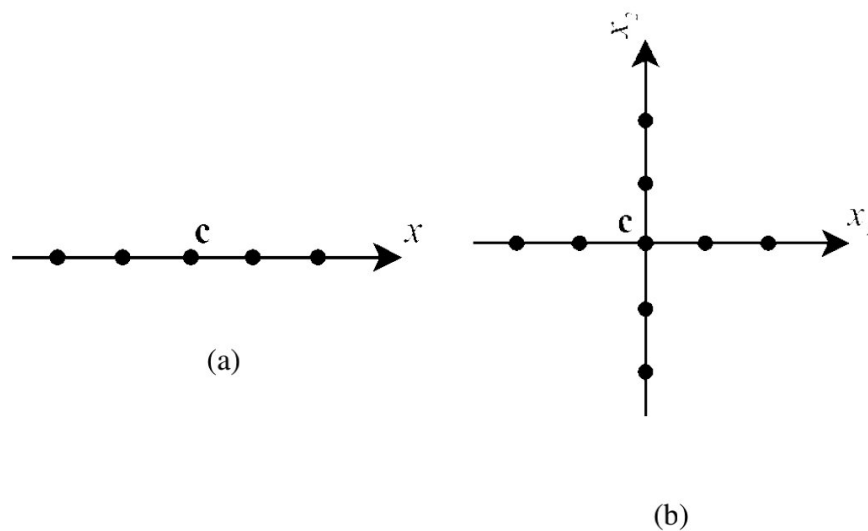


Figure 4.18 Sampling points along each variable axis in first-order HDMR

Significant computational savings are achieved by employing interpolation instead of full model simulations for output determination. In the first-order HDMR approximation, the variable axis x_i is populated with n (where n can be 3, 5, 7, or 9) equally spaced sample points. These sample points are distributed along the axis x_i as $\mu_i - (n-1)\sigma_i/2, \mu_i - (n-3)\sigma_i/2, \dots, \mu_i, \dots, \mu_i + (n-3)\sigma_i/2, \mu_i + (n-1)\sigma_i/2$. Here, μ_i represents the mean and σ_i represents the standard deviation of the variable x_i , with respect to the reference point. High dimensional model representation in conjunction with UGT has been developed and the flow chart for the proposed approach is shown in Figure 4.19.

The first-order HDMR generates a response surface that can be represented by a simple polynomial function. As the number of sample points increases, the polynomial function's degree correspondingly increases. However, the application of UGT to the HDMR response function can cause a shrinkage effect on the output when the degree of polynomial and number of input interval variable increases. This shrinkage phenomenon occurs as a result of the normalization effect caused by the upper bound during each arithmetic operation. During these operations, each uncertain parameter x_i exerts a distinct influence on the final result, with variations in the effects of these parameters. To determine the effect of each input parameter on the error, a weight factor w_i is assigned. The width coefficient for the input variable error can be expressed as:

$$\Delta_i = \left| \frac{\bar{x}_i - x_i}{x_0} \right| \quad (4.54)$$

where $x_0 = \frac{\bar{x}_i + x_i}{2}$. The weight factor assigned to each input variable is described as (Rao and Berke, 1997):

$$w_i = \frac{\Delta_i}{\sum_{i=1}^n \Delta_i} \quad (4.55)$$

To avoid excessive shrinking in the output response resulting from employing UGT, the truncation method is employed to evaluate the truncated factor, which is expressed as:

$$K = \sum_{i=1}^n \Delta_i w_i, \quad n = 1, 2, \dots, n \quad (4.56)$$

where n represents the number of uncertain parameters. Further, the improved universal grey number theory (Liu et al., 2021) is utilized to extend the output results of UGT, ensuring a more accurate representation. The output $\left(\bar{x}, \left[\frac{x}{\bar{x}}, 1 \right] \right)$ of UGT is modified as $\left(\bar{x} \left(1 + \frac{K}{2} \right), \left[\frac{x \left(1 - \frac{K}{2} \right)}{\bar{x} \left(1 + \frac{K}{2} \right)}, 1 \right] \right)$.

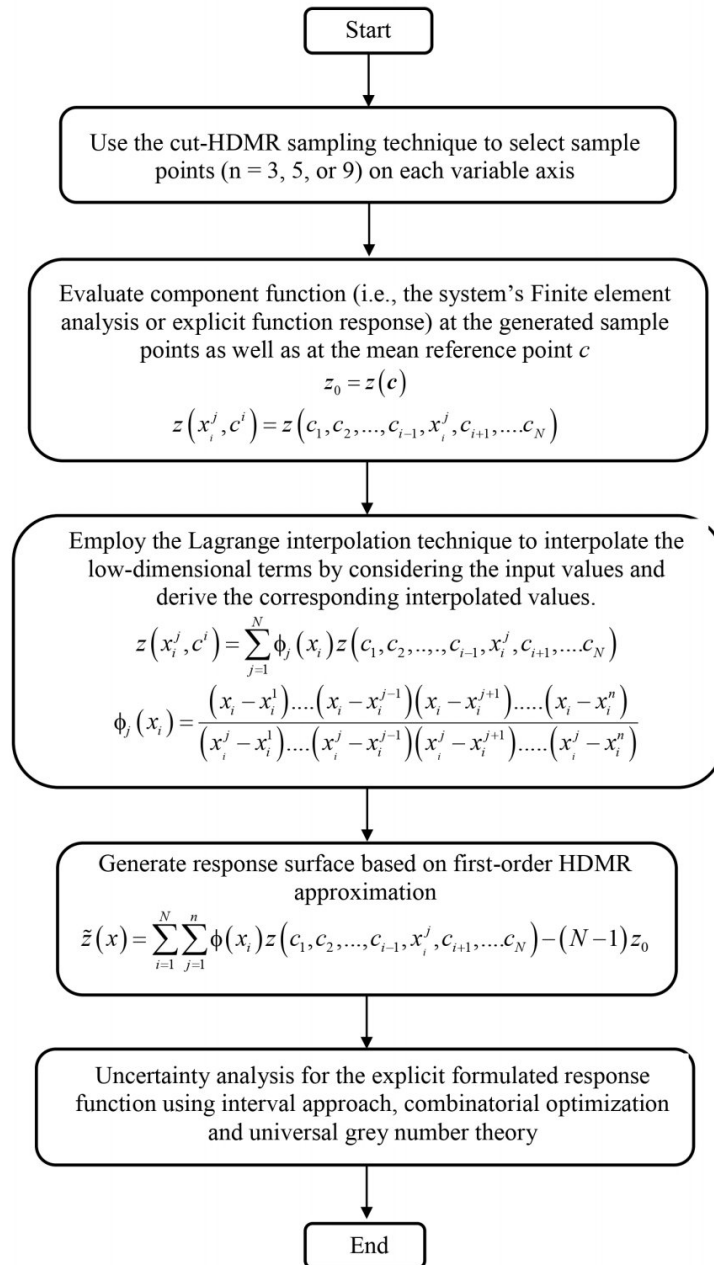


Figure 4.19 UGT–HDMR based uncertainty analysis

4.7 NUMERICAL EXAMPLES

Three numerical examples are solved using proposed HDMR–UGT approach and comparisons are made with the conventional techniques. During the UGT analysis, each uncertain parameter described in intervals was rewritten as a universal grey number. The variation in the parameters δ_i is studied by considering a uniform steps size i.e., $\alpha\delta_i$, with α ranging from 0 to 1. When $\alpha = 1$, the maximum variability is evident across all the parameters under consideration. Uncertain analysis for the first-order HDMR function is performed using UGT, interval approach, and combinatorial optimization.

4.7.1 A Truncated Conical Structure

A conical structure under a compressive axial load P and a bending moment M is considered. The buckling criterion is the failure mode of this structure, which can be defined as the following performance function equation (G) (Keshtegar, 2018).

$$G = 1 - \frac{\sqrt{3(1-\mu^2)}}{\pi Et^2 \cos^2 \theta} \times \left(\frac{P}{0.66} + \frac{M}{0.41 r_1} \right) \quad (4.57)$$

The uncertainty in the material, loading, and geometry of the conical structure is considered ($E = [69300, 70700]$ MPa, $t = [0.0022, 0.0025]$ m, $P = [68000, 70000]$ N) and other parameters are considered deterministic (θ (rad) = 0.524, $\mu = 0.3$, r_1 (m) = 0.9, M (N-m) = 80000). Using cut-HDMR sampling technique, the sample points ($n = 3$ and 5) were generated along each variable axis. The number of interval variables (N) considered for the analysis is 3. The process of constructing a first-order HDMR approximation equation necessitates a total of $(n-1)N+1$ function evaluations. Hence, 7 and 13 function evaluation are performed on explicit function. The Lagrange interpolation technique was employed to interpolate the low-dimensional terms by considering the input values to derive the corresponding interpolated values. Finally, the response surfaces were generated based on first-order HDMR approximation function. Eq. (4.58) and (4.59) represent the first-order HDMR performance function obtained for the conical structure for sample points $n = 3$ and 5, respectively.

$$\begin{aligned} \tilde{G}(t, P, E)_{n=3} = & -240000 t^2 + 1614 t - 1.020 \times 10^{-22} E^2 \\ & + 2.164 \times 10^{-11} E - 2.428 \times 10^{-6} P - 2.897 \end{aligned} \quad (4.58)$$

$$\begin{aligned}
\tilde{G}(t, P, E)_{n=5} = & -4.338 \times 10^{-20} P^4 + 1.214 \times 10^{-14} P^3 - 1.275 \times 10^{-9} P^2 \\
& + 5.704 \times 10^{-5} P - 213333333432 t^4 + 2144000003 t^3 \\
& - 8099866.650 t^2 + 13736.200 t + 29.709 E^4 - 832.870 E^3 \\
& + 8755.319 E^2 - 40904.077 E + 71649.945
\end{aligned} \tag{4.59}$$

The formulated HDMR response surface function was subjected to epistemic uncertainty in its material and geometrical properties. Due to the order of explicit function and complexity of problem, the bound predicted by the UGT found to be over conservative (shrink) when compared with the combinatorial. Hence, to avoid excessive shrinking in the output response resulting from employing UGT, the truncation method is employed. Initially, weight factor of each input variable towards the output error is found and then K value is calculated Eq. (4.60). Finally the correction in the output results of UGT are made with the K value. For $\alpha = 0.1$, the shrinkage factor is determined as follows:

$$K = \sum_{i=E, P, t} \Delta_i w_i = \Delta_E w_E + \Delta_P w_P + \Delta_t w_t \tag{4.60}$$

$$\Delta_P = \frac{70.28 - 69.720}{70} = 0.008$$

$$\Delta_E = \frac{70070 - 69930}{70000} = 0.002$$

$$\Delta_t = \frac{0.002505 - 0.002495}{0.0025} = 0.004$$

$$\sum \Delta_{E, P, t} = 0.014$$

$$w_P = \frac{\Delta_P}{\sum \Delta_{E, P, t}} = 0.5714$$

$$w_E = \frac{\Delta_E}{\sum \Delta_{E, P, t}} = 0.1428$$

$$w_t = \frac{\Delta_t}{\sum \Delta_{E, P, t}} = 0.2857$$

Substituting the above values in Eq. (4.60), gives the K value as 0.006. The output of the UGT is corrected using K value. Similarly the K value is obtained for the other α values. The variation in the performance function of the truncated conical structure is obtained by considering the percentage variation in the input variable and is illustrated graphically in Figure 4.20.

It is observed that when n is set to 5, the proposed HDMR–UGT method yields a convergent estimation of the response bounds with combinatorial optimization. For $n = 3$, the bounds obtained by HDMR–INT ($n = 3$) using interval arithmetic procedure

are larger in width. For $n = 5$, the results were comparatively much wider because of the dependency issue in the interval approach; therefore, the response bounds of HDMR-INT ($n = 5$) response surface analysis were neglected and are not shown in Figure 4.20.

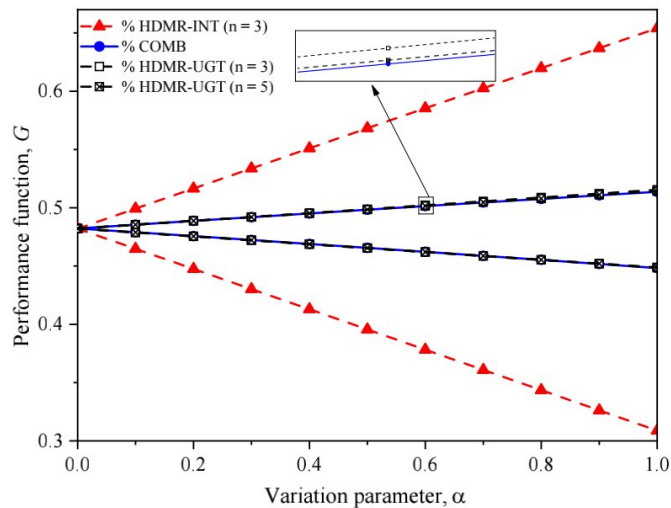


Figure 4.20 Performance function, G

The lower bound predicted by HDMR-UGT ($n = 3$) and combinatorial optimization (COMB) for the maximum percentage variation in the input parameters differ by 0.14% while their upper bounds differ by 0.34%. Similarly, for HDMR-UGT ($n = 5$) and COMB, the differences observed in the lower and upper bounds were 0.127% and 0.130%, respectively. In the interval approach, the bounds differed by 31.12% and 27.31% in its lower and upper bounds, respectively, when compared to the combinatorial optimization.

4.7.2 Static Analysis of Fixed Beam

The behavior of a fixed beam of size $0.23 \text{ m} \times 0.23 \text{ m}$ subjected to uniformly distributed load over the entire span was studied by considering interval uncertainty in its dimension and material property whose values are presented in Table 4.15. The static interval response of the fixed beam was computed using the proposed first-order HDMR-UGT technique. The percentage variation in the considered parameters was: $\pm 5\%$ in E^0 , $\pm 2.5\%$ in L^0 , and $\pm 12\%$ in w^0 , where E^0 , L^0 , w^0 are mean value of the respective variables.

Table 4.15 Material and geometrical properties of fixed beam

variables	Description	Mean	Interval
E	Young's modulus (Mpa)	1.9×10^7	$[1.8 \times 10^7, 2 \times 10^7]$
L	Length (m)	4.0	[3.90, 4.10]
w	Load per meter (kN/m)	9.0	[8, 10]

The impact of the number of sample points employed for the first-order HDMR approximation of the original response function was investigated in the explicit formulation. The value of n was varied from 3 to 5 to assess this effect. Finite element analysis was performed at each of the generated sample points, including at mean reference point c . Eq. (4.61) and (4.62) represent the first-order HDMR approximation function obtained for the fixed beam subjected to UDL for sample points $n = 3$ and 5 respectively.

$$\begin{aligned} \tilde{U}_{\max}(w, L, E)_{n=3} = & 0.375E^2 - 2.139E + 0.510L^2 - 2.725L + 0.1505w \\ & + 5.451 \end{aligned} \quad (4.61)$$

$$\begin{aligned} \tilde{U}_{\max}(w, L, E)_{n=5} = & -2.400L^4 + 38.480L^3 - 230.825L^2 + 615.322L \\ & + 2.2204 \times 10^{-16}w^4 + 0.0001w^3 - 0.0035w^2 + 0.1827w \\ & - 0.666E^4 + 4.866E^3 - 12.918E^2 + 13.961E - 621.073 \end{aligned} \quad (4.62)$$

Similar to the previous problem truncation procedure is adopted to obtain the accurate bounds using UGT. The analysis revealed that when n is set to 5, the proposed method yielded a convergent estimation of the response bounds. Figure 4.21 presents the variation in the maximum deflection of the beam at mid span for the developed HDMR explicit formulation with UGT and interval approach for $n = 3$ and 5 in conjunction with the combinatorial optimization.

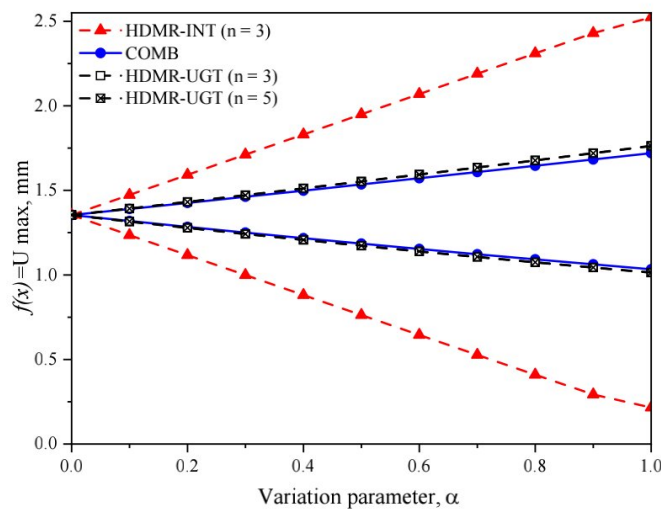


Figure 4.21 Maximum deflection at mid span

The lower bound predicted by HDMR-UGT ($n = 3$) and combinatorial optimization (COMB) for the maximum percentage variation in the input parameters differ by 1.96% while their upper bounds differ by 2.43%. Similarly, for HDMR-UGT ($n = 5$) and COMB, the differences observed in the lower and upper bounds were 1.87% and 2.24%, respectively. In the interval approach, the lower and upper bounds differ by 79.15% and 43.93%, respectively, when compared to that in the combinatorial optimization. The significant error produced by the interval approach is evidently untenable when applied to practical engineering problems.

4.7.3 Shear Wall Frame Subjected to Lateral Load

In this example, a building consisting of four columns and two shear walls was considered. The floor plan of the building is shown in Figure 4.22; the columns and shear walls collectively serve as the lateral force resisting system against force F . The square-shaped columns have dimensions of t by t and the shear walls have a thickness of t . The contribution of shear deformation is considered for the shear walls and neglected for the columns. The height of each storey is H . Geometric stiffness was disregarded; however, the torsion effect was considered for all building components, assuming unrestricted warping of the cross-sections. The floor was assumed to possess three degrees of freedom owing to its rigid in-plane nature. The columns and shear walls exhibit three degrees of freedom, as indicated in Figure 4.23.

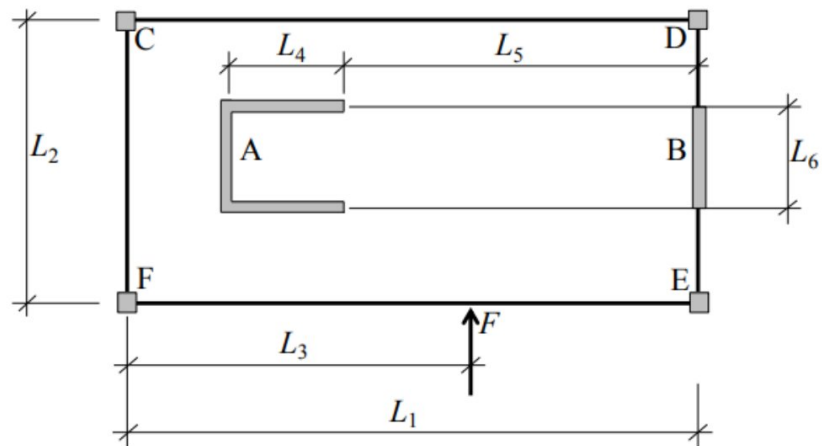


Figure 4.22 Floor plan of the building

For the subsequent calculations, numbers “1” and “2” directions 1 and 2, respectively, corresponding to the degrees of freedom depicted in Figure 4.23. This designation establishes the axis-1 as the conventional y-axis and the axis-2 as the conventional z-axis.

The first-order HDMR technique was employed to generate the response surface for the single-storey building subjected to lateral forces. The sample points were generated using a cut-HDMR sampling scheme along each variable axis. This involved distributing a specific number of sample points ($n = 3$ and 5) along each variable axis and considering the mean values of the interval variables as the reference point, denoted as c . The input data for this example is presented in Table 4.16.

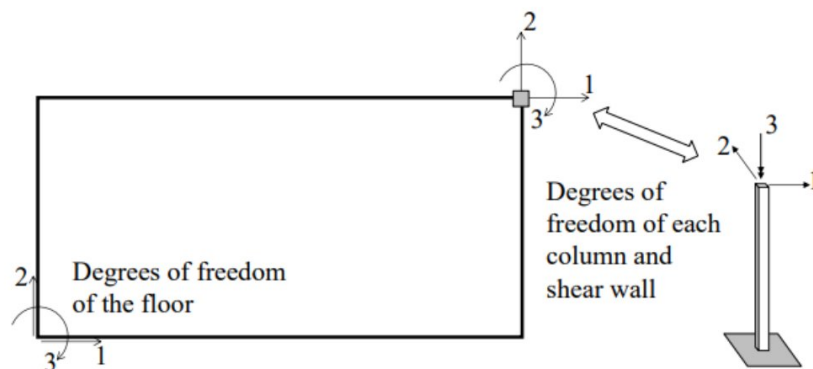


Figure 4.23 Rigid floor plan with degree of freedom

Table 4.16 Material and geometric properties of the single-storey building

variables	Description
E	$[59.9, 60.1] \times 10^6$ kN/m ²
t	0.2 m
μ	0.2
L_1	20 m
L_2	10 m
L_3	$[9.95, 10.05]$ m
L_4	2 m
L_5	14 m
L_6	2 m
H	4.5 m
F	$[3000, 3240]$ kN

The percentage variation in each of the parameter was: $\pm 0.1\%$ in E^0 , $\pm 0.5\%$ in L_3^0 , and $\pm 3.8\%$ in F^0 , where E^0 , L_3^0 , and F^0 are the mean values of the respective parameters. Using first-order HDMR approximation, the explicit formulation for the displacement function in directions 1 and 2 (i.e., U_1 and U_2 , respectively) was obtained. The formulated HDMR functions were subjected to considered interval uncertainty for the uncertainty analysis. Eq.(4.63)–(4.66) represent the first-order HDMR functions for displacements U_1 and U_2 obtained for the sample points $n = 3$ and 5 respectively.

$$\begin{aligned} \tilde{U}_1(F, L_3, E)_{n=3} = & -2.986 \times 10^{-9} F^2 + 6 \times 10^{-4} F + 1.5 \times 10^{-3} L_3^2 + 1.051 L_3 \\ & + 0.057 E^2 - 1.027 E - 6.595 \end{aligned} \quad (4.63)$$

$$\begin{aligned} \tilde{U}_1(F, L_3, E)_{n=5} = & -3.922 \times 10^{-13} F^4 + 4.932 \times 10^{-9} F^3 - 2.325 \times 10^{-5} F^2 \\ & + 0.049 F + 6.794 L_3^4 - 272.270 L_3^3 + 4091.553 L_3^2 - 0.004 E^4 \\ & - 27325.951 L_3 + 0.091 E^3 - 0.686 E^2 + 1.634 E + 68394.146 \end{aligned} \quad (4.64)$$

$$\begin{aligned} \tilde{U}_2(F, L_3, E)_{n=3} = & -3.4722 \times 10^{-9} F^2 - 1 \times 10^{-4} F - 2.984 \times 10^{-13} L_3^2 \\ & - 0.216 L_3 - 0.011 E^2 + 0.203 E + 1.308 \end{aligned} \quad (4.65)$$

$$\begin{aligned} \tilde{U}_2(F, L, E)_{n=5} = & -2.658 \times 10^{-8} F^4 + 3 \times 10^{-4} F^3 - 1.513 F^2 + 3108.633 F \\ & - 4.266 L_3^4 + 170.560 L_3^3 - 2556.789 L_3^2 + 17032.694 L_3 - 0.333 E^4 \\ & - 72.094 E^2 + 8.019 E^3 + 285.389 E - 2436216.499 \end{aligned} \quad (4.66)$$

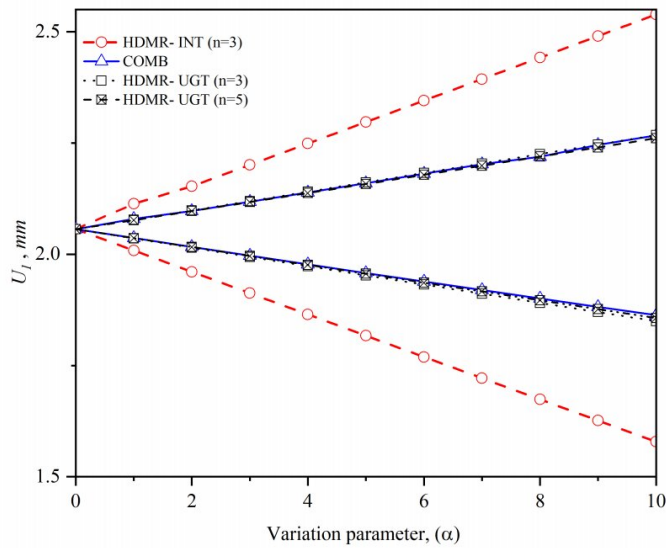


Figure 4.24 Displacement, U_1

Uncertainty analysis for the first-order HDMR functions (for $n=3$ and 5) is performed using UGT, interval approach, and combinatorial optimization. Similar to the first problem truncation procedure is adopted to obtain the accurate bounds using UGT. The graphical representation of displacements (U_1 and U_2) of the single-storey building obtained by the three methods considering variation in the input parameters is shown in Figures 4.24 and 4.25, respectively.

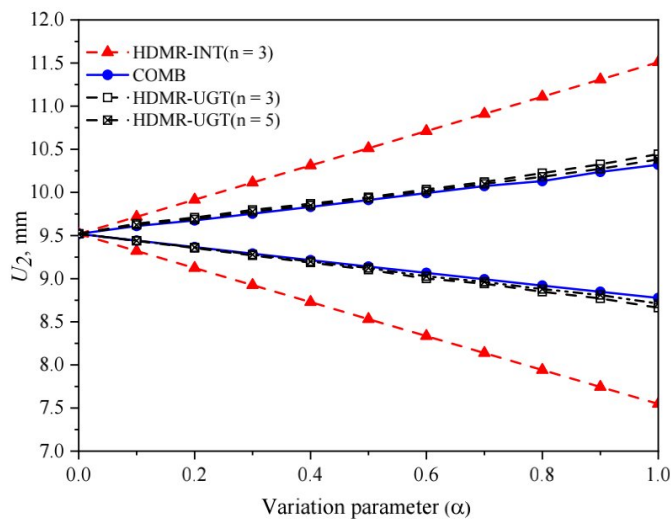


Figure 4.25 Displacement, U_2

The lower bound of U_1 predicted by HDMR-UGT ($n = 3$) and combinatorial optimization (COMB) for the maximum percentage variation in the input parameters differ by 0.72% while their upper bounds differ by 0.32%. Similarly, for U_1 predicted by HDMR-UGT ($n = 5$) and COMB, the differences observed in the lower and upper bounds were 0.34% and 0.3%, respectively. In the interval approach, the lower and upper bounds predicted by HDMR-INT ($n = 3$) differ by 15.27% and 12.30%, respectively, when compared to that predicted by COMB. Similar trends were observed in the displacement U_2 .

4.7.4 Multi-Storied Frame Structure

The deflection at the top story is determined for the three bay five story frame structure subjected to horizontal load as shown in Figure 4.26. Interval uncertainty in the material, geometry and load parameter is considered for the uncertainty analysis and their values are depicted in Table. 4.17. The analysis is performed using proposed HDMR techniques in conjunction with the UGT to evaluate the response of the structure. Similar to the previous examples the response surface is generated using first order HDMR approximation technique for the sample points (n) 3 and 5. The number of variables (N) considered for the frame analysis is 6. The process of constructing a first-order HDMR approximation equation necessitates a total of $(n-1)N+1$ function evaluations. Hence, 13 and 25 functional evaluation are performed by employing an FEA package. Using first-order HDMR approximation technique, the explicit function for the displacement at top story is obtained for $n = 3$ and 5.

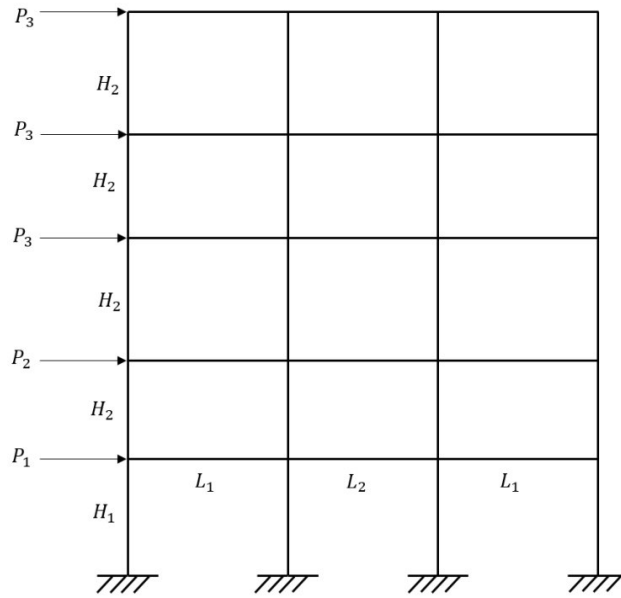


Figure 4.26 Five story three bay portal frame

$$\begin{aligned} \tilde{U}_{x(n=3)} = & -3.587H_1^2 + 41.80H_1 - 4.95H_2^2 + 57.10H_2 - 0.026P_1^2 \\ & + 7.736P_1 - 0.006P_2^2 + 1.612P_2 - 0.009P_3^2 + 2.27P_3 \\ & - 3.60 \times 10^{-12}E^2 + 0.00017E - 3191.472 \end{aligned} \quad (4.67)$$

$$\begin{aligned} \tilde{U}_{x(n=5)} = & 577.083H_1^4 - 9233.083H_1^3 + 55370.329H_1^2 - 147494.869H_1 \\ & + 1823.868H_2^4 - 21885.827H_2^3 + 98437.562H_2^2 - 196658.46H_2 \\ & + 0.0114P_1^4 - 6.844P_1^3 + 1539.871P_1^2 - 153961.463P_1 - 1.028P_2^4 \\ & + 490.399P_2^3 - 87679.357P_2^2 + 6964094.789P_2 + 0.00147P_3^4 \\ & - 0.5913P_3^3 + 88.661P_3^2 - 5904.249P_3 - 4.4612 \times 10^{-22}E^4 \\ & + 4.4526 \times 10^{-14}E^3 + 1.6665 \times 10^{-6}E^2 + 27.7214E \\ & - 374037352.312 \end{aligned} \quad (4.68)$$

The obtained explicit function from the first order HDMR evaluation is subjected to interval uncertainty. Uncertainty analysis is performed using interval method and UGT to evaluate the response bounds of the frame structure, and the results are compared with the deterministic (mean) analysis result. Similar to the first problem truncation procedure is adopted to obtain the accurate bounds using UGT. Figure 4.27 illustrates the variation in top displacement in response to changes in input uncertainty as a percentage, predicted by various methods such as deterministic, Interval method and UGT.

Table 4.17 Input data for the frame structure

Variables	Value
E	$[2.475, 2.525] \times 10^7$ kN/m ²
P_1	[147, 153] kN
P_2	[114, 126] kN
P_3	[95, 105] kN
H_1	[3.8, 4.2] m
H_2	[2.85, 3.15] m

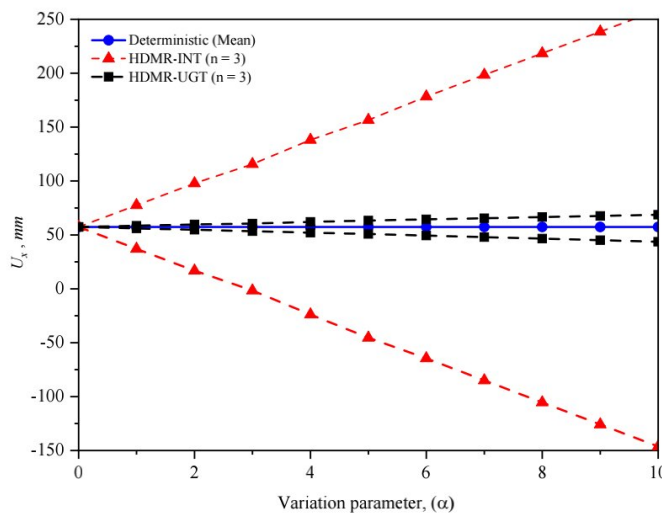


Figure 4.27 Displacement, U_x

The lower bound of top displacement U_x predicted by HDMR-UGT ($n = 3$) and deterministic analysis for the maximum percentage variation in the input parameters differ by 23.89% while their upper bounds differ by 19.8%. Whereas, the results predicted by the interval method are significantly much larger and meaning less. When evaluating the HDMR function Eq.(4.68) using the proposed method, the predicted results were significantly wider and erroneous. The results for $n = 5$ started diverging from the results obtained for $n = 3$. It may be due to the sensitivity of the uncertain variable considered for the numerical example.. Due to these errors, the results were not plotted for HDMR with $n=5$. An attempt was made for $n = 7$, the results were not converging though.

CHAPTER 5

SUMMARY AND CONCLUSION

5.1 SUMMARY AND RESEARCH FINDINGS

It is inevitable to avoid uncertainties in structural analysis and design. Depending on the source and nature of these uncertainties, it is essential to employ appropriate techniques, as no single approach can universally satisfy all the necessary physical laws within the uncertain environment. The present study exclusively focuses on addressing epistemic uncertainty. When the information about the uncertainty is grey (i.e., partially available as range or interval), methods such as combinatorial approach, interval methods, and universal grey theory (UGT) are commonly employed. However, as the dimension of the uncertain system increases, challenges emerge. Combinatorial optimization, although effective, becomes computationally expensive for large systems, and interval analysis tends to overestimate due to violations of physical laws and dependency issues. To mitigate these challenges, UGT offers a promising solution by obeying distributive laws, ensuring free from dependency problems, and enhancing computational efficiency. Few examples are solved using traditional UGT.

In the case of explicit non-linear response function, for the maximum percentage variation in the input variable, UGT predicted better results, with maximum variation in accuracy of 7.19 % and 21.54 % in its lower and upper bound when compared with the combinatorial optimization, whereas the interval method results differ by 57.21 % and 171.28 %. Similarly for spring mass damper system, the maximum percentage variation in the displacement transmissibility ratio predicted by UGT is 3.19 % and 8.25 % for $\zeta = 0.3$; and 4.68 % and 4.85 % for $\zeta = 0.5$ respectively. whereas the interval method results differ by 14.52 % and 17.27 % for $\zeta = 0.3$; and 13.26 % and 15.45 % for $\zeta = 0.5$.

However, traditional UGT encounters limitations when dealing with situations where one or both bounds are negative. Therefore, a necessary modification has been proposed within the UGT framework. Numerical examples demonstrate the computational efficiency of the proposed methodology. In explicit nonlinear function case, UGT required only 5 function evaluations compared to the 80 needed by the combinatorial approach. Moreover, UGT yielded much better results, with a maximum

variation in accuracy of 11.83 % for the lower bound and 1.30% for the upper bound, compared to interval analysis, which showed variations of 102.82% and 6.44%, respectively. Similarly in the case of planar truss system the results from the proposed UGT are comparable to those from the combinatorial optimization. It shows that among the truss members with the high stresses, the stress error ranged from 0.153 % to 3.49 %, whereas the deviations are larger for the stresses which has smaller magnitude of stresses. Similar trends were observed in structural mechanics examples.

Additionally, efficient analysis of epistemic uncertainty involves managing computational expenses. Traditional analytical methods often fall short while dealing with complex problems, necessitating the use of finite element analysis, which demands substantial computational time. Meta-modeling methods like RSM and Kriging become expensive with growing dimensions. The HDMR offers cost-efficient computational advantages for larger systems.

To address the quantification of epistemic uncertainty in large-dimensional systems, this study proposes, the HDMR based UGT formulation. Proposed method integrates the finite element modeling, eliminate the model errors by developing the response surface model using HDMR technique, and employing the UGT for the uncertainty analysis to predict the response bounds. In cases with high-dimensional uncertain systems, UGT might exhibit a tendency for inward oscillations that is taken care by the truncation procedure.

Numerical examples presented showcase the computational efficiency of proposed HDMR based UGT formulation, in terms of effort and accuracy. Compared to the combinatorial optimization, the results of the conical structure obtained using the HDMR based UGT differ by 0.14 % and 0.34 % for the lower and upper bounds respectively. The improvement in the difference has been achieved (i.e., 0.127 % and 0.130 % for lower and upper bounds), when the number of sample points in HDMR is increased from 3 to 5. In contrast, the direct interval approach exhibits much larger disparities, differing by 31.12 % and 27.31 % in lower and upper bounds. Similarly, in the case of the multi-storey building, the results obtained by proposed method differ by 23.89 % while their upper bounds differ by 19.8 %. Whereas, the results predicted by the interval method are significantly much larger and meaning less.

The proposed HDMR based UGT formulation is particularly valuable for research application where accurate results are essential, but computational resources are limited. Nonetheless, the utilization of UGT effectively mitigates dependency problems inherent to interval arithmetic processes.

5.2 FUTURE SCOPE

1. In the present work, we employed first-order HDMR expansions to formulate the response equations. To achieve higher accuracy, the utilization of second-order HDMR is possible, although with a slightly computational time.
2. In the present study, we employed Lagrange interpolation functions. Moreover, alternative interpolation methods, such as moving least squares, can be explored to assess the precision in output responses.
3. Reliability analysis of the system can be performed by developing the hybrid techniques where in epistemic uncertainty is handled by UGT and aleatory uncertainty by any probabilistic technique.



APPENDIX A

Universal grey number arithmetic relations

Let x and y be two interval variable expressed in universal grey number

$x = [\underline{x}, \bar{x}] = \left(\bar{x}, \left[\frac{x}{\bar{x}}, 1 \right] \right)$ and $y = [\underline{y}, \bar{y}] = \left(\bar{y}, \left[\frac{y}{\bar{y}}, 1 \right] \right)$, if $|\bar{x}| \leq |\underline{x}|$, $|\bar{y}| \leq |\underline{y}|$ then, the UGN arithmetic operation are defined as

Addition ($x + y$)

$$\left(\bar{x} + \bar{y}, \left[\frac{x+y}{\bar{x}+\bar{y}}, 1 \right] \right)$$

Subtraction ($x - y$)

$$\text{if } \underline{x} - \underline{y} \leq \bar{x} - \bar{y}, \quad \left(\bar{x} - \bar{y}, \left[\frac{x-y}{\bar{x}-\bar{y}}, 1 \right] \right)$$

$$\text{if } \bar{x} - \bar{y} \leq \underline{x} - \underline{y}, \quad \left(\underline{x} - \underline{y}, \left[\frac{\bar{x}-\bar{y}}{\underline{x}-\underline{y}}, 1 \right] \right)$$

Multiplication ($x \times y$)

$$\left(\bar{x} \times \bar{y}, \left[\frac{x \times y}{\bar{x} \times \bar{y}}, 1 \right] \right)$$

Division ($x \div y$)

$$\text{if } \underline{x} \times \bar{y} \leq \bar{x} \times \underline{y}, \quad \left(\frac{\bar{x}}{\bar{y}}, \left[\frac{x \times \bar{y}}{\bar{x} \times \underline{y}}, 1 \right] \right)$$

$$\text{if } \bar{x} \times \underline{y} < \underline{x} \times \bar{y}, \quad \left(\frac{\underline{x}}{\underline{y}}, \left[\frac{\bar{x} \times \underline{y}}{\underline{x} \times \bar{y}}, 1 \right] \right)$$

Interval arithmetic relations

Let x and y be two interval variable

$x = [\underline{x}, \bar{x}]$ and $y = [\underline{y}, \bar{y}]$, if $|\bar{x}| \leq |\underline{x}|$, $|\bar{y}| \leq |\underline{y}|$ then, the interval arithmetic operation are defined as

Addition ($x + y$)

$$[\underline{x} + \underline{y}, \bar{x} + \bar{y}]$$

Subtraction ($x - y$)

$$[\underline{x} - \bar{y}, \bar{x} - \underline{y}]$$

Multiplication ($x \times y$)

$$[\min(\bar{x} \times \bar{y}, \underline{x} \times \bar{y}, \underline{x} \times \underline{y}, \bar{x} \times \underline{y}), \max(\bar{x} \times \bar{y}, \underline{x} \times \bar{y}, \underline{x} \times \underline{y}, \bar{x} \times \underline{y})]$$

Division ($x \div y$)

$$[\min(\bar{x} \div \bar{y}, \underline{x} \div \bar{y}, \underline{x} \div \underline{y}, \bar{x} \div \underline{y}), \max(\bar{x} \div \bar{y}, \underline{x} \div \bar{y}, \underline{x} \div \underline{y}, \bar{x} \div \underline{y})], \text{ if } 0 \notin [\underline{y}, \bar{y}]$$

MATLAB code using INTLAB tool for arithmetic operation for the UGN:

% A and B are interval parameter (Addition of two universal grey number)

function [z] = add (A, B)

if 0 <= inf(A) && 0 <= inf(B)

[z] = infsup(inf(A) + inf(B), sup(A) + sup(B));

end

if 0 > inf(A) && 0 <= inf(B)

if inf(B) - abs(sup(A)) > sup(B) - abs(inf(A))

[z] = infsup(sup(B) - abs(inf(A)), inf(B) - abs(sup(A)));

else

[z] = infsup(inf(B) - abs(sup(A)), sup(B) - abs(inf(A)));

end

end

```

if 0 > inf(A) && 0 > inf(B)
    if -(abs(sup(A)) + abs(sup(B))) > -(abs(inf(A)) + abs(inf(B)))
        [z] = infsup(-(abs(inf(A)) + abs(inf(B))), -(abs(sup(A)) + abs(sup(B))));
    else
        [z] = infsup(-(abs(sup(A)) + abs(sup(B))), -(abs(inf(A)) + abs(inf(B))));
    end
end

end

% A and B are interval parameter (Subtraction of two universal grey number)
function [z] = sub (A, B)
    if 0 <= inf(A) && 0 <= inf(B)
        if inf(A) - inf(B) <= sup(A) - sup(B)
            [z] = infsup(inf(A) - inf(B), sup(A) - sup(B));
        else
            [z] = infsup(sup(A) - sup(B), inf(A) - inf(B));
        end
    end

end

if 0 > inf(A) && 0 > inf(B)
    if abs(sup(B)) - abs(sup(A)) >= abs(inf(B)) - abs(inf(A))
        [z] = infsup(abs(inf(B)) - abs(inf(A)), abs(sup(B)) - abs(sup(A)));
    else
        [z] = infsup(abs(sup(B)) - abs(sup(A)), abs(inf(B)) - abs(inf(A)));
    end
end

end

if 0 <= inf(A) && 0 > inf(B)
    if inf(A) + abs(sup(B)) < sup(A) + abs(inf(B))
        [z] = infsup(inf(A) + abs(sup(B)), sup(A) + abs(inf(B)));
    else
        [z] = infsup(inf(A) + abs(sup(B)), sup(A) + abs(inf(B)));
    end
end

end

```

```

if 0 > inf(A) - 0.2cm & 0 <= inf(B)
    if -(abs(sup(A)) + inf(B)) < -(abs(inf(A)) + sup(B))
        [z] = infsup(-(abs(sup(A)) + inf(B)), -(abs(inf(A)) + sup(B)));
    else
        [z] = infsup(-(abs(inf(A)) + sup(B)), -(abs(sup(A)) + inf(B)));
    end
end
end
end

```

% A and B are interval parameter (Multiplication of two universal grey number)

```

function [z] = mul (A, B)
    if 0 <= inf(A) & 0 <= inf(B)
        [z] = infsup(inf(A) * inf(B), sup(A) * sup(B));
    end
    if 0 > inf(A) & 0 > inf(B)
        if inf(A) * inf(B) >= sup(A) * sup(B)
            [z] = infsup(sup(A) * sup(B), inf(A) * inf(B));
        else
            [z] = infsup(sup(A) * sup(B), inf(A) * inf(B));
        end
    end
    if 0 <= inf(A) & 0 > inf(B)
        if inf(A) * sup(B) < sup(A) * inf(B)
            [z] = infsup(inf(A) * sup(B), sup(A) * inf(B));
        else
            [z] = infsup(sup(A) * inf(B), inf(A) * sup(B));
        end
    end
end
end

```

```

if 0 > inf(A) & 0 <= inf(B)
    if sup(A)*inf(B) < inf(A)*sup(B)
        [z] = infsup(sup(A)*inf(B), inf(A)*sup(B));
    else
        [z] = infsup(inf(A)*sup(B), sup(A)*inf(B));
    end
end
end

```

% A and B are interval parameter (Division of two universal grey number)

```

function [z] = div (A, B)
    if 0 <= inf(A) && 0 <= inf(B)
        if inf(A)*sup(B) <= sup(A)*inf(B)
            [z] = infsup(inf(A)/inf(B), sup(A)/sup(B));
        else
            [z] = infsup(sup(A)/sup(B), inf(A)/inf(B));
        end
    end
end
    if 0 > inf(A) && 0 <= inf(B)
        if sup(A)/inf(B) <= inf(A)/sup(B)
            [z] = infsup(sup(A)/inf(B), inf(A)/sup(B));
        else
            [z] = infsup(inf(A)/sup(B), sup(A)/inf(B));
        end
    end
end
    if 0 > inf(A) && 0 > inf(B)
        if sup(A)/sup(B) <= inf(A)/inf(B)
            [z] = infsup(sup(A)/sup(B), inf(A)/inf(B));
        else
            [z] = infsup(inf(A)/inf(B), sup(A)/sup(B));
        end
    end
end
end

```

```

if 0 <= inf(A) && 0 > inf(B)
    if inf(A)/sup(B) <= sup(A)/inf(B)
        [z] = infsup(inf(A)/sup(B), sup(A)/inf(B));
    else
        [z] = infsup(sup(A)/inf(B), inf(A)/sup(B));
    end
end
end

```

Gauss elimination code for the UGN arithmetic

E = young's modulus

Aug = Augmented matrix

N = Length of the matrix

X = Nodal displacement matrix

N = length(B);

X = intval(zeros(N,1));

Aug = [A B];

function [z] = *gauss*(Aug, N, E, L, X)

for j = 1 : N - 1

for i = j + 1 : N

 m = *div*(Aug(i, j), Aug(j, j));

 Aug(i, j) = *sub*(Aug(i, j), (*mul*(m, Aug(j, j))));

for count = j + 1 : N + 1

 Aug(i, count) = *sub*(Aug(i, count), (*mul*(m, Aug(j, count))));

end

end

end

Aug;

```

X(N) = div(Aug(N, N+1), Aug(N, N));
for k = N-1 : -1 : 1
    X(k) = div(sub(Aug(k, N+1), smt([Aug(k, k+1:N)], [X(k+1:N)])), Aug(k, k));
end
X;
end
stress(1) = div(mul(E(1), X(1)), L(1));
for i = 2 : N;
    stress(i) = div(mul(E(i), (sub(X(i), X(i-1)))), L(i));
end

```



REFERENCES

- Akpan, U., Koko, T., Orisamololu, I., and Gallant, B. (2001). Practical fuzzy finite element analysis of structures. *Finite Elements in analysis and Design*, 38(2):93–111.
- Alam, F. M., McNaught, K. R., and Ringrose, T. J. (2004). A comparison of experimental designs in the development of a neural network simulation metamodel. *Simulation Modelling Practice and Theory*, 12(7-8):559–578.
- Alazwari, M. A. and Rao, S. S. (2019). Modeling and analysis of composite laminates in the presence of uncertainties. *Composites Part B: Engineering*, 161:107–120.
- Alazwari, M. A. and Rao, S. S. (2022). Uncertainty analysis of large structures using universal grey number theory. *Applied Mathematics and Computation*, 416:126735.
- Alefeld, G. and Herzberger, J. (2012). *Introduction to interval computation*. Academic press.
- Alış, Ö. F. and Rabitz, H. (2001). Efficient implementation of high dimensional model representations. *Journal of Mathematical Chemistry*, 29:127–142.
- Averbakh, I. (2001). On the complexity of a class of combinatorial optimization problems with uncertainty. *Mathematical programming*, 90:263–272.
- Balu, A. S. and Rao, B. N. (2012a). High dimensional model representation based formulations for fuzzy finite element analysis of structures. *Finite Elements in Analysis and Design*, 50:217–230.
- Balu, A. S. and Rao, B. N. (2012b). Inverse structural reliability analysis under mixed uncertainties using high dimensional model representation and fast fourier transform. *Engineering structures*, 37:224–234.
- Balu, A. S. and Rao, B. N. (2014). Efficient assessment of structural reliability in presence of random and fuzzy uncertainties. *Journal of Mechanical Design*, 136(5):051008.
- Baran, I., Cinar, K., Ersoy, N., Akkerman, R., and Hattel, J. H. (2017). A review on the mechanical modeling of composite manufacturing processes. *Archives of Computational Methods in Engineering*, 24:365–395.

- Ben-Haim, Y. (1994). Convex models of uncertainty: applications and implications. *Erkenntnis*, 41(2):139–156.
- Ben-Haim, Y. and Elishakoff, I. (2013). *Convex models of uncertainty in applied mechanics*. Elsevier.
- Berleant, D. J., Ferson, S., Kreinovich, V., and Lodwick, W. A. (2005). Combining interval and probabilistic uncertainty: foundations, algorithms, challenges-an overview. In *4th International Symposium on Imprecise Probabilities and their Applications*.
- Chen, S., Lian, H., and Yang, X. (2002). Interval static displacement analysis for structures with interval parameters. *International Journal for Numerical Methods in Engineering*, 53(2):393–407.
- Chen, S. H. and Yang, X. W. (2000). Interval finite element method for beam structures. *Finite Elements in Analysis and Design*, 34(1):75–88.
- Degrauwe, D., Lombaert, G., and De Roeck, G. (2010). Improving interval analysis in finite element calculations by means of affine arithmetic. *Computers & structures*, 88(3-4):247–254.
- Der Kiureghian, A. and Ditlevsen, O. (2009). Aleatory or epistemic? does it matter? *Structural Safety*, 31(2):105–112.
- Dessombz, O., Thouverez, F., Laîné, J.-P., and Jézéquel, L. (2001). Analysis of mechanical systems using interval computations applied to finite element methods. *Journal of Sound and Vibration*, 239(5):949–968.
- Dey, S., Mukhopadhyay, T., and Adhikari, S. (2015). Stochastic free vibration analysis of angle-ply composite plates—a rs-hdmr approach. *Composite Structures*, 122:526–536.
- Dey, S., Mukhopadhyay, T., and Adhikari, S. (2017). Metamodel based high-fidelity stochastic analysis of composite laminates: A concise review with critical comparative assessment. *Composite Structures*, 171:227–250.
- Du, L., Choi, K. K., and Youn, B. D. (2006). Inverse possibility analysis method for possibility-based design optimization. *AIAA Journal*, 44(11):2682–2690.
- Dubois, D. and Prade, H. (2015). Possibility theory and its applications: Where do we stand? *Springer Handbook of Computational Intelligence*, pages 31–60.
- Elishakoff, I. and Thakkar, K. (2014). Overcoming overestimation characteristic

to classical interval analysis. *AIAA Journal*, 52(9):2093–2097.

Fedele, F., Muhanna, R. L., Xiao, N., and Mullen, R. L. (2015). Interval-based approach for uncertainty propagation in inverse problems. *Journal of Engineering Mechanics*, 141(1):06014013.

Ferson, S. and Ginzburg, L. R. (1996). Different methods are needed to propagate ignorance and variability. *Reliability Engineering & System Safety*, 54(2-3):133–144.

Ferson, S. and Hajagos, J. G. (2004). Arithmetic with uncertain numbers: rigorous and (often) best possible answers. *Reliability Engineering & System Safety*, 85(1-3):135–152.

Forrester, A., Sobester, A., and Keane, A. (2008). *Engineering design via surrogate modelling: a practical guide*. John Wiley & Sons.

Ge, W., Wang, X., Li, Z., Zhang, H., Guo, X., Wang, T., Gao, W., Lin, C., and Van Gelder, P. (2021). Interval analysis of the loss of life caused by dam failure. *Journal of Water Resources Planning and Management*, 147(1):04020098.

Gong, Z. and Forrest, J. Y.-L. (2014). Special issue on meteorological disaster risk analysis and assessment: on basis of grey systems theory. *Natural Hazards*, 71(2):995–1000.

Hang Hou, Y., jia Li, Y., and Liang, X. (2019). Mixed aleatory/epistemic uncertainty analysis and optimization for minimum eedi hull form design. *Ocean Engineering*, 172:308–315.

Hansen, E. and Walster, G. (1992). Global optimization using interval analysis, volume 165 of. *Pure and Applied Mathematics*.

Hansen, E. and Walster, G. W. (2003). *Global optimization using interval analysis: revised and expanded*, volume 264. CRC Press.

Huang, G., Baetz, B. W., and Patry, G. G. (1992). A grey linear programming approach for municipal solid waste management planning under uncertainty. *Civil Engineering Systems*, 9(4):319–335.

Impollonia, N. and Muscolino, G. (2011). Interval analysis of structures with uncertain-but-bounded axial stiffness. *Computer Methods in Applied Mechanics and Engineering*, 200(21-22):1945–1962.

Jansson, C. (1991). Interval linear systems with symmetric matrices,

skew-symmetric matrices and dependencies in the right hand side. *Computing*, 46(3):265–274.

Ji, L., Chen, G., Qian, L., Ma, J., and Tang, J. (2022). An iterative interval analysis method based on kriging-hdmr for uncertainty problems. *Acta Mechanica Sinica*, 38(7):521378.

Jiang, C., Han, X., Guan, F., and Li, Y. (2007). An uncertain structural optimization method based on nonlinear interval number programming and interval analysis method. *Engineering Structures*, 29(11):3168–3177.

Joslyn, C. (2004). Approximate representations of random intervals for hybrid uncertainty quantification in engineering modeling. Technical report, Los Alamos National Lab.(LANL), Los Alamos, NM (United States).

Julong, D. et al. (1989). Introduction to grey system theory. *The Journal of Grey System*, 1(1):1–24.

Kaya, H., Kaplan, M., and Saygın, H. (2004). A recursive algorithm for finding hdmr terms for sensitivity analysis. *Computer Physics Communications*, 158(2):106–112.

Kesava Rao, B. and Balu, A. S. (2019). Modeling of delamination in fiber-reinforced composite using high-dimensional model representation-based cohesive zone model. *Journal of the Brazilian Society of Mechanical Sciences and Engineering*, 41:1–14.

Keshtegar, B., B.-S. . E.-S. (2018). Self-adaptive conjugate method for a robust and efficient performance measure approach for reliability-based design optimization. *Engineering with Computers*, 34,187–202.

Khodaparast, H. H., Mottershead, J. E., and Badcock, K. J. (2011). Interval model updating with irreducible uncertainty using the kriging predictor. *Mechanical Systems and Signal Processing*, 25(4):1204–1226.

Kleijnen, J. P. (1987). *Statistical tools for simulation practitioners*. Marcel Dekker.

Köylüoğlu, H. U., Ş. Çakmak, A., and Nielsen, S. R. (1995). Interval algebra to deal with pattern loading and structural uncertainties. *Journal of Engineering Mechanics*, 121(11):1149–1157.

Li, G., Lu, Z., Li, L., and Ren, B. (2016). Aleatory and epistemic uncertainties analysis based on non-probabilistic reliability and its kriging solution. *Applied*

Mathematical Modelling, 40(9-10):5703–5716.

Li, G., Rosenthal, C., and Rabitz, H. (2001a). High dimensional model representations. *The Journal of Physical Chemistry A*, 105(33):7765–7777.

Li, G., Wang, S.-W., Rabitz, H., Wang, S., and Jaffé, P. (2002). Global uncertainty assessments by high dimensional model representations (hdmr). *Chemical Engineering Science*, 57(21):4445–4460.

Li, G., Wang, S.-W., Rosenthal, C., and Rabitz, H. (2001b). High dimensional model representations generated from low dimensional data samples. i. mp-cut-hdmr. *Journal of Mathematical Chemistry*, 30:1–30.

Liang, Z., Liu, X., Yansong, W., and Wang, X. (2021). Universal grey number theory for the uncertainty presence of wiper structural system. *Assembly Automation*, 41(1):55–70.

Lin, Y., Chen, M., and Liu, S. (2004). Theory of grey systems: capturing uncertainties of grey information. *Kybernetes*, 33(2):196–218.

Liu, S. and Forrest, J. Y. (2010). *Advances in grey systems research*. Springer.

Liu, S., Yang, Y., and Forrest, J. (2017). Grey data analysis. *Springer Singapore, Singapore, Doi*, 10(1007):978–981.

Liu, X., Geng, S., Yu, X., Tong, J., and Wang, Y. (2021). Improved uncertain method for safety analysis of aircraft landing gear. *Proceedings of the Institution of Mechanical Engineers, Part G: Journal of Aerospace Engineering*, 235(16):2547–2560.

LiuSF, L. et al. (2010). Grey information: theory and practical applications.

Makino, K. and Berz, M. (1999). Efficient control of the dependency problem based on Taylor model methods. *Reliable Computing*, 5(1):3–12.

Mazyavkina, N., Sviridov, S., Ivanov, S., and Burnaev, E. (2021). Reinforcement learning for combinatorial optimization: A survey. *Computers & Operations Research*, 134:105400.

Moore, R. E. (1966). *Interval analysis*, volume 4. Prentice-Hall Englewood Cliffs.

Moore, R. E., Kearfott, R. B., and Cloud, M. J. (2009). *Introduction to interval analysis*. SIAM.

- Muhanna, R. L. and Mullen, R. L. (1999). Formulation of fuzzy finite-element methods for solid mechanics problems. *Computer-Aided Civil and Infrastructure Engineering*, 14(2):107–117.
- Muhanna, R. L. and Mullen, R. L. (2001). Uncertainty in mechanics problems—interval-based approach. *Journal of Engineering Mechanics*, 127(6):557–566.
- Muhanna, R. L., Mullen, R. L., and Zhang, H. (2005). Penalty-based solution for the interval finite-element methods. *Journal of Engineering Mechanics*, 131(10):1102–1111.
- Muhanna, R. L., Zhang, H., and Mullen, R. L. (2007). Interval finite elements as a basis for generalized models of uncertainty in engineering mechanics. *Reliable Computing*, 13:173–194.
- Naveen, B. O. and Balu, A. S. (2019). Hdmr-based model update in structural damage identification. *International Journal of Computational Methods*, 16(05):1840004.
- Nedialkov, N. S., Kreinovich, V., and Starks, S. A. (2004). Interval arithmetic, affine arithmetic, taylor series methods: why, what next? *Numerical Algorithms*, 37:325–336.
- Nejadpak, A. and Rao, S. S. (2020). Universal gray finite elements for heat transfer analysis in the presence of uncertainties. *ASCE-ASME Journal of Risk and Uncertainty in Engineering Systems, Part B: Mechanical Engineering*, 6(3):031004.
- Neumaier, A. (1990). *Interval methods for systems of equations*. Number 37. Cambridge University Press.
- Oberkampf, W. L. and Helton, J. C. (2004). Evidence theory for engineering applications. In *Engineering Design Reliability Handbook*, pages 197–226. CRC Press.
- Pan, Q. and Dias, D. (2017). An efficient reliability method combining adaptive support vector machine and monte carlo simulation. *Structural Safety*, 67:85–95.
- Polyak, B. T. and Nazin, S. A. (2004). Interval solutions for interval algebraic equations. *Mathematics and Computers in Simulation*, 66(2-3):207–217.
- Qiu, Z., Chen, S., and Song, D. (1996). The displacement bound estimation for

structures with an interval description of uncertain parameters. *Communications in Numerical Methods in Engineering*, 12(1):1–11.

Qiu, Z. and Elishakoff, I. (1998). Antioptimization of structures with large uncertain-but-non-random parameters via interval analysis. *Computer Methods in Applied Mechanics and Engineering*, 152(3-4):361–372.

Rabitz, H. and Aliş, Ö. F. (1999). General foundations of high-dimensional model representations. *Journal of Mathematical Chemistry*, 25(2-3):197–233.

Ranganathan, R. (1999). *Structural reliability analysis and design*. Jaico Publishing House.

Rao, S. S. and Alazwari, M. A. (2020). Failure modeling and analysis of composite laminates: Interval-based approaches. *Journal of Reinforced Plastics and Composites*, 39(21-22):817–836.

Rao, S. S. and Berke, L. (1997). Analysis of uncertain structural systems using interval analysis. *AIAA Journal*, 35(4):727–735.

Rao, S. S. and Jin, H. (2014). Analysis of coupled bending-torsional vibration of beams in the presence of uncertainties. *Journal of Vibration and Acoustics*, 136(5):051004.

Rao, S. S. and Liu, X. T. (2017). Universal grey system theory for analysis of uncertain structural systems. *AIAA Journal*, 55(11):3966–3979.

Rao, S. S. and Wang, S. (2019). Uncertainty-based structural optimization using universal grey number theory. *AIAA Journal*, 57(11):5002–5013.

Rohn, J. (1989). Systems of linear interval equations. *Linear Algebra and its Applications*, 126:39–78.

Rump, S. M. (1999). Intlab-interval laboratory. In *Developments in Reliable Computing*, pages 77–104. Springer.

Santoro, R., Failla, G., and Muscolino, G. (2020). Interval static analysis of multi-cracked beams with uncertain size and position of cracks. *Applied Mathematical Modelling*, 86:92–114.

Sentz, K. and Ferson, S. (2002). Combination of evidence in dempster-shafer theory.

Shary, S. P. (2001). Interval gauss-seidel method for generalized solution sets to interval linear systems. *Reliable computing*, 7(2):141–155.

- Shi, H. and Deng, Y. (2012). A grey model for evaluation of information systems security. *J. Comput.*, 7(1):284–291.
- Sobol', I. M. (2003). Theorems and examples on high dimensional model representation. *Reliability Engineering and System Safety*, 79(2):187–193.
- Sofi, A. and Romeo, E. (2016). A novel interval finite element method based on the improved interval analysis. *Computer Methods in Applied Mechanics and Engineering*, 311:671–697.
- Sudret, B. (2012). Meta-models for structural reliability and uncertainty quantification. *arXiv preprint arXiv:1203.2062*.
- The Mathworks, I. (2021). Matlab r2021b.
- Tunga, M. A. and Demiralp, M. (2006). Hybrid high dimensional model representation (hhdmr) on the partitioned data. *Journal of Computational and Applied Mathematics*, 185(1):107–132.
- Walley, P. (1991). *Statistical reasoning with imprecise probabilities*, volume 42. Springer.
- Wan, H.-P., Mao, Z., Todd, M. D., and Ren, W.-X. (2014). Analytical uncertainty quantification for modal frequencies with structural parameter uncertainty using a gaussian process metamodel. *Engineering Structures*, 75:577–589.
- Wang, L., Zhao, X., Wu, Z., and Chen, W. (2022a). Evidence theory-based reliability optimization for cross-scale topological structures with global stress, local displacement, and micro-manufacturing constraints. *Structural and Multidisciplinary Optimization*, 65(1):23.
- Wang, L., Zhao, Y., Liu, J., and Zhou, Z. (2023). Uncertainty-oriented optimal pid control design framework for piezoelectric structures based on subinterval dimension-wise method (sdwm) and non-probabilistic time-dependent reliability (ntdr) analysis. *Journal of Sound and Vibration*, 549:117588.
- Wang, L., Zhou, Z., and Liu, J. (2022b). Interval-based optimal trajectory tracking control method for manipulators with clearance considering time-dependent reliability constraints. *Aerospace Science and Technology*, 128:107745.
- Wei, Z., Zhigeng, F., and Changjun, C. (2009). The constitutive error and optimize operator research in the grey number's addition and subtraction inverse

operation. In *2009 IEEE International Conference on Grey Systems and Intelligent Services (GSIS 2009)*, pages 429–433. IEEE.

Wu, W. and Rao, S. (2004). Interval approach for the modeling of tolerances and clearances in mechanism analysis. *J. Mech. Des.*, 126(4):581–592.

Xia, B. and Yu, D. (2013). Modified interval perturbation finite element method for a structural-acoustic system with interval parameters. *Journal of Applied Mechanics*, 80(4):041027.

Xiao, N., Muhanna, R. L., Fedele, F., and Mullen, R. L. (2015). Interval finite element analysis of structural dynamic problems. *SAE International Journal of Materials and Manufacturing*, 8(2):382–389.

Yang, X., Liu, J., Chen, X., Qing, Q., and Wen, G. (2018). Hybrid structural reliability analysis under multisource uncertainties based on universal grey numbers. *Shock and Vibration*, 2018.

Zadeh, L. A. (1965). Fuzzy sets. *Information and control*, 8(3):338–353.

Zavadskas, E. K., Turskis, Z., and Tamošaitiene, J. (2010). Risk assessment of construction projects. *Journal of Civil Engineering and Management*, 16(1):33–46.

Zhang, L., Lu, Z., and Wang, P. (2015). Efficient structural reliability analysis method based on advanced kriging model. *Applied Mathematical Modelling*, 39(2):781–793.

Zhao, H., Yue, Z., Liu, Y., Gao, Z., and Zhang, Y. (2015). An efficient reliability method combining adaptive importance sampling and kriging metamodel. *Applied Mathematical Modelling*, 39(7):1853–1866.

Zhou, Y., Jiang, C., and Han, X. (2006). Interval and subinterval analysis methods of the structural analysis and their error estimations. *International Journal of Computational Methods*, 3(02):229–244.

Zhou, Z., Ong, Y. S., Nguyen, M. H., and Lim, D. (2005). A study on polynomial regression and gaussian process global surrogate model in hierarchical surrogate-assisted evolutionary algorithm. In *2005 IEEE Congress on Evolutionary Computation*, volume 3, pages 2832–2839. IEEE.

Zuhe, S., Neumaier, A., and Eiermann, M. (1990). Solving minimax problems by interval methods. *BIT Numerical Mathematics*, 30:742–751.

PUBLICATIONS

Journals

1. **Kumar, A., and Balu, A.S.** (2023). Epistemic uncertainty quantification in structural systems using improved universal grey theory. *Structures*, (56):104872. <https://doi.org/10.1016/j.istruc.2023.104872>
2. **Kumar, A., and Balu, A.S.** (2023). High dimensional model representation based universal grey theory for uncertainty quantification. *International Journal of Non-Linear Mechanics* (Under review).

Book Chapter

1. **Kumar, A., and Balu, A.S.** (2024). Stability analysis of structural systems with epistemic uncertainties. *Springer Proceedings in Materials*, 35, pp. 221 - 233. https://doi.org/10.1007/978-981-99-6255-6_19

Conferences

1. **Kumar, A., and Balu, A.S.** (2022). Universal grey number systems for uncertainty quantification. *Recent Advances in Materials, Mechanics and Structures. Lecture Notes in Civil Engineering, vol 269* Springer, Singapore. https://doi.org/10.1007/978-981-19-3371-4_17

CURRICULUM VITAE

Akshay Kumar

DoB: September 20, 1994

H.NO-5-2(A), Opposite of Khadi bhandar, Sardar Chowk, Chitguppa,
Bidar, Karnataka, India-585412.

Mobile: +91 9611647313

Email: akshaymankal2@gmail.com

EDUCATIONAL QUALIFICATIONS Doctor of Philosophy (Ph.D.),

2019-Present (In progress)

Institution : National Institute of Technology Karnataka, Surathkal

University : National Institute of Technology Karnataka, Surathkal

Specialization : Structural Engineering, (Civil Engineering)

MASTER OF ENGINEERING (M.TECH.), 2017-2019

Institution : R V College of Engineering

University : Visvesvaraya Technological University, Belagavi

Specialization : Structural Engineering, (Civil Engineering)

BACHELOR OF ENGINEERING (B.E.), 2012-2016

Institution : Bangalore Institute of Technology, Bangalore

University : Visvesvaraya Technological University, Belagavi

Specialization : Civil Engineering